Development of enzymatic synthesis of chiral cyclic amines

Yuta Fukawa

March 2023

Department of Engineering Science,

Graduate School of Engineering,

Gifu University

Contents

Chapter 1
Introduction and Background Information

1.1 Introduction

Chiral amines are constituents of physiologically active substances such as alkaloids and antibiotics, as well as biomolecules like amino acids and carbohydrates. Amines exhibit basicity and electrostatically interact with anions by having a positive charge after binding to a proton. When chiral amines with a certain structure interact specifically with proteins such as receptors and enzymes in vivo, they transmit specific signals within cells or regulate enzyme activities, resulting in giving a variety of effects on living organisms. Therefore, chiral amines are important raw materials for synthesizing pharmaceuticals and agricultural chemicals. In recent years, from the background that many pharmaceuticals have been developed and that the process with low environment load have been required, more efficient synthetic process has been demanded. There are many synthetic methods for amine compounds such as nucleophilic substitution-reduction with cyanide or azide ions, reduction of amides, Gabriel synthesis with phthalimide, reductive amination with hydride reagents including sodium cyanoborohydride and sodium triacetoxyborohydride, Hofmann rearrangement, Mannich reaction, etc. However, these chemical syntheses generally yield racemic amines, and require optical resolutions to obtain single enantiomer which is structurally important for interaction with the binding site of specific protein. Therefore, chemical amine synthesis is generally used for reactions that do not form asymmetric centers (**Figure 1**). In the synthesis of the anticoagulant drug edoxaban, an amino group is introduced into the reaction substrate by azidation and reduction.[1,2] Hofmann rearrangement is applied in the synthesis of (1*R*, 2*S*)-Methyl 1-Boc-amino-2-vinylcyclopropanecarboxylate, which is used as the building block of antiviral drug such as Asunaprevir and Grazoprevir.[3–5] It could be a useful method for synthesis of unnatural amino acids from diester derivatives since rearrangement reactions retains the stereochemistry of the molecule. Reductive amination and Mannich reaction have been applied in the synthesis of pharmaceuticals including Ambroxol and Tramadol.[6,7] Since the synthesis of amine compounds generates an asymmetric center, stereoselective synthesis of amines with various chiral catalysis have recently been developed.

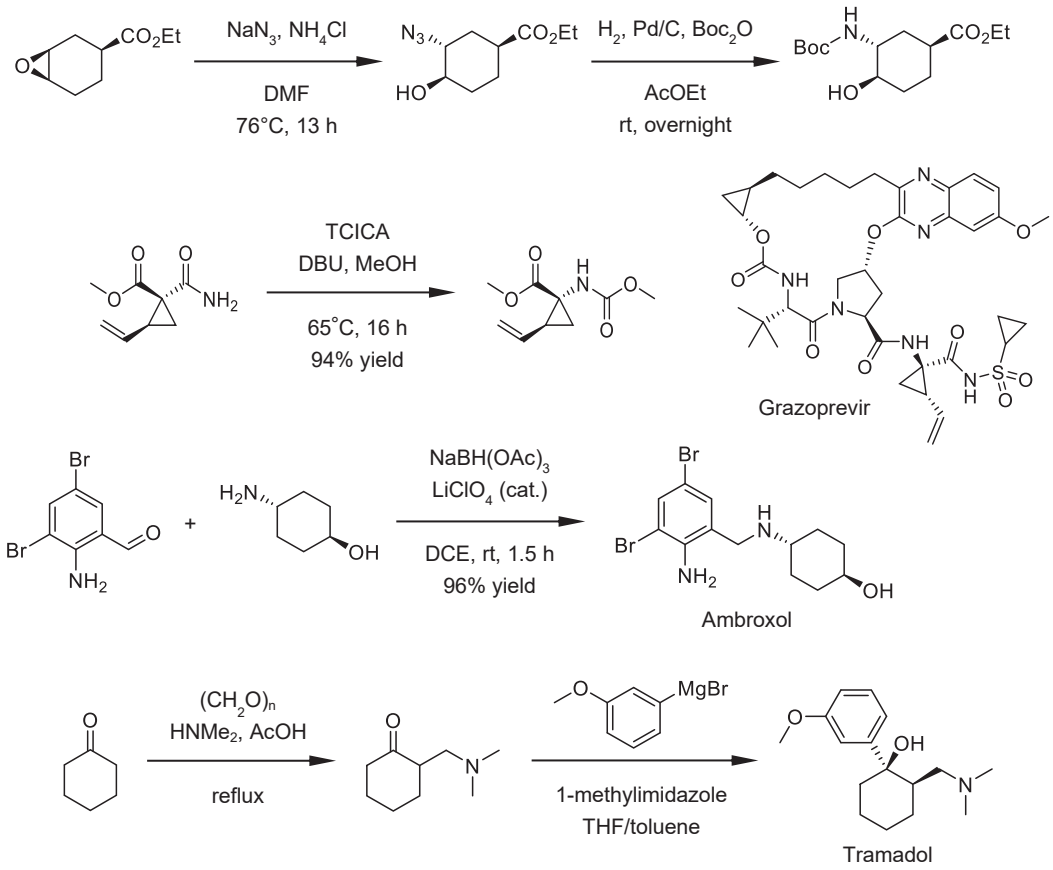

Figure 1. Examples of synthesis of amine compounds

1.2. Chemical synthesis of chiral amines

Chemical syntheses of chiral amines are performed by using chiral catalysts for reductive amination, nitroaldol reaction, Mannich reaction, and Strecker reaction. In reductive amination, iridium or rhodium complexes are commonly used, but nickel or palladium complexes may also be used.[8–12] By using hydrosilane as a hydrogen source, base metals such as copper and zinc can also be used as catalysts.[13,14] Enantioselective reductive amination was first reported in the production process of metolachlor by Solvias (**Figure 2**).[15,16] It has been found that this reaction proceeds with a very small amount of an asymmetric iridium complex (0.01 mol%), and the addition of acetic acid, trifluoroacetic acid or methanesulfonic acid improves its catalytic activity and stereoselectivity. In 2003, reductive amination of acetophenone derivatives was investigated.[17] All the reactions presented in the study showed complete transformations with high stereoselectivities up to 96% ee, but required iodine and isopropyl titanate. Reactions using frustrated Lewis pairs (FLP), Hantzsch esters or optically active phosphoric acid catalysts (Akiyama-Terada Catalyst) have also been reported as reactions that do not use transition metals.[18,19]

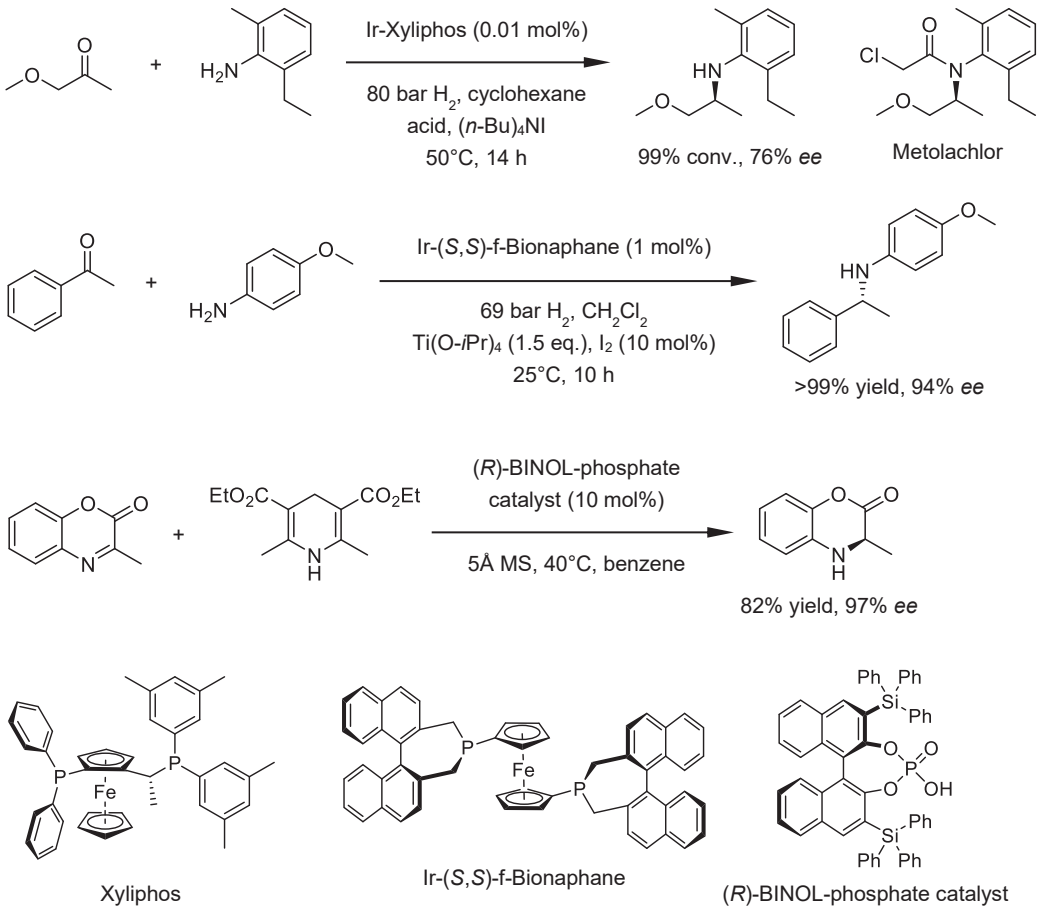

Figure 2. Examples of chemical synthesis of chiral amines by enantioselective reduction.

Asymmetric nitroaldol reactions produce β-nitroalcohols to synthesis 1,2-aminoalcohols found in many bioactive natural products and pharmaceuticals. Reactions of nitroalkanes with carbonyl compounds is performed under basic conditions in the presence of a chiral catalyst and provides the target product with excellent selectivity. Asymmetric phosphonium catalysts synthesized from valine have been reported to exhibit excellent stereoselectivity (anti:syn>19:1, 96–99% *ee*) for aromatic aldehydes.[20] There are also reports of synthesis to give efinaconazole and albaconazole using metal catalysts prepared by mixing $NdCl_3$, diamide ligand, and *t*-BuONa in a 1:1:6 ratio (**Figure 3**).[21,22] Asymmetric Mannich reactions using chiral catalysts including thioureas, phosphate diesters, or proline derivatives can give optically active β-aminocarbonyl compounds.[23–26] Many asymmetric catalysts have been developed based on the chiral structures of natural product molecules such as proline, quinine, and camphor, which can reduce the environmental burden associated with the synthesis of asymmetric catalysts.[27–30] Asymmetric Strecker reactions can give various α-amino acids by using cyanide ions with chiral Lewis acid catalysts or organocatalysts.[31,32] α-Amino acids can also be synthesized from glycine derivatives with an organocatalyst (Maruoka catalyst), which was commercialized by Nagase & Co., Ltd.[33]

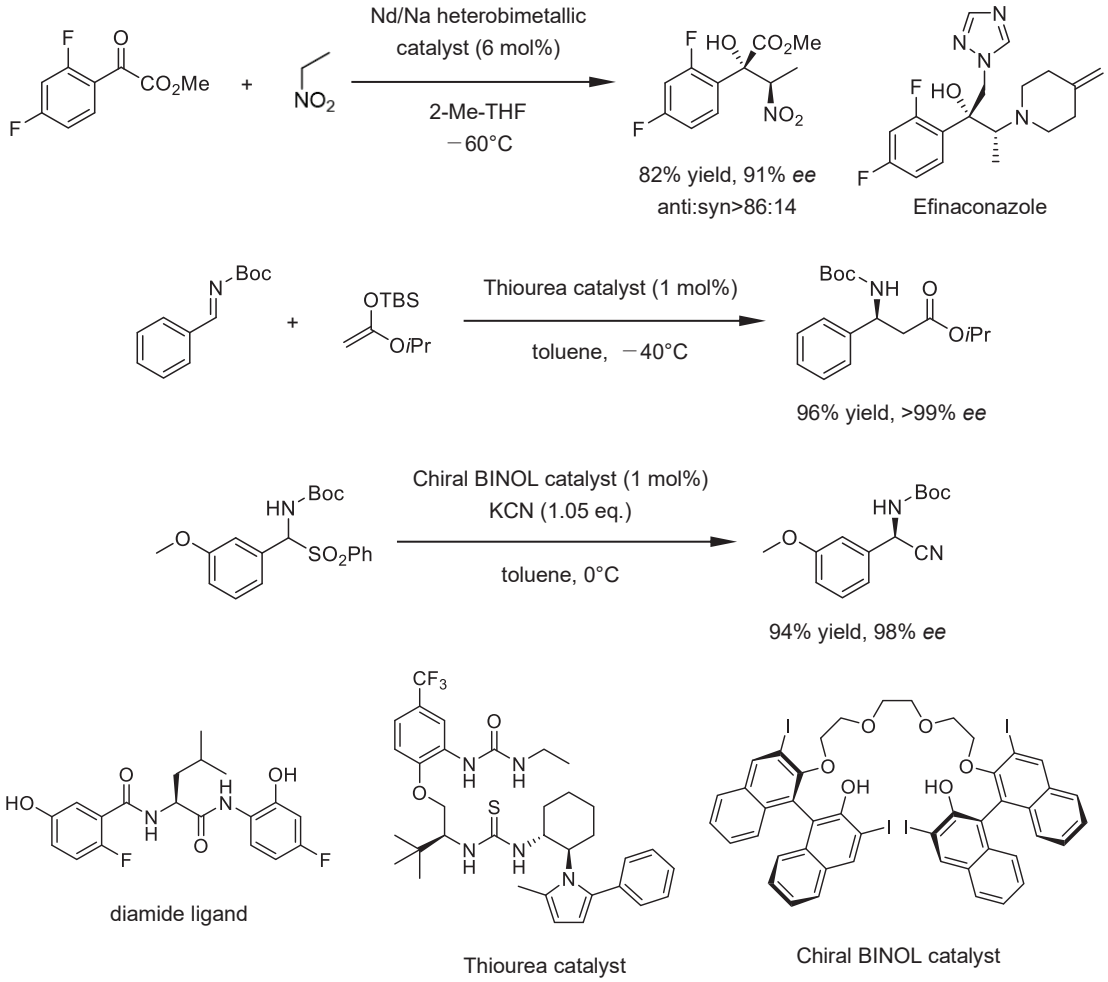

Figure 3. Examples of chemical synthesis of chiral amines by intermolecular addition.

1.3. Biocatalytic synthesis of chiral amines

In recent years, it has been shown that chiral amines can be efficiently synthesized with hydrolases, transaminase, and dehydrogenases. Hydrolases including lipase and acylase are mainly used for optical resolution of racemic amines, which have the advantage that racemic amines are inexpensive or can be easily synthesized. The disadvantage, however, is that even if one enantiomer can be isolated, the other undesired enantiomer remains. Therefore, for practical use, it is desirable to racemate a substrate in the reaction system, and this reaction process is called dynamic kinetic resolution (DKR). Transaminase can catalyze amination of carbonyl groups with an amino donor such as alanine and isopropylamine. Its reaction generally reaches equilibrium, not achieving full conversion of a carbonyl compound, but it can stereoselectively aminate carbonyl compounds with a high conversion rate by using an excess amount of amino donor. Amine dehydrogenase and imine reductase catalyze the asymmetric reduction of imine using NADPH. These enzymatic reactions yield a by-product $NADP^+$ and require a NADPH-regenerating enzyme for efficient reactions. However, unlike transaminase

catalyzing the equilibrium reaction, reductive aminations using the reductase and a NADPH-regenerating enzyme proceed irreversibly, thus avoiding excessive substrate use and achieving high atomic efficiency.

Enzymes in living organisms are known as biocatalysts that catalyze extremely regio- or stereo-selective reactions, and thus their practical use has been desired. Initially, due to the delicate nature of enzymes, it was thought to be difficult to make practical use of enzymes because it is often unstable under the reaction conditions required on an industrial scale. However, recent developments in genetic engineering have led to the discovery of various enzymes with higher durability. Furthermore, a high-throughput screening has identified useful mutations that contribute to the enhancement of enzyme activity or stability, leading to the creation of an extremely stable enzyme variants that can efficiently catalyze reactions under conditions that generally inactivate and denature wild-type enzymes in the presence of high substrate concentrations of 100 g/L or more. These biocatalysts can reduce the environmental burden and the cost in the manufacturing process, and are currently in practical use in several pharmaceutical manufacturing processes.[34] Examples of drugs that consist of chiral amines synthesized enzymatically include pregabalin, sitagliptin, GSK2879552, and abrocitinib (**Figure 4**). Pregabalin is synthesized using nitrilases or lipases in the presence of extremely high concentrations of substrates.[35,36] The kinetic resolution by the lipase from *Thermomyces lanuginosus* yields the *S*-enantiomer of Pregabalin precursor, while the remaining *R*-enantiomer is racemized and can be used in the reaction again. The production of Sitagliptin at Merck uses transaminases mutated over 11 rounds.[37] The original enzyme used in the mutations is a homolog of the enzyme from *Arthrobacter* sp. KNK168, which was discovered by Kaneka Corporation and exhibits excellent (*R*)-selectivity. The transaminase differs from the enzyme from *Arthrobacter* sp. KNK168 in having a substitution of isoleucine (I) at residue position 306 with valine (V).[38,39] The substrate binding site of this enzyme was extended stepwise while improving stability, resulting in an efficient reaction process in the presence of 200 g/L of substrate. Imine reductases has also been used in practical processes. The enzymes was only discovered about 15 years ago, and it remains unclear which substrate imine reductases originally act on in the living organisms.[40,41] Nevertheless, GSK and Pfizer have succeeded in dramatically improving enzyme activity or stability through a high-throughput screening.[42,43] Currently, several research groups, especially in the pharmaceutical industry, are now developing efficient enzymatic syntheses of drugs. In addition to chiral amines, artificial nucleotides that are difficult to synthesize chemically, e.g. Islatravir, Molnupiravir, Ulevostinag (MK-1454), have also been developed in efficient and short step processes with improved biocatalysts.[44–46] It is expected that even more various enzymes will be engineered and used as efficient synthetic tools in drug synthesis in the future.

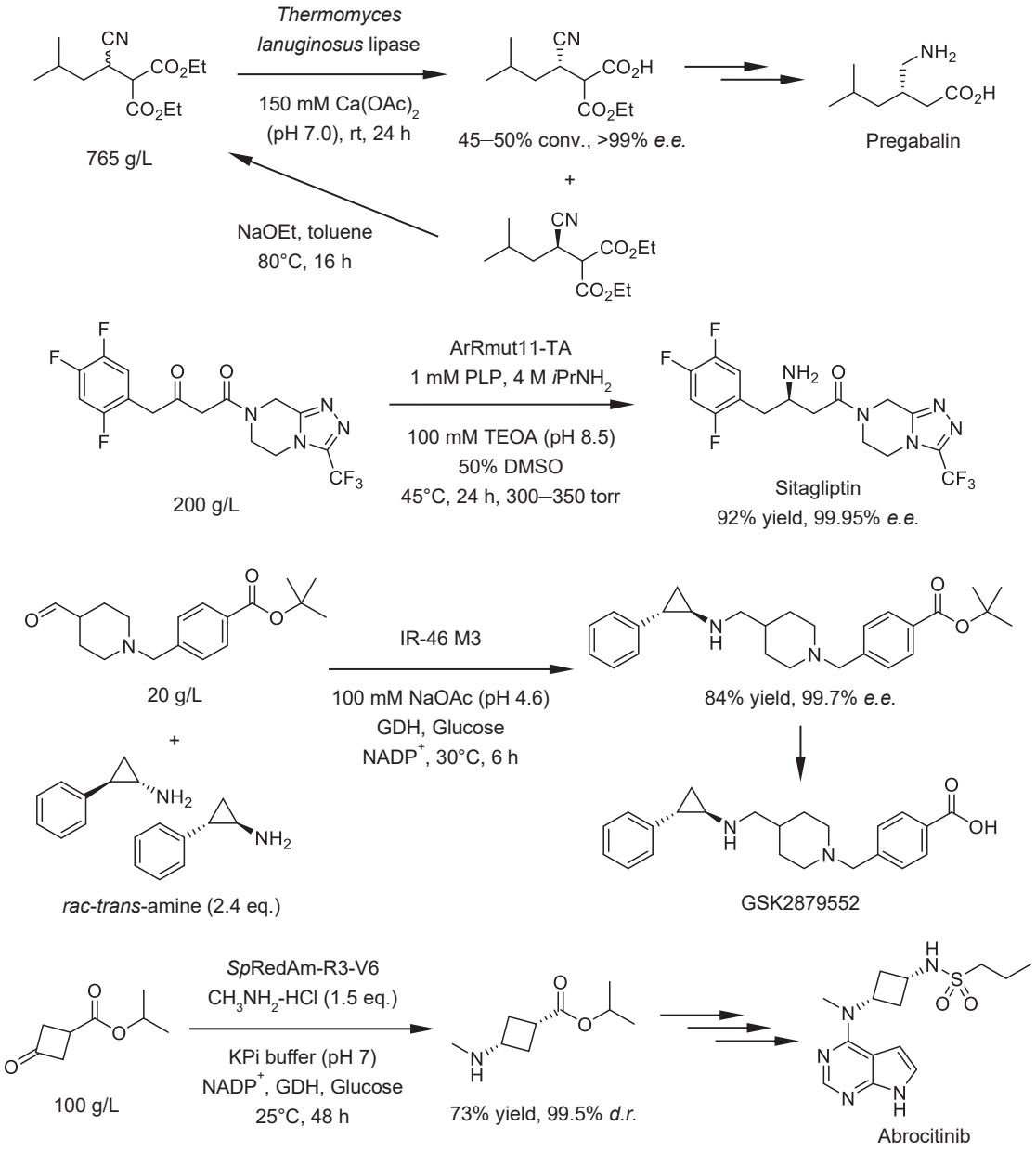

Figure 4. Examples of biocatalytic synthesis of chiral amines

1.4. Purpose of this study

For many years, our laboratory has been searching for microbial enzymes that can be used to synthesize chiral compounds, and has discovered nitrilases, hydrolases, reductases, and other enzymes that are highly useful. Although enzymatic syntheses of chiral amines have been developed, these have often been limited to chain amines, and there are interestingly few reported examples of enzymatic syntheses of cyclic amines such as pyrrolidine and piperidine. On the other hand, our laboratory has discovered hydrolases that act on cyclic amines and imine reductases that act on cyclic imines, respectively, and is pioneering an efficient approach to the synthesis of chiral cyclic amines. Among

them, (*S*)-selective hydrolase K5 (SHA K5) and (*S*)-selective imine reductase GF3546 (SIR46) can be used for the synthesis of (*S*)-chiral cyclic amines. SHA K5 is a novel enzyme that catalyzes (*S*)-stereoselective hydrolysis of racemic *N*-acyl piperidines. There are few enzymes that directly hydrolyze such *N*-acyl cyclic amine. In several hydrolase for kinetic resolution, it has been reported that some hydrolases catalyze enantioselective acylation or carbamoylation of racemic cyclic amines or hydrolyze an intramolecular ester of them stereoselectively. In addition, an enantioselective Cbz-deprotecting enzyme reported in 2003 can deprotect various *N*-Cbz-amino acids including pipecolic acid to afford corresponding chiral products.[47] On the other hand, only SIR46 exhibits (*S*)-selectivity among the five imine reductases found by screening in our laboratory. The reduction activity of the enzyme is about 1/100 of that of imine reductase GF3587 that exhibits (*R*)-selectivity. Since its discovery, several groups have found (*S*)-selective IREDs with higher activity, but most of them still have challenges in stability and stereoselectivity.

Based on these backgrounds, I aimed to develop an enzymatic synthesis of (*S*)-chiral cyclic amines. In Chapter 1, I report the screening, characterization and enzymatic purification of SHA, then construction of a heterologous expression system for SHA K5. In Chapter 2, I investigated practical application of SIR46 showing low reductive activity. SIR46 is the first (*S*)-selective imine reductases, and still shows higher stereoselectivity for many cyclic imines compared to other enzymes. Therefore, I refocused on SIR46 to investigate the effects of improved stabilization of the enzyme by mutations on the enzymatic reaction. These processes may provide a series of chiral cyclic amines for the building blocks of biologically active compounds (**Figure 5**).[48–51]

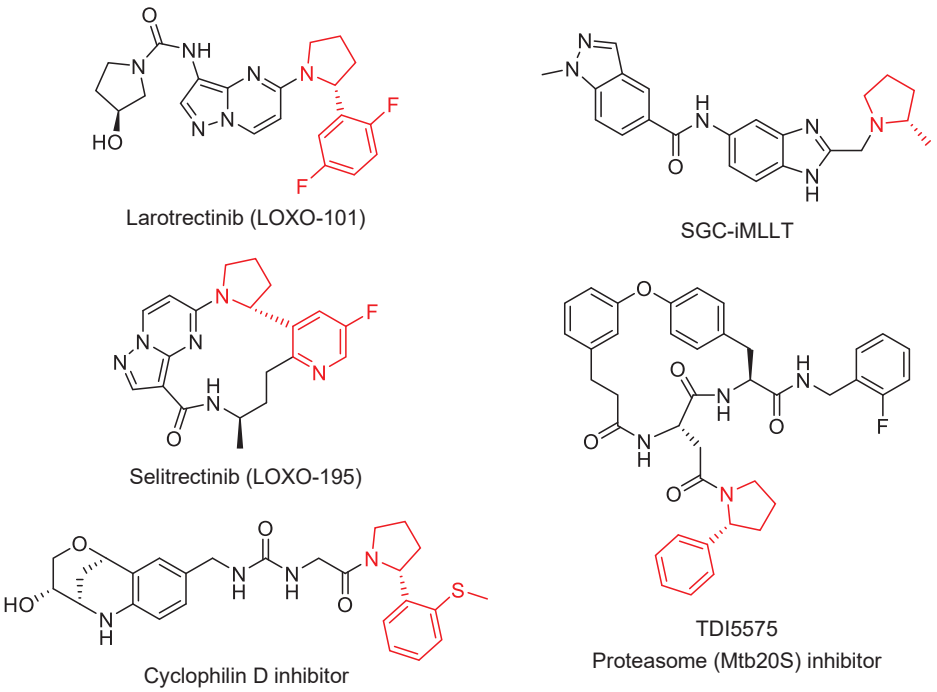

Figure 5. Biologically active compounds containing chiral cyclic amines.

In both studies, I finally designed a heterologous expression system using *Rhodococcus* as a host. One reason for using this host is that both of enzymes dealt with in this study are all derived from actinomycetes, so there is no need to perform codon optimization of the enzyme genes. The second reason is that *Rhodococcus* sp. has a more robust cell wall than *E. coli* and contributes to stabilizing enzymes, expecting to be more resistant to organic solvents and high-concentration substrates. In the case of *E. coli* cell, it tends to lysis during the whole-cell reaction, resulting in inactivation or denaturation of enzymes. Therefore, it is desirable to use *Rhodococcus* cell for a long reaction time or in the presence of high-concentration substrate. Furthermore, it has been reported that *Rhodococcus* could prepare some proteins that become insoluble when expressed in *E. coli*. Despite these advantages, there are still few examples of heterologous expression constructions using *Rhodococcus* as a host cell. Therefore, I constructed recombinant *Rhodococcus* cells expressing SHA K5 or SIR46 gene to enhance their performances. In addition, stabilization of enzyme itself by introducing amino acid mutations is also important for efficient enzymatic synthesis. Since SIR46 exhibits high (*S*)-selectivity but low stability, I evaluated the performances of recombinant *E. coli* or *Rhodococcus* expressing SIR46 gene, and furthermore improved the enzyme stability by mutagenesis for practical synthesis of chiral cyclic amines.

References

(1) T. Ohta, S. Komoriya, T. Yoshino, K. Uoto, Y. Nakamoto, H. Naito, A. Mochizuki, T. Nagata, H. Kanno, N. Haginoya, K. Yoshikawa, M. Nagamochi, S. Kobayashi, M. Ono, Diamine derivatives, US 20050020645A1, Jan. 27, 2005.

(2) K. Yoshikawa, S. Kobayashi, Y. Nakamoto, N. Haginoya, S. Komoriya, T. Yoshino, T. Nagata, A Mochizuki, K. Watanabe, M. Suzuki, H. Kanno, T. Ohta, Design, synthesis, and SAR of cis-1,2-diaminocyclohexane derivatives as potent factor Xa inhibitors. Part II: Exploration of 6–6 fused rings as alternative S1 moieties, *Bioorg. Med. Chem.*, **2009**, 17, 8221–8233.

(3) P. M. Scola, L.-Q. Sun, A. X. Wang, J. Chen, N. Sin, B. L. Venables, S.-Y. Sit, Y. Chen, A. Cocuzza, D. M. Bilder, S. V. D'Andrea, B. Zheng, P. Hewawasam, Y. Tu, J. Friborg, P. Falk, D. Hernandez, S. Levine, C. Chen, F. Yu, A. K. Sheaffer, G. Zhai, D. Barry, J. O. Knipe, Y.-H. Han, R. Schartman, M. Donoso, K. Mosure, M. W. Sinz, T. Zvyaga, A. C. Good, R. Rajamani, K. Kish, J. Tredup, H. E. Klei, Q. Gao, L. Mueller, R. J. Colonno, D. M. Grasela, S. P. Adams, J. Loy, P. C. Levesque, H. Sun, H. Shi, L. Sun, W. Warner, D. Li, J. Zhu, N. A. Meanwell, F. McPhee, The discovery of asunaprevir (BMS-650032), an orally efficacious NS3 protease inhibitor for the treatment of hepatitis C virus infection, *J. Med. Chem.*, **2014**, 57, 1730–1752.

(4) F. Xu, J. Kim, J. Waldman, T. Wang, P. Devine, Synthesis of Grazoprevir, a Potent NS3/4a Protease Inhibitor for the Treatment of Hepatitis C Virus, *Org. Lett.*, **2018**, 20, 22, 7261–7265.

(5) M. M. Littleson, C. M. Baker, A. J. Dalençon, E. C. Frye, C. Jamieson, A. R. Kennedy, K. B. Ling, M. M. McLachlan, M. G. Montgomery, C. J. Russell, A. J.B. Watson, Scalable total synthesis and comprehensive structure–activity relationship studies of the phytotoxin coronatine, *Nat. Commun.*, **2018**, 9, 1105.

(6) S. Sun, C. Cao, Y. Zhou, Y. Zhu, G. Xu, Preparation method of ambroxol hydrochloride, CN 111072500A, Apr. 28, 2020.

(7) M. Borie-Guichot, M. L. Tran, Y. Génisson, S. Ballereau, C. Dehoux, Pharmacological Chaperone Therapy for Pompe Disease, *Molecules*, **2021**, 26, 7223.

(8) M. Subedi, S. Bajaj, M.S. Kumar, M. Yc, An overview of tramadol and its usage in pain management and future perspective, *Biomed. Pharmacother.*, **2019**, 111, 443–451.

(9) T. C. Nugenta, M. El-Shazly, Chiral Amine Synthesis – Recent Developments and Trends for Enamide Reduction, Reductive Amination, and Imine Reduction, *Adv. Synth. Catal.*, **2010**, 352, 753–819.

(10) C. T. Nandhu, T. Aneeja, G. Anilkumar, Advances and perspectives in the rhodium catalyzed reductive amination reactions, *J. Organomet. Chem.*, **2022**, 965−966, 122332.

(11) Z. Wu, W. Wang, H. Guo, G. Gao, H. Huang, M. Chang, Iridium-catalyzed direct asymmetric reductive amination utilizing primary alkyl amines as the N-sources, *Nat. Commun.*, **2022**, 13, 3344.

(12) Y. Liu, Z. Yi, X. Tan, X.-Q. Dong, X. Zhang, Nickel-Catalyzed Asymmetric Hydrogenation of Cyclic Sulfamidate Imines: Efficient Synthesis of Chiral Cyclic Sulfamidates, *iScience*, **2019**, 19, 63–73.

(13) C.-B. Yu, D.-W. Wang, Y.-G. Zhou, Highly Enantioselective Synthesis of Sultams via Pd-Catalyzed Hydrogenation, *J. Org. Chem.*, **2009**, 74, 5633–5635.

(14) B. H. Lipshutz, H. Shimizu, Copper(I)-Catalyzed Asymmetric Hydrosilylations of Imines at Ambient Temperatures, *Angew. Chem. Int. Ed.*, **2004**, 43, 2228–2230

(15) I. Węglarz, K. Michalak, J. Mlynarski, Zinc-Catalyzed Asymmetric Hydrosilylation of Cyclic Imines: Synthesis of Chiral 2-Aryl-Substituted Pyrrolidines as Pharmaceutical Building Blocks, *Adv. Synth. Catal.*, **2021**, 363, 1317–1321.

(16) H.-U. Blaser, H.-P. Buser, H.-P. Jalett, B. Pugin, F. Spindler, Iridium Ferrocenyl Diphosphine Catalyzed Enantioselective Reductive Alkylation of a Hindered Aniline, *Synlett*, **1999**, 867–868.

(17) H.-U. Blaser, The Chiral Switch of (*S*)-Metolachlor: A Personal Account of an Industrial Odyssey in Asymmetric Catalysis, *Adv. Synth. Catal.*, **2002**, 344, 17–31.

(18) Y. Chi, Y.-G. Zhou, X. Zhang, Highly Enantioselective Reductive Amination of Simple Aryl Ketones Catalyzed by Ir−f-Binaphane in the Presence of Titanium(IV) Isopropoxide and Iodine, *J. Org. Chem.*, **2003**, 68, 4120–4122.

(19) D. Chen, Y. Wang, J. Klankermayer, Enantioselective Hydrogenation with Chiral Frustrated Lewis Pairs, *Angew. Chem. Int. Ed.*, **2010**, 49, 9475–9478.

(20) R. I. Storer, D. E. Carrera, Y. Ni, D. W. C. MacMillan, Enantioselective Organocatalytic Reductive Amination, *J. Am. Chem. Soc.*, **2006**, 128, 84–86.

(21) T. Lundrigan, E. N. Welsh, T. Hynes, C.-H. Tien, M. R. Adams, K. R. Roy, K. N. Robertson, A. W. H. Speed, Enantioselective Imine Reduction Catalyzed by Phosphenium Ions, *J. Am. Chem. Soc.*, **2019**, 141, 14083−14088.

(22) D. Uraguchi, S. Sakaki, T. Ooi, Chiral Tetraaminophosphonium Salt-Mediated Asymmetric Direct Henry Reaction, *J. Am. Chem. Soc.*, **2007**, 129, 12392–12393.

(23) T. Nitabaru, A. Nojiri, M. Kobayashi, N. Kumagai, M. Shibasaki, anti-Selective Catalytic Asymmetric Nitroaldol Reaction via a Heterobimetallic Heterogeneous Catalyst, *J. Am. Chem. Soc.*, **2009**, 131, 13860–13869.

(24) T. Karasawa, R. Oriez, N. Kumagai, M. Shibasaki, anti-Selective Catalytic Asymmetric Nitroaldol Reaction of α-Keto Esters: Intriguing Solvent Effect, Flow Reaction, and Synthesis of Active Pharmaceutical Ingredients, *J. Am. Chem. Soc.*, **2018**, 140, 12290−12295.

(25) C. R. Jones, G. Dan Pantoş, A. J. Morrison, M. D. Smith, Plagiarizing Proteins: Enhancing Efficiency in Asymmetric Hydrogen-Bonding Catalysis through Positive Cooperativity, *Angew. Chem. Int. Ed.*, **2009**, 48, 7391–7394.

(26) M. Terada, Binaphthol-derived phosphoric acid as a versatile catalyst for enantioselective carbon–

carbon bond forming reactions, *Chem. Commun.*, **2008**, 4097–4112.
(27) J. W. Yang, M. Stadler, B. List, Proline-Catalyzed Mannich Reaction of Aldehydes with N-Boc-Imines, *Angew. Chem. Int. Ed.*, **2007**, 46, 609–611.
(28) A. Moran, A. Hamilton, C. Bo, P. Melchiorre, A Mechanistic Rationale for the 9-Amino(9-deoxy)epi Cinchona Alkaloids Catalyzed Asymmetric Reactions via Iminium Ion Activation of Enones, *J. Am. Chem. Soc.*, **2013**, 135, 9091−9098.
(29) M.M. Heravi, V. Zadsirjan, Recent advances in the application of the Oppolzer camphorsultam as a chiral auxiliary, *Tetrahedron: Asymmetry*, **2014**, 25, 1061–1090.
(30) F. Scharinger, Á. M. Pálvölgyi, V. Zeindlhofer, M. Schnürch, C. Schröder, K. Bica-Schröder, Counterion Enhanced Organocatalysis: A Novel Approach for the Asymmetric Transfer Hydrogenation of Enones, *ChemCatChem*, **2020**, 12, 3776–3782.
(31) H. Yan, J. S. Oh, J.-W. Lee, C. E. Song, Scalable organocatalytic asymmetric Strecker reactions catalysed by a chiral cyanide generator, *Nat. Commun.*, **2012**, 3, 1212.
(32) T. Ooi, Y. Uematsu, K. Maruoka, Asymmetric Strecker Reaction of Aldimines Using Aqueous Potassium Cyanide by Phase-Transfer Catalysis of Chiral Quaternary Ammonium Salts with a Tetranaphthyl Backbone, *J. Am. Chem. Soc.*, **2006**, 128, 2548–2549.
(33) M. Kitamura, S. Shirakawa, K. Maruoka, Powerful Chiral Phase-Transfer Catalysts for the Asymmetric Synthesis of α-Alkyl- and α,α-Dialkyl-α-amino Acids, *Angew. Chem. Int. Ed.*, **2005**, 44, 1549–1551.
(34) S. Simić, E. Zukić, L. Schmermund, K. Faber, C. K. Winkler, W. Kroutil, Shortening Synthetic Routes to Small Molecule Active Pharmaceutical Ingredients Employing Biocatalytic Methods, *Chem. Rev.*, **2022**, 122, 1052−1126.
(35) C. A. Martinez, S. Hu, Y. Dumond, J. Tao, P. Kelleher, L. Tully, Development of a Chemoenzymatic Manufacturing Process for Pregabalin, *Org. Process Res. Dev.*, **2008**, 12, 3, 392–398.
(36) Q. Zhang, Z.-M. Wu, S. Liu, X.-L. Tang, R.-C. Zheng, Y.-G. Zheng, Efficient Chemoenzymatic Synthesis of Optically Active Pregabalin from Racemic Isobutylsuccinonitrile, *Org. Process Res. Dev.*, **2019**, 23, 2042–2049.
(37) C. K. Savile, J. M. Janey, E. C. Mundorff, J. C. Moore, S. Tam, W. R. Jarvis, J. C. Colbeck, A. Krebber, F. J. Fleitz, J. Brands, P. N. Devine, G. W. Huisman, G. J. Hughes, Biocatalytic Asymmetric Synthesis of Chiral Amines from Ketones Applied to Sitagliptin Manufacture, *Science*, **2010**, 329, 305–309.
(38) A. Iwasaki, Y. Yamada, N. Kizaki, Y. Ikenaka, J. Hasegawa, Microbial synthesis of chiral amines by (*R*)-specific transamination with *Arthrobacter* sp. KNK168, *Appl. Microbiol. Biotechnol.*, **2006**, 69, 499–505.
(39) C. Saville, E. Mundorff, J. C. Moore, P. N. Devine, J. M. Janey, Transaminase biocatalysts, US

20100285541A1, Nov. 11, 2010.
(40) K. Mitsukura, M. Suzuki, S. Shinoda, T. Kuramoto, T. Yoshida, T. Nagasawa, Purification and Characterization of a Novel (*R*)-Imine Reductase from *Streptomyces* sp. GF3587, *Biosci. Biotechnol. Biochem.*, **2011**, 75, 1778–1782.
(41) K. Mitsukura, T. Kuramoto, T. Yoshida, N. Kimoto, H. Yamamoto, T. Nagasawa, A NADPH-dependent (*S*)-imine reductase (SIR) from *Streptomyces* sp. GF3546 for asymmetric synthesis of optically active amines: purification, characterization, gene cloning, and expression, *Appl. Microbiol. Biotechnol.*, **2013**, 97, 8079–8086.
(42) M. Schober, C. MacDermaid, A. A. Ollis, S. Chang, D. Khan, J. Hosford, J. Latham, L. A. F. Ihnken, M. J. B. Brown, D. Fuerst, M. J. Sanganee, G.-D. Roiban, Chiral synthesis of LSD1 inhibitor GSK2879552 enabled by directed evolution of an imine reductase, *Nat. Catal.*, **2019**, 2, 909–915.
(43) R. Kumar, M. J. Karmilowicz, D. Burke, M. P. Burns, L. A. Clark, C. G. Connor, E. Cordi, N. M. Do, K. M. Doyle, S. Hoagland, C. A. Lewis, D. Mangan, C. A. Martinez, E. L. McInturff, K. Meldrum, R. Pearson, J. Steflik, A. Rane, J. Weaver, Biocatalytic reductive amination from discovery to commercial manufacturing applied to abrocitinib JAK1 inhibitor, *Nat. Catal.*, **2021**, 4, 775–782.
(44) M. A. Huffman, A. Fryszkowska, O. Alvizo, M. Borra-Garske, K. R. Campos, K. A. Canada, P. N. Devine, D. Duan, J. H. Forstater, S. T. Grosser, H. M. Halsey, G. J. Hughes, J. Jo, L. A. Joyce, J. N. Kolev, J. Liang, K. M. Maloney, B. F. Mann, N. M. Marshall, M. McLaughlin, J. C. Moore, G. S. Murphy, C. C. Nawrat, J. Nazor, S. Novick, N. R. Patel, A. Rodriguez-Granillo, S. A. Robaire, E. C. Sherer, M. D. Truppo, A. M. Whittaker, D. Verma, L. Xiao, Y. Xu, H. Yang, Design of an in vitro biocatalytic cascade for the manufacture of islatravir, *Science*, **2019**, 366, 1255–1259.
(45) T. Benkovics, J. McIntosh, S. Silverman, J. Kong, P. Maligres, T. Itoh, H. Yang, M. Huffman, D. Verma, W. Pan, H.-I. Ho, J. Vroom, A. Knight, J. Hurtak, W. Morris, N. Strotman, G. Murphy, K. Maloney, P. Fier, Evolving to an Ideal Synthesis of Molnupiravir, an Investigational Treatment for COVID-19, *ChemRxiv*, Dec. 23, **2020**, Version 1.
(46) J. A. McIntosh, Z. Liu, B. M. Andresen, N. S. Marzijarani, J. C. Moore, N. M. Marshall, M. Borra-Garske, J. V. Obligacion, P. S. Fier, F. Peng, J. H. Forstater, M. S. Winston, C. An, W. Chang, J. Lim, M. A. Huffman, S. P. Miller, F.-R. Tsay, M. D. Altman, C. A. Lesburg, D. Steinhuebel, B. W. Trotter, J. N. Cumming, A. Northrup, X. Bu, B. F. Mann, M. Biba, K. Hiraga, G. S. Murphy, J. N. Kolev, A. Makarewicz, W. Pan, I. Farasat, R. S. Bade, K. Stone, D. Duan, O. Alvizo, D. Adpressa, E. Guetschow, E. Hoyt, E. L. Regalado, S. Castro, N. Rivera, J. P. Smith, F. Wang, A. Crespo, D. Verma, S. Axnanda, Z. E. X. Dance, P. N. Devine, D. Tschaen, K. A. Canada, P. G. Bulger, B. D. Sherry, M. D. Truppo, R. T. Ruck, L.-C. Campeau, D. J. Bennett, G. R. Humphrey, K. R. Campos, M. L. Maddess, A kinase-cGAS cascade to synthesize a therapeutic STING activator, *Nature*, **2022**, 603, 439–444.
(47) R. N. Patel, V. Nanduri, D. Brzozowski, C. McNamee, A. Banerjee, Enantioselective Enzymatic Cleavage of *N*-Benzyloxycarbonyl Groups, *Adv. Synth. Catal.*, **2003**, 345, 830–834.

(48) F. H. Wilson, R. S. Herbst, Larotrectinib in *NTRK*-Rearranged Solid Tumors, *Biochemistry*, **2019**, 58, 1555−1557.
(49) U. Grädler, D. Schwarz, M. Blaesse, B. Leuthner, T. L. Johnson, F. Bernard, X. Jiang, A. Marx, M. Gilardone, H. Lemoine, D. Roche, C. Jorand-Lebrun, Discovery of novel Cyclophilin D inhibitors starting from three dimensional fragments with millimolar potencies, *Bioorganic Med. Chem. Lett.*, **2019**, 29, 126717.
(50) M. Moustakim, T. Christott, O. P. Monteiro, J. Bennett, C. Giroud, J. Ward, C. M. Rogers, P. Smith, I. Panagakou, L. Díaz-Sáez, S. L. Felce, V. Gamble, C. Gileadi, N. Halidi, D. Heidenreich, A. Chaikuad, S. Knapp, K. V. M. Huber, G. Farnie, J. Heer, N. Manevski, G. Poda, R. Al-awar, D. J. Dixon, P. E. Brennan, O. Fedorov, Discovery of an MLLT1/3 YEATS Domain Chemical Probe, *Angew. Chem. Int. Ed.*, **2018**, 57, 16302.
(51) H. Zhang, G. Lin, Microbial proteasomes as drug targets, *PLoS Pathog.*, **2021**, 17, e1010058.

Chapter 2
Enzymatic kinetic resolution of cyclic amines

2.1. Introduction

Chiral cyclic amines, which comprise piperidine, piperazine, or pyrrolidine skeleton, are widely used as building blocks of pharmaceuticals and pesticides.[1–9] Among them, 2-methylpiperidine (2-MPI) is used for the synthesis of piperocaine, piperalin, menabitan, SS220 (**Figure 1**),[6–9] and promising candidates for developing pharmaceuticals.[3–5] In the synthesis of SS220, (*S*)-2-MPI moiety makes it effective or more effective than the most widely used insect repellent, *N*,*N*-diethyl-*m*-toluamide (DEET).[10–12] The enzymatic synthesis of optically active cyclic amines has been successfully done via asymmetric reduction using imine reductases;[13–16] however, the method requires the synthesis of cyclic imines as substrates. Kinetic resolution is another approach for preparing chiral compounds, in which the racemates are used as substrates. Since racemic cyclic amines can be commercially available as inexpensive raw materials, in this study, I focused on stereoselective hydrolases for 2-MPI production.

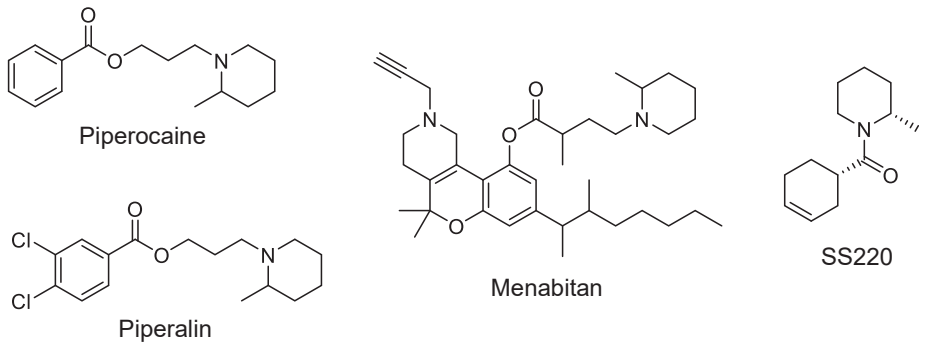

Figure 1. Biologically active compounds containing 2-MPI moiety.

Optically active amines can be prepared from racemic amine by diastereomeric salt formation using chiral carboxylic acids[17] or by stereoselective bioconversion of racemic *N*-acyl amine using enzymes.[18–20] Several studies on chiral cyclic amines' preparation via chemical or enzymatic resolution have been reported.[21–33] In the enzymatic method, racemic piperidines are stereoselectively acylated or hydrolyzed by a lipase or protease to obtain the desired enantiomer.[21–24] Conversely, the racemates are chemically resolved by chiral acylating reagents to provide enantioenriched amines (**Scheme 1**).[25–27] Other chemical resolutions have been reported;[28–30] however, these chemical processes require chiral reagents for kinetic resolution. Considering the need of chiral compounds that

are also synthesized from chiral precursors, the discovery of highly stereoselective hydrolase is desired for chiral cyclic amines' preparation. Until now, the existing hydrolases described above have been used to synthesize chiral secondary amines; however, their variation was limited. Other enzymatic processes need cyclic amines with functional groups, such as 2-hydroxymethylpiperidine, to yield products with low enantioselectivity in many cases due to the low chirality-recognition ability of enzyme.[31–33] Interestingly, there is no kinetic resolution to directly obtain chiral 2-substituted piperidines from *N*-acyl derivatives of them by enzymatic hydrolysis. Given these backgrounds, it is necessary to improve the enantioselectivity of existing hydrolases or find a novel hydrolase.

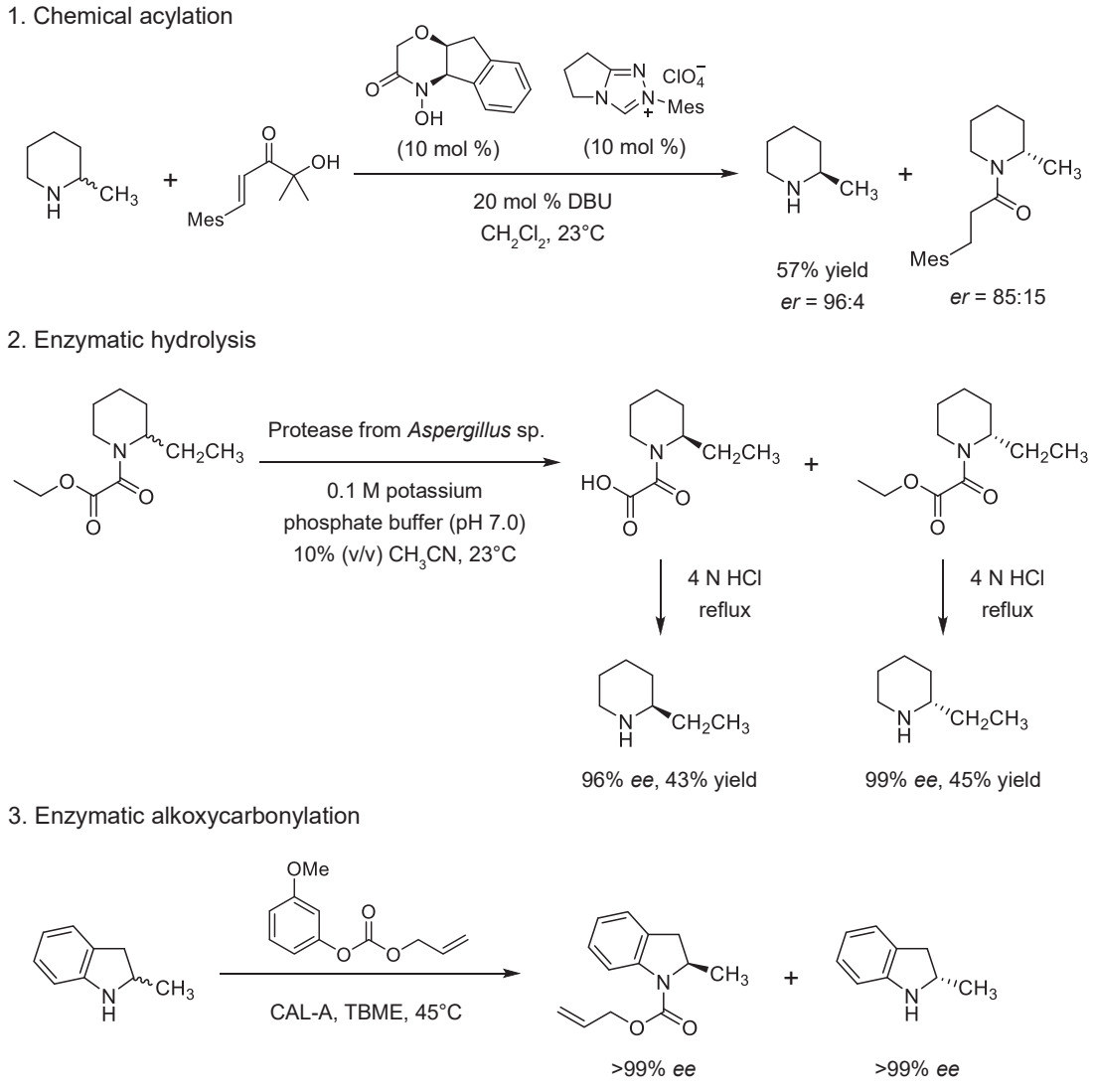

Scheme 1. Examples of reported processes for preparation of chiral cyclic amine.

In this study, a stereoselective hydrolase acting on *rac*-*N*-acyl-2-MPI was screened from soil microorganisms for one-step preparation of chiral 2-MPI (**Scheme 2**). Then the hydrolase was purified

for characterization. To ensure efficient chiral piperidine preparation, I constructed recombinant cells expressing the hydrolase gene and investigated the optically pure 2-MPI production via whole-cell reaction.

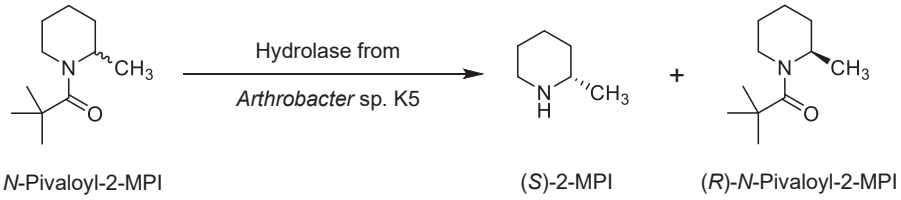

Scheme 2. Stereoselective hydrolysis of *N*-pivaloyl-2-MPI by *Arthrobacter* sp. K5 hydrolase.

2.2 Results and Discussion

2.2.1. Screening of microorganisms

To obtain microorganisms exhibiting hydrolase activity toward *N*-acyl-2-MPI, 294 strains were isolated from soil samples using a medium containing *N*-acetyl-2-MPI as the sole carbon source. Among 60 bacteria that hydrolyzed *N*-acetyl-2-MPI, the majority of them did not display high stereoselectivity. Only the strain K5 revealed moderate (*S*)-selectivity kinetically, yielding racemic 2-MPI (Figure 2a). It was predicted that the acyl group affected the enantiomeric recognition of the hydrolase in strain K5. To improve the enantioselectivity of the hydrolysis, the acetyl group of *N*-acetyl-2-MPI was substituted with a bulky pivaloyl group for appropriate chiral recognition. The reaction using whole cells of strain K5 exhibited good (*S*)-stereoselectivity toward *N*-pivaloyl-2-MPI to yield (*S*)-2-MPI with 88% *ee* in 72 h (Figure 2b). The strain K5 was identified as *Arthrobacter* sp. based on 16S rDNA sequence analysis.

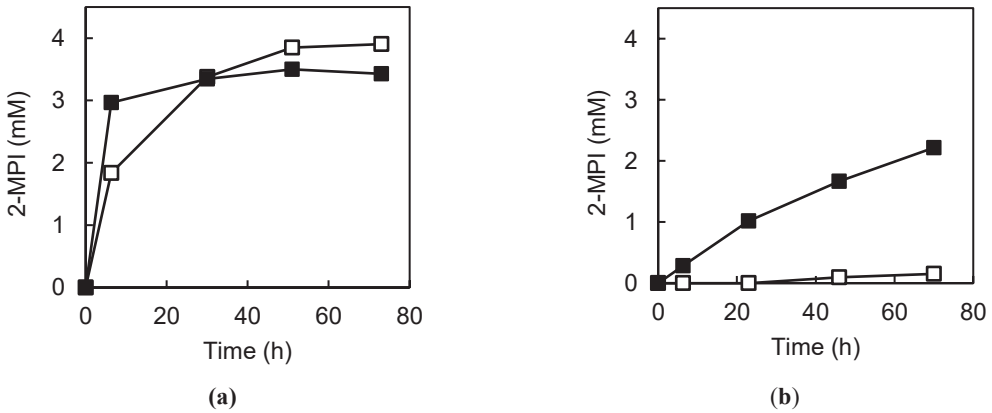

Figure 2. Hydrolysis of *N*-acetyl-2-MPI (**a**) and *N*-pivaloyl-2-MPI (**b**) using *Arthrobacter* sp. K5 cells. Closed squares; (*S*)-2-MPI, open squares; (*R*)-2-MPI. The reactions were performed at 30°C in 2 mL of 100 mM potassium phosphate buffer (pH 7.0) containing 10 mM *N*-acyl-2-MPI and whole cells derived from 4 mL culture broth.

2.2.2. Optimization of culture conditions and kinetic resolution using optimized whole cells

To enhance the hydrolase activity in *Arthrobacter* sp. K5 cells, cyclic amine derivatives were added to the culture medium, and the hydrolase activity was examined. The addition of *N*-acetyl-2-MPI, *N*-acetylpiperidine, or *N*-acetyl-2-methylpyrrolidine resulted in a high induction of the hydrolase activity, with the best compound being *N*-acetylpiperidine, which also enhanced *Arthrobacter* sp. K5 growth (Table S1). The highest activity was found in the cells cultivated for 1 day with 0.4% (v/v) *N*-acetylpiperidine (Table S2, S3). Prolonged cultivation (≥2 days) decreased enzyme activity. The culture conditions were optimized as follows: time, 24 h; culture medium, 0.4% (v/v) *N*-acetylpiperidine, 5 g L^{-1} polypeptone, 5 g L^{-1} meat extract, 2 g L^{-1} NaCl, and 0.5 g L^{-1} yeast extract in tap water (pH 7). Using the cells cultivated under optimal conditions, the kinetic resolution of *N*-pivaloyl-2-MPI was performed. In the reaction with 100 mM concentration of *N*-pivaloyl-2-MPI, 38.2 mM (*S*)-2-MPI was formed at 80.2% *ee* after 115 h. However, the whole cells reaction stopped after 75 h, not achieving 50% conversion of the substrate.

2.2.3. Properties of the hydrolase

To obtain a homogeneous enzyme, the hydrolase was purified from the cell-free extract of *Arthrobacter* sp. K5 through 5 steps, including ammonium sulfate fractionation, ion-exchange chromatography on DEAE-Sephacel, and hydrophobic interaction chromatography on phenyl-Sepharose and butyl-Toyopearl (Table S4). The purified enzyme was obtained with a specific activity of 35.5 μmol min^{-1} mg^{-1}. The overall purification was 10.8-fold (yield = 22%). The molecular mass of the hydrolase was estimated to be 50 kDa by SDS-PAGE and 238 kDa by gel permeation high performance liquid chromatography (HPLC), which suggests it to be a homo-tetrameric hydrolase. The optimum reaction temperature and pH of the hydrolase were 45°C and pH 8.0 (Tris-HCl), respectively (Figure S3, S4). The enzyme retained 75% of its maximum activity <40°C; however, its activity decreased at a temperature >45°C (Figure S5). Conversely, it retained 80% of its maximum activity at pH 6.0–7.5 and more than 80% inhibition of the hydrolase activity was observed at other pH values (Figure S6). According to amino acid sequence analysis, the N-terminal and internal amino acid sequences of the hydrolase were obtained as ATQTVITNGTLIDGTGNQPQ and GGVTTVFDTWNA, respectively. Based on the amino acid sequence and genome DNA sequence of *Arthrobacter* sp. K5, I identified (*S*)-selective hydrolase (SHA). The enzyme gene was composed of 1,384 bp, and coded for a protein of 481 amino acids with a molecular mass of 49,725 Da. This value is in agreement with molecular mass determined on SDS-PAGE. A BLAST search with full-length amino acid sequence of SHA revealed moderate sequence identity with the amidohydrolase protein family, including phenylurea hydrolases (<66%), and the highest sequence identity (67%) with the molinate hydrolase from *Gulosibacter molinativorax*. These results suggest SHA as a novel enzyme.

2.2.4. Substrate specificity

The substrate specificity of purified SHA was examined using various *N*-acyl cyclic amines and comparing the activity toward them with the activity toward *N*-benzoyl-2-MPI (Table 1). The hydrolase exhibited almost the same activity toward *N*-benzoyl-2-MPI and *N*-pivaloyl-2-MPI; however, the latter was more hydrolyzed with higher (*S*)-selectivity. *N*-Acetyl-2-MPI was hydrolyzed with 24.8-fold higher activity than *N*-benzoyl-2-MPI. SHA displayed high activity on *N*-acyl 2-unsubstituted cyclic amines, such as *N*-benzoylpiperidine, *N*-benzoyl-3-MPI, *N*-pivaloyl-3-MPI, *N*-benzoyl-4-MPI, and *N*-benzoylpyrrolidine but showed no stereoselectivity toward *N*-acyl-3-MPI. *N*-benzoyl-2-methylpyrrolidine displayed 4-fold higher reactivity than *N*-benzoyl-2-MPI, whereas enantioselectivity was low in slight favor of the (*R*)-enantiomer (11% *ee*). *N*-benzoyl-2-methylindoline was also a preferable substrate, reacting with medium enantioselectively (*S*- or *R*-enantiomers not determined); however, *N*-pivaloyl-2-methylindoline and *N*-benzoyl-1,2,3,4-tetrahydroquinaldine were not hydrolyzed. The reactivity and stereoselectivity of SHA for tested compounds depended on the acyl groups and the distance between the acyl group and chiral center. SHA exhibited no activity toward *N*-acetyl D- or L-amino acid (data not shown).

Table 1. Substrate specificity of SHA. [1]

Substrate	Relative activity (%)	Conv. (%) and *ee* values (%)	
N-Benzoyl-2-MPI	100 (0.123 U mg^{-1})	21 (48 h) [4]	63 (*S*)
N-Pivaloyl-2-MPI	102	31 (48 h) [4]	88 (*S*)
N-Acetyl-2-MPI	2480	46 (2 h) [4]	43 (*S*)
N-Crotonoyl-2-MPI	1210	56 (4 h) [4]	55 (*S*)
N-Benzoylpiperidine	81200	n.d. [3]	n.d.
N-Benzoyl-3-MPI	7640	50 (2 h) [4]	0
N-Pivaloyl-3-MPI	3120	42 (24 h) [4]	0
N-Benzoyl-4-MPI	9320	n.d.	n.d.
N-Benzoylpyrrolidine	1280	n.d.	n.d.
N-Benzoyl-2-methylpyrrolidine	409	49 (24 h) [4]	11 (*R*)
N-Benzoyl-2-methylindoline [2]	40	53 (48 h) [4]	50 (n.d.[3])
N-Acetyl-2-methylindoline [2]	101	56 (3 h) [4]	45 (n.d.)
N-Pivaloyl-2-methylindoline [2]	0	n.d.	n.d.
N-Acetyl-1,2,3,4-tetrahydroquinaldine [2]	trace	n.d.	n.d.
N-Benzoyl-1,2,3,4-tetrahydroquinaldine [2]	0	n.d.	n.d.

[1] The reaction was performed at 30°C in 100 mM potassium phosphate buffer (pH 7.0) containing 10 mM substrate and 0.0158 mg mL^{-1} purified enzyme.
[2] 1 mM Substrate instead of 10 mM was added to the reaction with 5% (v/v) acetonitrile.
[3] n.d. = not determined.
[4] Reaction time in bracket.

2.2.5. (*S*)-2-MPI synthesis using recombinant cells

Since SHA gene sequence has GC-content, I overexpressed the gene in *Rhodococcus erythropolis* L88, which are high GC-content bacteria that can express high GC-content genes.[34] *Rhodococcus* sp. has robust cells which show resistance to various stress conditions, expecting tolerance to organic solvent, high concentration of substrates, and long-time reaction.[35] The reaction with 100 mM *N*-pivaloyl-2-MPI using the recombinant cells produced 48.4 mM (*S*)-2-MPI with 83.5% *ee* in 74 h (Figure 3, closed circles). Compared with the reaction using *Arthrobacter* sp. K5 cells that almost stopped after 60 h with the conversion level of <40% (Figure 3, closed triangles), *R. erythropolis* transformant retained the hydrolase activity and the reaction proceeded to 50% conversion after 72 h. The 2-MPI productivity is comparable with that of the enzymatic process using oxalamic ester. Moreover, the kinetic resolution by SHA achieved one-step preparation of (*S*)-2-MPI requiring only inexpensive reagents. However, optical purity of 2-MPI was decreased due to gradual hydrolysis of the (*R*)-enantiomer. For the kinetic resolution of chiral 2-MPI production, it is essential to improve the stereoselectivity of SHA toward *N*-pivaloyl-2-MPI using protein engineering.

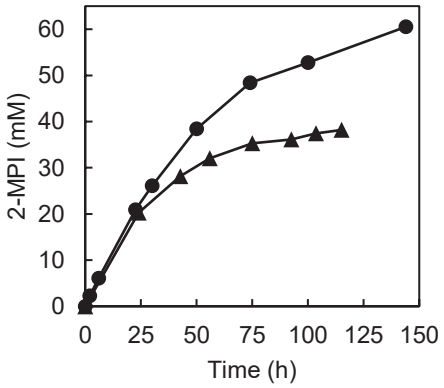

Figure 3. Synthesis of (*S*)-2-MPI from *N*-pivaloyl-2-MPI by *Arthrobacter* sp. K5 cells (closed triangles) or recombinant cells (closed circles). The reactions were performed at 30°C in 100 mM potassium phosphate buffer (pH 7.0) containing 100 mM *N*-pivaloyl-2-MPI and whole cells derived from the culture broth equivalent to 5-fold amount of reaction volume.

2.3. Conclusions

SHA exhibited high (*S*)-selectivity toward *N*-pivaloyl-2-MPI to produce (*S*)-2-MPI with 80.2% *ee*. I successfully overexpressed SHA gene in *R. erythropolis* L88 and improved the hydrolase activity. The biocatalytic process achieved a kinetic resolution of 100 mM *N*-pivaloyl-2-MPI to 48.4 mM (*S*)-2-MPI with 83.5% *ee* in one step using only inexpensive materials. As a potential enzyme for practical applications, SHA may allow highly enantioenriched (*S*)-MPI production by improving its stereoselectivity in the future.

2.4. Materials and Methods

2.4.1 General information

Commercially available reagents were used without purification and purchased from Tokyo Chemical Industry Co. Ltd. (Tokyo, Japan), FUJIFILM Wako Pure Chemical Corporation (Osaka, Japan) and Sigma-Aldrich (Darmstadt, Germany) unless stated otherwise. The following products from each supplier were used: polypeptone (Nippon Seiyaku, Tokyo, Japan), meat extract (Kyokuto Seiyaku, Tokyo, Japan), and yeast extract (Oriental Yeast, Tokyo, Japan). Thin-layer chromatography (TLC) was performed on TLC silica gel $60F_{254}$ (Merck KGaA, Darmstadt, Germany). Column chromatography was performed on Wakosil® 60 (FUJIFILMWako Pure Chemical Corporation, spherical, 64–210 μm). HPLC analyses were performed using LC-10AT pump, SPD-10A detector (Shimadzu, Kyoto, Japan), Atlantis dC18 5μm 4.6 × 150 mm column (Waters, Massachusetts, USA), CHIRALPAK AD-H 4.6 × 250 mm column (Daicel, Osaka, Japan), and TSK-GEL G-3000SW column (7.5 × 600 mm; Tosoh, Tokyo, Japan). The conversion rate and optical purity were determined by HPLC after derivatization of amines with 2,3,4,6-tetra-*O*-acetyl-β-D-glucopyranosyl isothiocyanate (GITC) at 40°C for 1 h. The *E* value was calculated using Chen's equation.[36] ^{1}H and ^{13}C NMR spectra were recorded on a JEOL ECA600 spectrometer (600 MHz for ^{1}H and 150 MHz for ^{13}C) in $CDCl_3$ or CD_3OD using tetramethylsilane as an internal standard (δ = 0 ppm). Polymerase chain reaction (PCR), restriction enzyme digestion, and DNA ligation were performed using TaKaRa PCR Thermal Cycler Dice® mini (Takara Bio, Shiga, Japan).

2.4.2 Synthesis of *N*-pivaloyl-2-MPI

A solution of pivaloyl chloride (13 mL, 107 mmol) in acetonitrile (10 mL) was added to a solution of 2-methylpiperidine (12 mL, 102 mmol) and triethylamine (14.2 mL, 102 mmol) in acetonitrile (60 mL) at 0°C with stirring. The reaction mixture was warmed to room temperature and stirred overnight. The reaction mixture was filtered to remove triethylamine hydrochloride and the resulting supernatant was concentrated under reduced pressure with a rotary evaporator (EYELA, Tokyo, Japan). The residue was purified by column chromatography (silica gel, *n*-hexane:ethyl acetate = 6:1) to yield *N*-pivaloyl-2-methylpiperidine (17.06 g, 91%) as a colorless oil. ^{1}H NMR configurations are as follows: $CDCl_3$ (600 MHz), δ (ppm) 1.19, (3H, brs), 1.27 (9H, s), 1.36–1.43 (1H, m), 1.51–1.53 (1H, m), 1.59–1.71 (4H, m), 2.93 (1H, brs), 4.18 (1H, brs), and 4.73 (1H, brs). ^{13}C NMR configurations are as follows: $CDCl_3$ (150 MHz), δ (ppm) 15.84, 18.88, 26.06, 27.11, 27.89, 28.43, 30.11, 38.83, and 176.12.

2.4.3 Synthesis of *N*-acyl cyclic amines

Acyl chloride (50 mmol) was added to a solution of cyclic amine (50 mmol) and pyridine (50 mmol) in dichloromethane (200 mL) at 0°C. The reaction was performed overnight at room temperature with stirring. The reaction mixture was concentrated under reduced pressure. Ethyl acetate was added to

the residue, and pyridine hydrochloride was removed by filtration. The supernatant was concentrated under reduced pressure and purified by column chromatography (silica gel, *n*-hexane:ethyl acetate = 6:1) to obtain *N*-acyl cyclic amines in moderate to good yield.

2.4.4 Screening of microorganisms degrading *N*-acetyl-2-MPI

Soil samples were collected from various area of Japan. A few grams of the soil sample was put in 5 mL of medium containing 1.88 g L^{-1} *N*-acetyl-2-MPI, 1 g L^{-1} NH_4Cl, 5 g L^{-1} Na_2HPO_4, 2 g L^{-1} KH_2PO_4, 0.5 g L^{-1} $MgSO_4 \cdot 7H_2O$, 1% (v/v) metal solution and 1% (v/v) vitamin mixture in tap water, pH 7. Metal solution consists of 0.3 g L^{-1} H_3BO_3, 0.4 g L^{-1} $CaCl_2 \cdot 2H_2O$, 0.2 g L^{-1} $FeSO_4 \cdot 7H_2O$, 0.1 g L^{-1} KI, 0.4 g L^{-1} $MnCl_2 \cdot 4H_2O$, 0.04 g L^{-1} $CuSO_4 \cdot 5H_2O$, 0.22 g L^{-1} $Na_2MoO_4 \cdot 2H_2O$ and 1% (v/v) HCl (6 M) in distilled water. Vitamin mixture consists of 100 mg L^{-1} biotin, 20 mg L^{-1} pantothenate・Ca, 100 mg L^{-1} inositol, 20 mg L^{-1} nicotinic acid, 20 mg L^{-1} pyridoxine・HCl, 10 mg L^{-1} 4-aminobenzoic acid, 10 mg L^{-1} riboflavin and 0.5 mg L^{-1} folic acid in distilled water. Cultivation was aerobically carried out at 28°C with shaking (120 rpm). After 7–10 days, 0.1 mL of culture broth was inoculated into new medium and cultivated at the same conditions. This process was repeated once more. The final culture broth was spread onto 2% (w/v) agar plates of the above medium. The colonies isolated on the agar plates were cultivated in 5 mL medium with 0.2% (w/v) yeast extract at 28°C for 2–6 days. Cells were harvested by centrifugation and washed with 0.85% (w/v) NaCl. The reaction mixture (2 mL) was consisted of 10 mM *N*-acetyl-2-MPI, 100 mM potassium phosphate buffer (pH 7.0), and cells derived from 5 mL culture broth. The mixture was incubated at 30°C for 24 h with shaking (120 rpm). The reaction was quenched by centrifugation for removal of cells and the resulting supernatants were analyzed by TLC and HPLC. Microorganisms exhibiting hydrolase activity for *rac*-*N*-acetyl-2-methylpiperidine were evaluated and the strains with high stereoselectivity for other *N*-acyl-2-MPI was selected. Among the microorganisms, strain K5 with the highest stereoselectivity was identified by Techno-Suruga Laboratory Co. Ltd. based on 16S rDNA gene analysis.

2.4.5 Optimization of culture conditions for *Arthrobacter* sp. K5

To optimize the culture medium, the following compounds were added to nutrient medium containing 5 g L^{-1} polypepton, 5 g L^{-1} meat extract, 2 g L^{-1} NaCl, 0.5 g L^{-1} yeast extract in tap water (pH 7, adjusted by 6M NaOH): *N*-acetyl-2-MPI, *N*-acetyl-2-methylpyrrolidine, *N*-acetylpiperidine, *N*-acetylpyrrolidine, *N,N'*-diacetyl-2-methylpiperazine, acetanilide, *N*-acetylaspartic acid, 2-MPI, benzamide and nicotinamide.

2.4.6 Cultivation of *Arthrobacter* sp. K5

Arthrobacter sp. K5 was cultivated at 28°C for 24 h in 5 mL nutrient medium containing 5 g L^{-1} polypepton, 5 g L^{-1} meat extract, 2 g L^{-1} NaCl, 0.5 g L^{-1} yeast extract in tap water (pH 7). Cultivation

was performed at 28°C and 120 rpm for 24 h in 40 mL scale containing nutrient medium with 0.4% (v/v) *N*-acetylpiperidine for the induction of hydrolase activity. Cells were harvested by centrifugation, washed twice with 0.85% (w/v) NaCl, and suspended in the same solution. The cell growth of *Arthrobacter* sp. K5 was estimated turbidimetrically at 610 nm.

2.4.7 Hydrolysis of *N*-pivaloyl-2-MPI using whole cells of *Arthrobacter* sp. K5

The reaction was performed at 30°C with shaking (120 rpm) in 25 mL of 100 mM potassium phosphate buffer (pH 7.0) containing 100 mM *N*-pivaloyl-2-MPI and whole cells derived from 125 mL culture broth. Samples were collected multiple times and analyzed by HPLC after derivatization of samples with GITC.

2.4.8 Preparation of cell-free extract

Cells of *Arthrobacter* sp. K5 were suspended in 100 mM potassium phosphate buffer (pH 7.0) containing 1 mM dithiothreitol and disrupted by ultrasonication at 100 W for 20 min at 4°C using a cell disrupter (19 kHz, Insonator 201 M; Kubota, Japan). The cell debris was removed by centrifugation at 4°C and 8,000 rpm for 30 min and the supernatant solution was used as cell-free extract.

2.4.9 Enzyme assay

Enzymatic reaction was assayed in the reaction mixture containing 10 mM *N*-benzoylpiperidine and 1 μL enzyme solution in 100 mM potassium phosphate buffer (pH 7.0). One unit (U) of hydrolase activity was defined as the amount of enzyme that catalyzed the formation of 1 μmol benzoate at 30°C per min. Enzyme activity was determined with HPLC using *N*-benzoylpiperidine by detecting benzoate released by hydrolysis. HPLC analysis was performed at 254 nm at a flow rate of 1.0 ml min^{-1} using an Atlantis dC18 5μm 4.6×150 mm column (Waters) and 10 mM sodium phosphate buffer (pH 2.8) /acetonitrile (3:2, v/v). Retention time of benzoate was 4 min under the above conditions.

2.4.10 Enzyme purification from *Arthrobacter* sp. K5

All purification steps were conducted at 4°C in 100 mM potassium phosphate buffer (pH 7.0) containing 0.1 mM dithiothreitol.

2.4.10a Ammonium sulfate fractionation

Solid ammonium sulfate was added to the cell-free extract to reach 30% saturation. Proteins precipitated was removed by centrifugation at 4°C and 8,000 rpm for 30 min. To the supernatant, solid ammonium sulfate was added to 60% saturation and resulting precipitate was collected by

centrifugation at 4°C and 8,000 rpm for 30 min. The precipitate was dissolved in 100 mM potassium phosphate buffer (pH 7.0) containing 1 mM dithiothreitol and dialyzed in the same dissolving solution.

2.4.10b DEAE-Sephacel column chromatography

Protein solution obtained by ammonium sulfate fractionation was applied to DEAE-Sephacel resin (GE-healthcare, Tokyo, Japan) equilibrated with 100 mM potassium phosphate buffer (pH 7.0) containing 100 mM potassium chloride. Proteins bound to the resin were eluted with stepwise concentration of 100, 150 and 200 mM potassium chloride in 100 mM potassium phosphate buffer (pH 7.0).

2.4.10c Phenyl-Sepharose column chromatography

Solid ammonium sulfate was added to the protein solution obtained by DEAE-Sephacel column chromatography to reach 20% saturation. This solution was applied to phenyl-Sepharose (GE-healthcare) column chromatography equilibrated with 100 mM potassium phosphate buffer (pH 7.0) containing 20% ammonium sulfate. Proteins bound to the resin were eluted with stepwise concentration of 20 and 15% ammonium sulfate in 100 mM potassium phosphate buffer (pH 7.0).

2.4.10d Butyl-Toyopearl column chromatography

Solid ammonium sulfate was added to the protein solution obtained by phenyl-Toyopearl (Tosoh, Tokyo, Japan) column chromatography to reach 20% saturation. This solution was applied to butyl-Sepharose column chromatography equilibrated with 100 mM potassium phosphate buffer (pH 7.0) containing 20% ammonium sulfate. Proteins bound to the resin were eluted with stepwise concentration of 20, 10, 2.5 and 0% ammonium sulfate in 100 mM potassium phosphate buffer (pH 7.0).

2.4.11 Protein analysis

Protein concentration was determined by the Bradford method, using a protein assay kit (Bio-Rad Laboratories, Inc., California, USA) and bovine serum albumin as a standard.[37] In column chromatography, absorbance at 280 nm was measured to detect eluted protein. SDS-PAGE was performed on 10% polyacrylamide gel with Tris-glycine buffer system according to Laemmli.[38] Protein were stained with Coomassie Brilliant Blue R250 and gels destained in ethanol/acetate/H_2O (3:1:6, v/v/v). Native molecular mass of the enzyme was estimated by gel permeation HPLC on a TSK G-3000SW column (7.5 × 600 mm; Tosoh, Tokyo, Japan) with 100 mM sodium phosphate buffer (pH 7.0) containing 200 mM NaCl as a mobile phase at a flow rate of 0.7 mL min^{-1}. The N-terminal and internal amino acid sequences of purified enzyme were determined by APRO Science Inc.

2.4.12 Effect of temperature and pH on purified enzyme

Optimal temperature of the hydrolase was examined in a 100 mM potassium phosphate buffer (pH 7.0) containing an appropriate amount of the purified enzyme and 10 mM *N*-benzoylpiperidine at temperatures from 15 to 60°C. Optimal pH was examined at 30°C using various 100 mM buffers with different pH values, including sodium citrate (pH 3.0–6.0), potassium phosphate buffer (pH 6.0–8.0), Tris-HCl (pH 7.5–9.0) and glycine-NaOH (pH 9.0–11.0). In all cases, incubation was carried out for 10 min. To determine the thermal stability of the hydrolase, the enzyme solution was pre-incubated at temperatures from 0 to 55°C for 30 min and cooled on ice. For evaluation of pH stability, the enzyme solution was pre-incubated at 30°C for 30 min using the various buffers with different pH values (3.0–11.0). The enzyme solutions incubated at various temperature or pH were used for reaction mixture containing 100 mM potassium phosphate buffer (pH 7.0) and 10 mM *N*-benzoylpiperidine at 30°C.

2.4.13 Substrate specificity of purified enzyme

Substrate specificity was investigated using the following 1 or 10 mM *N*-acyl cyclic amines: *N*-benzoyl-2-MPI, *N*-pivaloyl-2-MPI, *N*-acetyl-2-MPI, *N*-acryloyl-2-MPI, *N*-crotonoyl-2-MPI, *N*-benzoylpiperidine, *N*-benzoyl-3-MPI, *N*-pivaloyl-3-MPI, *N*-benzoyl-4-MPI, *N*-benzoylpyrrolidine, *N*-benzoyl-2-methylpyrrolidine, *N*-benzoyl-2-methylindoline, *N*-acetyl-2-methylindoline, *N*-pivaloyl-2-methylindoline, *N*-acetyl-1,2,3,4-tetrahydroquinaldine, *N*-benzoyl-1,2,3,4-tetrahydroquinaldine, and *N*-acetyl amino acids.

2.4.14 Genome sequence of *Arthrobacter* sp. K5

Arthrobacter sp. K5 cells were lysed at room temperature overnight with 0.5 mg mL^{-1} achromopeptidase (crude) in 10 mM Tris-HCl (pH 8.0). To this solution, 0.02 mg mL^{-1} proteinase K, 10 mM $CaCl_2$, and 0.5% (w/v) SDS were added, and the mixture was incubated overnight at 37°C. To an equal volume of the lysed cells, 2×CTAB solutions was added and incubated at 60°C for 1 h. The 2×CTAB solution contained 20 g L^{-1} cetyltrimethylammonium bromide, 50 mM Tris-HCl, 20 mM EDTA, 111 g L^{-1} NaCl, and 10 g L^{-1} polyvinylpyrrolidone in distilled H_2O. To an equal volume of the treatment solution, a mixture of phenol, chloroform, and isoamyl alcohol (25:24:1, v/v/v) was added, mixed gently, and centrifuged at 4°C and 8,000 rpm for 30 min. The supernatant was washed with chloroform and one-tenth volume of 3 M sodium acetate (pH 5.2) was added and mixed with isopropanol until genome DNA was thoroughly precipitated. The genome DNA obtained was washed twice with 70% (v/v) ethanol and diluted with distilled H_2O. Genome analysis was commissioned to Gifu University NGS service.

2.4.15 Hydrolase overexpression in *Rhodococcus erythropolis* L88

The SHA gene was identified based on the partial amino acid sequence of SHA and genome sequence analysis of *Arthrobacter* sp. K5. The gene sequence was deposited in the DDBJ database under the accession number LC633519. The gene amplification was performed via PCR using the primers 5'-CTATCCATGGCAACGCAGACAGTG-3' and 5'-TAATCTCGAGTCAGACGTTGTCGTCGAGG-3' with PrimeSTAR® Max DNA Polymerase (Takara Bio). The amplified DNA fragments and pTipQC1 vector (Hokkaido System Science, Hokkaido, Japan) were digested with *Nco* I and *Xho* I and ligated using DNA Ligation Kit (Takara Bio). The resulting plasmid was transformed into *Rhodococcus erythropolis* L88 cells (Hokkaido System Science) by electroporation with Eporator® (Eppendorf, Hamburg, Germany). The transformed cells were cultivated with 30 μg mL^{-1} chloramphenicol at 120 rpm and 28°C in 5 mL of the nutrient medium containing 10 g L^{-1} tryptone, 5 g L^{-1} yeast extract, 4 g L^{-1} Na_2HPO_4, 1 g L^{-1} KH_2PO_4, 1 g L^{-1} NaCl, 0.2 g L^{-1} $MgSO_4 \cdot 7H_2O$, and 0.01 g L^{-1} $CaCl_2 \cdot 2H_2O$ in tap water. The preculture was inoculated into 90 mL of the nutrient medium and 0.2 μg ml^{-1} thiostrepton was added and incubated at 20°C and 120 rpm for 24 h. The cells were harvested by centrifugation, washed twice with 0.85% (w/v) NaCl, and suspended in the same solution. This solution was used as whole cells.

2.4.16 (*S*)-2-MPI synthesis using recombinant cells

The reaction was performed at 30°C with shaking (120 rpm) in 2 mL of 100 mM potassium phosphate buffer (pH 7.0) containing 37 mg (100 mM) *N*-pivaloyl-2-MPI and whole cells obtained from 10 mL culture broth. Samples were collected multiple times and analyzed by HPLC after derivatization with GITC.

2.5 Supplementary information

Table S1. Effect of amine compound on *Arthrobacter* sp. K5 growth and hydrolase activity

Compound	**Growth [1] (OD_{610}) [2]**	**(*S*)-2-MPI [3] (mM)**
None	4.30	0.12
N-Acetyl-2-MPI	4.51	1.51
N-Acetyl-2-methylpyrrolidine	4.23	1.25
N-Acetylpiperidine	6.02	1.67
N-Acetylpyrrolidine	5.53	0.71
N,*N'*-Diacetyl-2-methylpiperazine	3.67	0.26
2-MPI	4.48	0.10
Acetanilide	5.47	0.09
Benzamide	0.56	0.18

[1] *Arthrobacter* sp. K5 was cultivated at 28°C and 120 rpm for 2 days with 0.2% (w/v) amine compound.
[2] OD_{610} = optical density at 610 nm.
[3] The reactions were performed at 30°C for 27 h in 2 mL of 100 mM potassium phosphate buffer (pH 7.0) containing 10 mM *N*-pivaloyl-2-MPI and whole cells derived from 4 mL culture broth.

Table S2. Effect of *N*-acetylpiperidine concentration on *Arthrobacter* sp. K5 growth and hydrolase activity

***N*-Acetylpiperidine (%, w/v)**	**Growth [1] (OD_{610})**	**(*S*)-2-MPI [2] (mM)**
0	4.30	0.12
0.05	4.69	1.10
0.1	4.48	1.21
0.2	5.90	1.98
0.3	5.91	1.99
0.4	6.91	2.65
0.5	6.02	1.44

[1] *Arthrobacter* sp. K5 was cultivated at 28°C and 120 rpm for 2 days.
[2] The reactions were performed at the same condition as described in table S1.

Table S3. Effect of culture time on *Arthrobacter* sp. K5 growth and hydrolase activity

Preculture (day)	Culture (day)	Growth [1] (OD_{610})	(*S*)-2-MPI [2] (mM)
1	1	8.24	3.27
1	2	6.16	2.28
2	1	9.91	3.91
2	2	6.65	2.19
2	3	4.13	1.38
3	1	9.95	3.80
3	2	7.01	2.84
3	3	4.24	1.45

[1] *Arthrobacter* sp. K5 was cultivated at 28°C and 120 rpm in 5 mL nutrient medium containing 5 g L^{-1} polypepton, 5 g L^{-1} meat extract, 2 g L^{-1} NaCl, 0.5 g L^{-1} yeast extract in tap water (pH 7), then 5 mL preculture was inoculated into 40 mL the nutrient medium and further cultivated at 28°C.

[2] The reactions were performed at the same condition as described in table S1.

Table S4. Purification of *Arthrobacter* sp. K5 hydrolase.

Purification step	Total protein (mg)	Total activity (U)	Specific activity (U mg^{-1})	Yield (%)	Purification (-fold)
Cell-free extract [1]	3340	11000	3.30	100	1
$(NH_4)_2SO_4$ (30–60%)	1440	5170	3.60	47	1.09
DEAE-Sephacel	364	4980	13.7	45	4.14
Phenyl-Sepharose	133	4110	30.9	37	9.36
Butyl-Toyopearl	68	2420	35.5	22	10.8

[1] The cell-free extract was prepared by disruption of cells obtained from 4.84 L of culture broth.

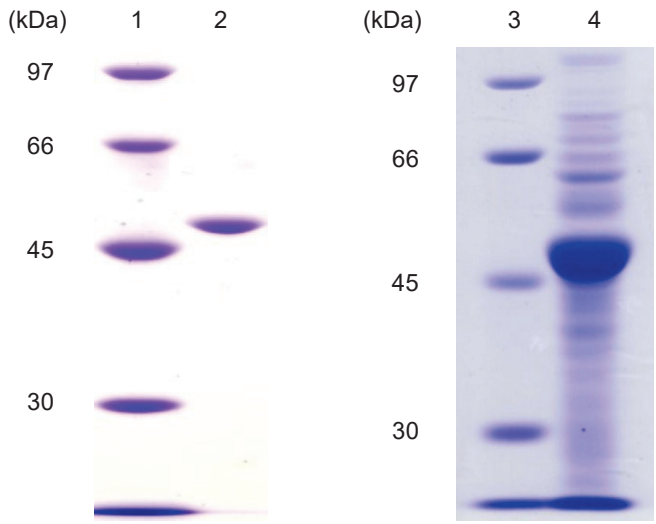

Figure S1. SDS-PAGE analysis of *Arthrobacter* sp. K5 hydrolase. Lanes 1, 3: molecular weight markers, 2: purified hydrolase from *Arthrobacter* sp. K5, 4: cell-free extract of recombinant *R. erythropolis* overexpressing (*S*)-selective hydrolase (SHA) gene.

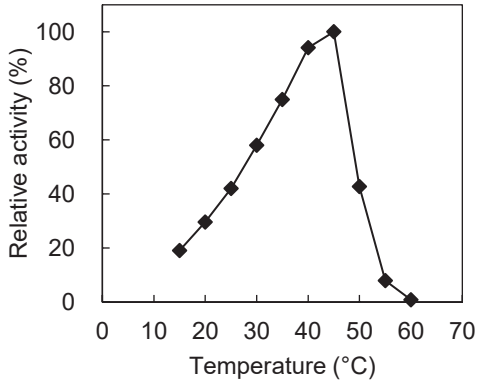

Figure S2. Optimum temperature of the purified hydrolase. 100% = 141 U mg^{-1}.

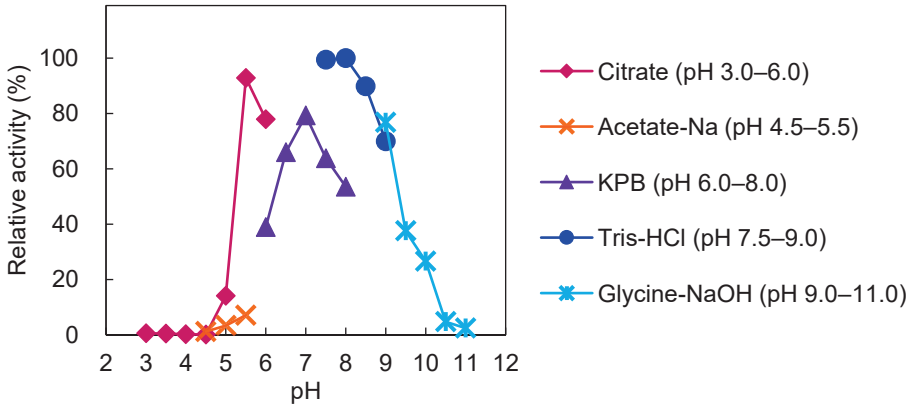

Figure S3. Optimum pH of the purified hydrolase. 100% = 114 U mg^{-1}.

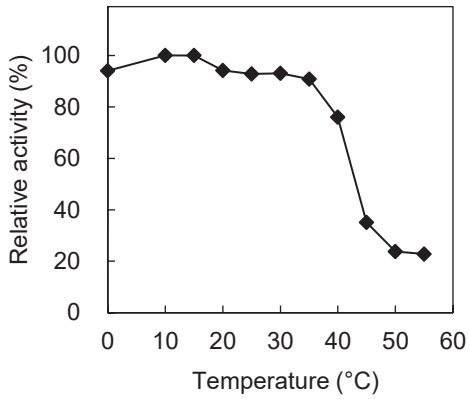

Figure S4. Thermal stability of the purified hydrolase. 100% = 89.1 U mg^{-1}.

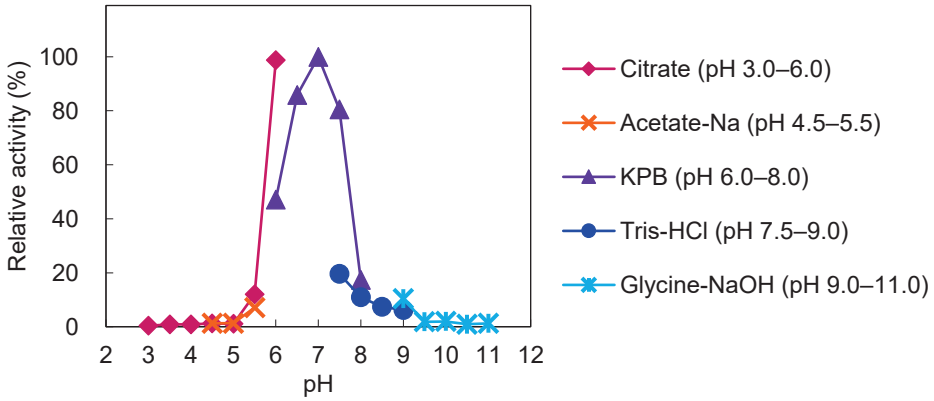

Figure S5. pH stability of the purified hydrolase. 100% = 76.3 U mg^{-1}.

Table S5. HPLC analysis conditions for detection of benzoate and cyclic amines.

Compound [1]	**Column**	**Solvent**	**Retention time (min)**
Benzoate	Atlantis dC18 5μm 4.6×150 mm	sodium phosphate buffer (10 mM, pH 2.8):MeCN = 3:2	4.0
2-MPI	Atlantis dC18 5μm 4.6×150 mm	sodium phosphate buffer (10 mM, pH 2.5):MeOH = 55:45	36.8 (*R*) [3] 38.5 (*S*)
N-Benzoyl-3-MPI [2]	CHIRALPAK AD-H 4.6×250 mm	*n*-hexane:*i*-PrOH = 95:5	9.1 10.4
2-Methylpyrrolidine	Atlantis dC18 5μm 4.6×150 mm	sodium phosphate buffer (10 mM, pH 2.5):MeOH = 55:45	20.8 (*S*) [3] 21.9 (*R*)
2-Methylindoline	Atlantis dC18 5μm 4.6×150 mm	60% (v/v) MeOH	17.3 19.4
1,2,3,4-tetrahydroquinaldine	Atlantis dC18 5μm 4.6×150 mm	60% (v/v) MeOH	21.0 22.3

[1] Cyclic amines except for 3-MPI were derivatized with GITC to determine the yield and optical purity.
[2] 3-MPI obtained by enzymatic hydrolysis was analyzed by chiral HPLC after acylation with benzoyl chloride.
[3] Absolute configurations of chiral cyclic amines were assigned using commercially available chiral reagents.

References

(1) Węglarz, I.; Michalak, K.; Mlynarski, J. Zinc-Catalyzed Asymmetric Hydrosilylation of Cyclic Imines: Synthesis of Chiral 2-Aryl-Substituted Pyrrolidines as Pharmaceutical Building Blocks. *Adv. Synth. Catal.*, **2021**, 363, 1317–1321.

(2) Jain, P.; Verma, P.; Xia, G.; Yu, J. Enantioselective amine α-functionalization via palladium-catalysed C–H arylation of thioamides. *Nat. Chem.*, **2017**, 9, 140–144.

(3) Chen, C.; Clark, R.B.; Deng, Y.; He, M.; Plamondon, L.; Sun, C.; Xiao, X.; Ronn, M. Tetracycline Compounds. US Patent 20120135968A1, 31 May 2012.

(4) Eis, Knut.; Ackerstaff, J.; Wagner, S.; Basting, D.; Golz, S.; Bender, E.; Li, V.M.; Lienau, P.; Liu, N.; Siegel, F.; Bauser, M.; et al. Amido-Substituted Azole Compounds. WO Patent 2015150449A2, 8 October 2015.

(5) Fischer, J.P.; Fell, J.B.; Blake, J.F.; Hinklin, R.J.; Mejia, M.J.; Hicken, E.J.; Chicarelli, M.J.; Gaudino, J.J.; Vigers, G.P.A.; Burgess, L.E.; et al. KRas G12C Inhibitors. WO Patent 2017201161A1, 23 November 2017.

(6) Gayda, R.C.; Henderson, G.W.; Markovitz, A. Neuroactive drugs inhibit trypsin and outer membrane protein processing in *Escherichia coli* K-12. *Proc. Natl. Acad. Sci.*, *USA* **1979**, 76, 2138–2142.

(7) Schneegurt, M.A.; Henry, M.J. Effects of piperalin and fenpropimorph on sterol biosynthesis in *Ustilago maydis*. *Pestic. Biochem. Physiol.*, **1992**, 43, 45–52.

(8) Green, K.; Kim, K. Acute dose response of intraocular pressure to topical and oral cannabinoids. *Proc. Soc. Exp. Biol. Med.*, **1977**, 154, 228–231.

(9) Klun, J.A.; Schmidt, W.F.; Debboun, M. Stereochemical Effects in an Insect Repellent. *J. Med. Entomol.*, **2001**, 38, 809–812.

(10) Klun, J.A.; Khrimian, A.; Margaryan, A.; Kramer, M.; Debboun, M.; Synthesis and Repellent Efficacy of a New Chiral Piperidine Analog: Comparison with Deet and Bayrepel Activity in Human-Volunteer Laboratory Assays Against *Aedes aegypti* and *Anopheles stephensi*. *J. Med. Entomol.*, **2003**, 40, 293–299.

(11) Klun, J.A.; Khrimian, A.; Debboun, M. Repellent and Deterrent Effects of SS220, Picaridin, and Deet Suppress Human Blood Feeding by *Aedes aegypti*, *Anopheles stephensi*, and *Phlebotomus papatasi*. *J. Med. Entomol.*, **2006**, 43, 34–39.

(12) Frances, S.P.; Mackenzie, D.O.; Klun, J.A.; Debboun, M. Laboratory and Field Evaluation of SS220 and Deet Against Mosquitoes in Queensland, Australia. *J. Am. Mosq. Control Assoc.*, **2009**, 25, 174–178.

(13) Mitsukura, K.; Suzuki, M.; Shinoda, S.; Kuramoto, T.; Yoshida, T.; Nagasawa, T. Purification and characterization of a novel (*R*)-imine reductase from Streptomyces sp. GF3587. *Biosci. Biotechnol.*

Biochem., **2011**, 75, 1778–1782.

(14) Mitsukura, K.; Kuramoto, T.; Yoshida, T.; Kimoto, N.; Yamamoto, H.; Nagasawa, T. A NADPH-dependent (*S*)-imine reductase (SIR) from Streptomyces sp. GF3546 for asymmetric synthesis of optically active amines: Purification, characterization, gene cloning, and expression. *Appl. Microbiol. Biotechnol.*, **2013**, 97, 8079–8086.

(15) Leipold, F.; Hussain, S.; Ghislieri, D.; Turner, N.J. Asymmetric Reduction of Cyclic Imines Catalyzed by a Whole-Cell Biocatalyst Containing an (*S*)-Imine Reductase. *ChemCatChem.*, **2013**, 5, 3505–3508.

(16) Hussain, S.; Leipold, F.; Man, H.; Wells, E.; France, S.P.; Mulholland, K.R.; Grogan, G.; Turner, N.J. An (*R*)-Imine Reductase Biocatalyst for the Asymmetric Reduction of Cyclic Imines. *ChemCatChem.*, **2015**, 7, 579–583.

(17) Siedlecka, R. Recent developments in optical resolution. *Tetrahedron*, **2013**, *69*, 6331–6363.

(18) Domínguez de María, P.; de Gonzalo, G.; Alcántara, A.R. Biocatalysis as Useful Tool in Asymmetric Synthesis: An Assessment of Recently Granted Patents (2014–2019). *Catalysts*, **2019**, 9, 802.

(19) Musa, M.M. Enzymatic racemization of alcohols and amines: An approach for bi-enzymatic dynamic kinetic resolution. *Chirality*, **2020**, 32, 147–157.

(20) Wu, S.; Snajdrova, R.; Moore, J.C.; Baldenius, K.; Bornscheuer, U.T. Biocatalysis: Enzymatic Synthesis for Industrial Applications. *Angew. Chem. Int. Ed.*, **2020**, 59, 2–34.

(21) Gotor-Fernández, V.; Fernández-Torres, P.; Gotor, V. Chemoenzymatic preparation of optically active secondary amines: A new efficient route to enantiomerically pure indolines. *Tetrahedron Asymmetry*, **2006**, 17, 2558–2564.

(22) Stirling, M.; Blacker, J.; Page, M.I. Chemoenzymatic dynamic kinetic resolution of secondary amines. *Tetrahedron Lett.*, **2007**, 48, 1247–1250.

(23) Hu, S.; Tat, D.; Martinez, C.A.; Yazbeck, D.R.; Tao, J. An efficient and practical chemoenzymatic preparation of optically active secondary amines. *Org. Lett.*, **2005**, 7, 4329–4331.

(24) Liljeblad, A.; Lindborg, J.; Kanerva, A.: Katajisto, J.; Kanerva, L.T. Enantioselective lipase-catalyzed reactions of methyl pipecolinate: Transesterification and *N*-acylation. *Tetrahedron Lett.*, **2002**, 43, 2471–2474.

(25) Binanzer, M.; Hsieh, S.; Bode, J.W. Catalytic Kinetic Resolution of Cyclic Secondary Amines. *J. Am. Chem. Soc.*, **2011**, 133, 19698–19701.

(26) Wanner, B.; Kreituss, I.; Gutierrez, O.; Kozlowski, M.C.; Bode, J.W Catalytic Kinetic Resolution of Disubstituted Piperidines by Enantioselective Acylation: Synthetic Utility and Mechanistic Insights. *J. Am. Chem. Soc.*, **2015**, 137, 11491–11497.

(27) Al-Sehemi, A.G.; Atkinson, R.S.; Fawcett, J.; Russell, D.R. 3-(*N*,*N*-Diacylamino)quinazolin-4(3*H*)-ones as enantioselective acylating agents for amines. *Tetrahedron Lett.*, **2000**, 41, 2239–2242.

(28) Saito, K.; Miyashita, H.; Akiyama, T. Chiral phosphoric acid catalyzed oxidative kinetic resolution of cyclic secondary amine derivatives including tetrahydroquinolines by hydrogen transfer to imines. *Chem. Commun.*, **2015**, 51, 16648–16651.

(29) Lackner, A.D.; Samant, A.V.; Toste, F.D. Single-Operation Deracemization of 3*H*-Indolines and Tetrahydroquinolines Enabled by Phase Separation. *J. Am. Chem. Soc.*, **2013**, 135, 14090–14093.

(30) Sakamoto, M.; Fujita, K.; Yagishita, F.; Unosawa, A.; Mino, T.; Fujita, T. Kinetic resolution of racemic amines using provisional molecular chirality generated by spontaneous crystallization. *Chem. Commun.*, **2011**, 47, 4267–4269.

(31) Perdicchia, D.; Christodoulou, M.S.; Fumagalli, G.; Calogero, F.; Marucci, C.; Passarella, D. Enzymatic Kinetic Resolution of 2-Piperidineethanol for the Enantioselective Targeted and Diversity Oriented Synthesis. *Int. J. Mol. Sci.*, **2016**, 17, 17.

(32) Saxon, R.E.; Leisch, H.; Hudlicky, T. Preliminary investigation of the yeast-mediated reduction of β-keto amides derived from cyclic amines as potential resolution methodology. *Tetrahedron Asymmetry*, **2008**, 19, 672–681.

(33) Solís, A.; Nava, A.; Pérez, H.I.; Manjarrez, N.; Luna, H.; Cassani, J. Enzymatic Hydrolysis of *N*–protected 2–Hydroxymethylpiperidine Acetates. *J. Mex. Chem. Soc.*, **2008**, 52, 181–184.

(34) Nakashima, N.; Tamura, T. A Novel System for ExpressingRecombinant Proteins Over a WideTemperature Range From 4 to 35 °C. *Biotechnol. Bioeng.*, **2004**, 86, 136–148.

(35) Cappelletti, M.; Presentato, A.; Piacenza, E.; Firrincieli, A.; Turner, R.J.; Zannoni, D. Biotechnology of *Rhodococcus* for the production of valuable compounds. *Appl. Microbiol. Biotechnol.*, **2020**, 104, 8567–8594

(36) Chen, C.S.; Fujimoto, Y.; Girdaukas, G.; Sih, C.J. Quantitative analyses of biochemical kinetic resolutions of enantiomers. *J. Am. Chem. Soc.*, **1982**, 104, 7294–7299.

(37) Bradford, M.M. A rapid and sensitive method for the quantitation of microgram quantities of protein utilizing the principle of protein-dye binding. *Anal. Biochem.* **1976**, 72, 248–254.

(38) Laemmli, U.K. Cleavage of structural proteins during the assembly of the head of bacteriophage T4. *Nature* **1970**, 227, 680–685.

Chapter 3
Enzymatic asymmetric reduction of cyclic imines

3.1 Introduction

Since imine reductases (IREDs) that asymmetrically reduce 2-methyl-1-pyrroline (2-MPN) were first discovered in soil actinomycetes, many types of IREDs have been identified based on the DNA sequences of (*R*)-selective IRED from *Streptomyces* sp. GF3587 (RIR87) and (*S*)-selective IRED from *Streptomyces* sp. GF3546 (SIR46).[1–4] Furthermore, some IREDs have been found to catalyze intermolecular reductive amination as well as the reduction of cyclic imines.[5–7] However, most IREDs exhibit low durability against high-concentration imines, and organic solvents are required to improve the efficiency of the reaction; thus, using IREDs for synthesizing chiral building blocks in pharmaceuticals has not been practical.[8] The specific activity and stability of various enzymes has been improved via mutations to provide resistance against heat or high-concentration substrates, which helps realize a high conversion rate.[9–13] In some cases, the efficient biocatalytic processes of chiral drugs, such as an LSD1 inhibitor (GSK2879552) and an abrocitinib JAK1 inhibitor, have been achieved on a practical scale by improving the activity and stability of IREDs via protein engineering.[14,15] However, among the known wild type IREDs or reductive aminases, the enzymes that exhibit a high conversion rate from imine to amine display highly specific activity or relatively high thermal stability.[8,16] I hypothesized that a lack of stability is one of the factors that limit the potential performance of IREDs. Because most reductive aminations require slightly water-soluble ketones, only enzymes tolerant of these ketones with the properties of organic solvents can catalyze the reaction efficiently. Of the two *Streptomyces*-derived IREDs found previously, the activity of SIR46 is lower than that of RIR87. Although many IREDs have been identified, SIR46 remains one of the most promising and versatile biocatalysts owing to its high (*S*)-selectivity toward various cyclic imines, despite its low durability against heat and high-concentration substrates. The imine reductase *Ao*IRED from *Amycolatopsis orientalis* exhibits higher specific activity than SIR46 as well as high (*S*)-selectivity (85% *ee*); however, when purified *Ao*IRED was stored at 4°C for 24 h and used for the biotransformation of 1-methyl-3,4-dihydroisoquinoline (1-MDIQ), its enantioselectivity was inverted from (S)- to (*R*)-preference with 98% *ee*.[17] *Sn*IR from *Stackebrandtia nassauensi* also exhibited high (*S*)-selectivity and performed full conversion of 100 mM 1-MDIQ into (*S*)-1-methyl-1,2,3,4-tetrahydroisoquinoline with >99% *ee*.[18] In both cases, however, the IREDs required high enzyme loading.

In a previous study, recombinant *Escherichia coli* overexpressing the *SIR46* gene exhibited reductive activity 2-fold higher than that of a cell-free extract of *Streptomyces* sp. GF3546, but the further research did not go.[2] I expected its potential utility, and therefore tested the reductive activity in several conditions using three types of coexpression systems with a glucose dehydrogenase gene from *Bacillus subtilis* (*BsGDH*) (Figures 1, S2 and S3, Table S1). It was shown that the productivity of (*S*)-2-methylpyrrolidine (*S*-2-MP) was improved, yielding around 30 mM *S*-2-MP in the presence of 30 or 40 mM 2-MPN (Table S1 and Figure S2). This result might be attributable to the low stability of the enzyme. Herein, I report an improved biocatalyst based on SIR46 for the practical synthesis of chiral cyclic amines.

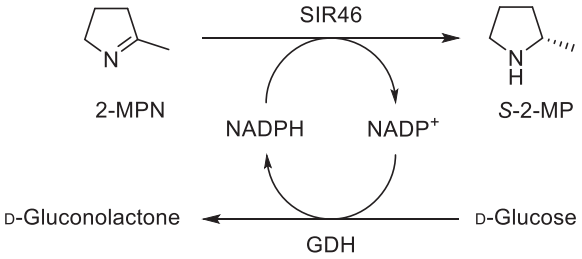

Figure 1. Asymmetric reduction of 2-MPN by SIR46 with NADPH regeneration system.

3.2 Results and discussion

To reduce the stress elicited by a high-concentration substrate on SIR46, I used *Rhodococcus erythropolis* cells as robust host cells for the construction of the expression system.[19] Recombinant *R. erythropolis* expressing the *SIR46* gene successfully led an efficient reaction, achieving full conversion of 100 mM 2-MPN (Figure S11). Moreover, the addition of only glucose drove the reaction without the expression of the *GDH* gene. To investigate this phenomenon, I evaluated NADPH-regenerating activity using cell-free extracts of the recombinant cells. The addition of glucose alone drove a low level of NADPH regeneration from $NADP^+$ in the cell-free extract. Given that NADPH regeneration occurred in the recombinant cells, membrane proteins related to oxidative phosphorylation were likely required. I hypothesized that NADPH regeneration requires ATP to yield glucose 6-phosphate, which is oxidized by glucose 6-phosphate dehydrogenase to obtain NADPH. This hypothesis was not supported by measuring the specific activity of the cell-free extract in the presence of glucose/ATP or glucose 6-dehydrogenase, but glucose 6-phosphate was found to drive NADPH regeneration (Table S2). Recombinant cells expressing the *SIR46* gene also achieved reduction with 2-MPN at >200 mM. This biocatalyst exhibited high productivity with a slow reaction time, i.e., the bioconversion was completed in about one week, which was due to the low catalytic efficiency of SIR46. Additionally, in the cell-free extract, thermal stability is initially low (<35°C), and the activity gradually decreases even during storage at 4°C. These properties are major disadvantages in terms of practical usage (Table S6).

To address these problematic SIR46 characteristics, I attempted to improve thermostability via site-directed mutagenesis. Modifying enzymes by substituting amino acid residues is generally time-consuming and labor-intensive because it requires a huge number of mutants. In the present study, I used a structure- and sequence-based design strategy to efficiently improve the stability of SIR46. Several mutation candidates were found using a method based on the comparison of amino acid sequences among several IREDs obtained via BLAST searches with the protein sequences of SIR46 and RIR87 (Figure S4) as well as the thermodynamic stability of protein secondary structure and the X-ray crystal structure of SIR46 (PDB 4oqy; Table S3). Mutations around the active site were prohibited to maintain the original enantioselectivity. The thermal stability of SIR46 variants was evaluated by measuring the specific activity of the cell-free extract after heat treatment at 40°C–60°C for 30 min (Tables 1 and S4). When I examined 10 single-site mutations selected based on the three concepts mentioned above, the R158L variant showed higher activity than the wild type as well as a slight improvement in thermal stability. Position 158 is generally occupied by leucine in D-type IREDs, including RIR87, *Asp*RedAm[7], IR-46 M3[14], and *Sp*RedAm-R3-V6[15], whereas arginine occupies this position in Y-type IREDs including the enzymes derived from *Streptomyces* sp. GF3546, *Streptomyces aurantiacus*[5], and *Bacillus cereus*[20]. Other mutations, including V48T, A103M, and S209R, also improved thermal stability or enzyme activity. Based on these results, several combinations of amino acid mutations could be examined, but I combined the beneficial mutations while retaining the enzyme activity. The obtained variants increased rather than decreased reductive activity while improving thermal stability. Although the single variant A90V exhibited one-third of the activity of the wild type, the variant M5 containing A90V maintained the activity and enhance the stability. The final variant M9 showed twice the activity of the wild type and thermal resistance at 50°C for 30 min, whereas the wild type lost its activity after incubation at 45°C.

In the SIR46 mutations, V48T and S209R were introduced considering secondary structural stability and hydrophilicity. In addition, A41P and A162P may contribute to the fixation of the helix kink and loop. Instead of V73M, the mutation A103M was designed for the preservation of internal hydrophobicity and the enhancement of hydrophobic interactions, although the alignment of SIR46 and similar enzymes according to a BLAST search showed that the major residue at position 73 is methionine. A90V and A103M probably play similar roles. V88T was introduced anticipating an effect similar to that of V48T. R158L and M207T presumably reduce steric hindrance around the residues (Table S3).

Table 1. Specific activity and thermostability of SIR46 variants.

SIR46 variant	Specific activity[1] (mU mg^{-1})	Residual activity[2] (%)				
		40°C	45°C	50°C	55°C	60°C
WT	12.6	66	0	n.d.	n.d.	n.d.
R158L (M1)	23.4	91	6	n.d.	n.d.	n.d.
M2 (M1 + V48T)	24.2	93	7	n.d.	n.d.	n.d.
M3 (M2 + S209R)	29.8	102	52	0	n.d.	n.d.
M4 (M3 + A103M)	31.0	n.d.[3]	84	9	n.d.	n.d.
M5 (M4 + A90V)	34.7	n.d.	95	74	n.d.	n.d.
M6 (M5 + A41P)	36.3	n.d.	92	87	n.d.	n.d.
M7 (M6 +A162P)	35.7	n.d.	n.d.	100	48	0
M8 (M7 + M207T)	36.6	n.d.	n.d.	94	63	0
M9 (M8 +V88T)	32.9	n.d.	n.d.	102	70	0

[1] Specific activity of SIR46 variant in the cell-free extract of the recombinant cell.
[2] Residual activity after incubation at 40°C–60°C for 30 min.
[3] n.d. = not determined.

The performance of SIR46 M9 was evaluated in the cell-free extract. Owing to the improved stability, the maximum specific activity was observed at 55°C (101 mU mg^{-1}), which was 3-fold higher than the activity at 30°C (Figure S6). Compared with wild type, the effect of pH on the activity was alleviated; thus, the activity was stable around pH 7.5 (Figure S7). When the cell-free extracts of wild type SIR46 and the variant M9 were stored at 4°C for one month, the activity of the wild type SIR46 decreased to 34% of the activity of the fresh cell-free extract, whereas the variant M9 did not exhibit a decrease in activity. Furthermore, the variant M9 retained its specific activity after incubation at 35°C for 24 h, which almost inactivated wild type SIR46 (Table S6). I also evaluated the effects of organic solvents on the activity because such solvents are often required in the reaction when imines or ketones with low water solubility are used for enzymatic reduction. Compared with several organic solvents, methanol resulted in low inhibition and elicited similar effects on the specific activities of the wild type SIR46 and variant M9. In addition, SIR46 M9 showed higher tolerance to DMSO than the wild type, with reductive activity maintained even in 20% DMSO, which inactivated wild type SIR46 (Figure S8). M9 showed higher tolerance to a high concentration of 2-MPN than the wild type, and M9 also showed a 90% or 70% conversion rate at 100 or 200 mM 2-MPN, respectively, whereas the wild type showed a 40% conversion rate (Figure S9). The K_m and V_{max} values for 2-MPN of SIR46 M9 in cell-free extract were 5.5 mM and 52 mU mg^{-1}, respectively, whereas the K_m and V_{max} values for wild type SIR46 were 14.0 mM and 42 mU mg^{-1}, respectively (Figure S10). These results suggest that structural changes in the enzyme, other than in the active site, affect specific activity and stability.

I hypothesized that SIR46 M9 exhibiting high durability would perform efficient conversion of high-concentration imines, which could not be performed by wild type SIR46. However, the

productivity of SIR46 in terms of converting 2-MPN into *S*-2-MP was improved only slightly, with variant M9 exhibiting relatively high activity (Figure S11). Given that both the wild type and variant SIR46 showed similar activity at more than 400 mM 2-MPN (Figure S11), it was predicted that the NADPH-regenerating activity in *Rhodococcus* cells was inhibited. To maximize the performance of M9, I coexpressed the *BsGDH* gene with the *SIR46* gene in the recombinant cells to keep NADPH regeneration enough for SIR46 to proceed the reaction efficiently. The DNA sequence of *BsGDH* was codon-optimized for expression in *R. erythropolis*. The constructed recombinant cells coexpressing *BsGDH* and *SIR46* M9 genes showed improved activity at >200 mM 2-MPN compared with the reaction involving wild type SIR46 (Figure 2). The reaction proceeded even with 500 mM substrate loading, but it took more than one week to complete the conversion. To further improve the conversion rate, the reaction was performed at 35°C to ensure that the variant retained its activity, but this resulted in a lower conversion than that achieved at 30°C (Figure S13). I used the biocatalyst to synthesize *S*-2-MP at 300 mM 2-MPN. After a one week reaction, the amine product was extracted following *N*-Boc protection and purified using column chromatography to give (*S*)-*N*-Boc-2-methylpyrrolidine at a 60% yield with 92.4% *ee*. The *S*-product can be used as a building block of SGC-iMLLT, a potent and selective inhibitor of MLLT1/3–histone interactions.[21]

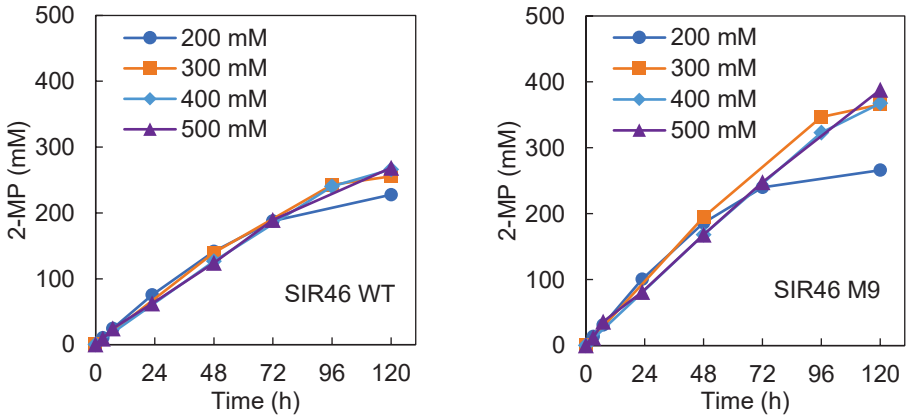

Figure 2. Biocatalytic reduction of 200–500 mM 2-MPN by SIR46 WT or M9. Reactions were performed at 30°C in potassium phosphate buffer (pH 7.5) containing approx. 200–500 mM 2-MPN, glucose (1.2 eq.), and whole cells expressing *SIR46* WT or M9 and *BsGDH* genes (OD_{610} = 25).

Next, I examined the activity of SIR46 M9 toward other imine substrates, including 2-phenyl-1-pyrroline (2-PPN), 2-(4-methoxyphenyl)-1-pyrroline (2-MeOPPN), and 1-MDIQ using the cell-free extract (Table 2). Although I initially used whole cells to perform the bioconversions of imines, the conversion rates were low compared with the reactions with the cell-free extract (data not shown). SIR46 M9 exhibited 3- or 5-fold higher activity toward 2-PPN than the wild type with enhanced enantioselectivity (95.5% *ee*). Similarly, SIR46 M9 exhibited a high conversion rate and slightly improved enantioselectivity (98.7% *ee*) toward 1-MDIQ even at a substrate concentration of 50 mM.

However, the activity toward 2-MeOPPN was decreased, which may have been caused by the small conformational alterations resulting from the mutations in the enzyme structure. I also examined the activity toward cyclohexanone with methylamine because SIR46 was reported to catalyze reductive amination in previous studies[5,6]. The improvement in reductive amination activity was higher in SIR46 M9 than in wild type SIR46 (Table 2 and Figure S14). The variant M9 exhibited a 5.5-fold improvement over the wild type in terms of the maximum conversion, despite showing only a 2-fold increase in specific activity through mutations; hence, the stability of the enzyme also contributes to enhancing the conversion. All reactions with the tested substrates proceeded almost within 24 h and ended after 48 h.

Table 2. Bioconversion of imines by a cell-free extract (CFE) of *R. erythropolis* expressing the *SIR46* and *BsGDH* genes.[1]

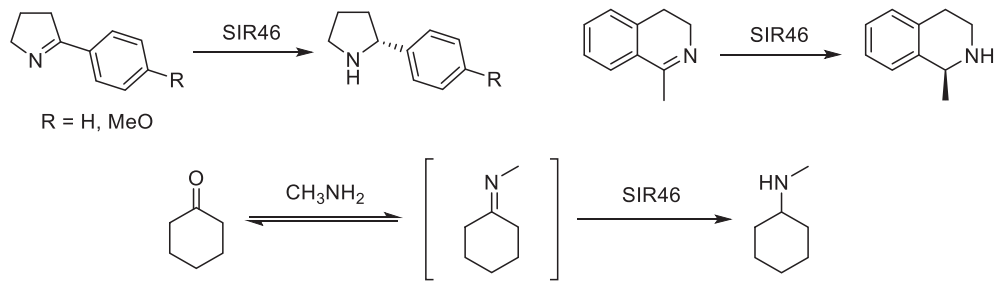

Substrate	Conc. (mM)	CFE (mg mL^{-1})	Conv. (%) and *ee* values (%)			
			Wild type		M9	
2-PPN[2]	10	1.5	10	90 (*R*)	52	95 (*R*)
	10	3.0	27	91 (*R*)	81	96 (*R*)
2-MeOPPN[2]	10	1.5	11	>99 (*R*)	6	>99 (*R*)
	10	3.0	26	>99 (*R*)	10	>99 (*R*)
1-MDIQ[2]	10	1.5	92	98 (*S*)	99	99 (*S*)
	20	1.5	58	98 (*S*)	99	99 (*S*)
	50	1.5	31	98 (*S*)	77	99 (*S*)
Cyclohexanone/CH_3NH_2	20/200	1.5	17	-	69	-
	50/200	1.5	6	-	33	-
	20/400	1.5	54	-	91	-
	50/400	1.5	21	-	51	-

[1] Reactions were performed at 30°C for 48 h in potassium phosphate buffer (pH 7.5) containing substrate(s), 50 or 100 mM glucose, 0.2 mM $NADP^+$, and CFE. Reductive amination of cyclohexanone with methylamine was performed at pH 8.0.

[2] Methanol was added to the reaction mixture to a final concentration of 2.5% (v/v) per 10 mM substrate.

3.3 Conclusions

In conclusion I successfully developed a whole-cell biocatalyst with high productivity in combination with BsGDH by improving the stability of SIR46, which is difficult to use practically. This biocatalyst will enable the efficient synthesis of *S*-2-MP. The cell-free extract of SIR46 M9 retained its activity even during storage at 4°C for more than one month. This level of stability will be a major advantage in terms of practical use and experimentation. Further improvement of the activity and stability of SIR46 will enable more efficient reactions at high concentrations of various imine substrates while reducing the amount of biocatalyst required.

3.4 Materials and methods

3.4.1 General information

Commercially available reagents were used without purification and purchased from Tokyo Chemical Industry Co. Ltd., FUJIFILM Wako Pure Chemical Corporation and Sigma-Aldrich unless stated otherwise. The following products from each supplier were used: polypeptone (Nippon Seiyaku, Tokyo, Japan), meat extract (Kyokuto Seiyaku, Tokyo, Japan), and yeast extract (Oriental Yeast, Tokyo, Japan). Thin-layer chromatography (TLC) was performed on TLC silica gel 60F_{254} (Merck KGaA, Darmstadt, Germany). Column chromatography was performed on Wakosil® 60 (FUJIFILM Wako Pure Chemical Corporation, spherical, 64–210 μm). HPLC analyses were performed using LC-20AD pump, SPD-10A detector (Shimadzu, Kyoto, Japan), Atlantis dC18 5μm 4.6 × 150 mm column (Waters, Massachusetts, USA), and CHIRALPAK AD-RH 5μm 4.6 × 250 mm column (Daicel, Osaka, Japan). Conversion rate and optical purity of amines were determined by HPLC after derivatization with 2,3,4,6-tetra-*O*-acetyl-β-D-glucopyranosyl isothiocyanate (GITC) or methyl isothiocyanate (MITC) at 40°C for 1 h. ^{1}H and ^{13}C NMR spectra were recorded on a JEOL ECA600 spectrometer (600 MHz for ^{1}H and 150 MHz for ^{13}C) in $CDCl_3$ or CD_3OD using tetramethylsilane as an internal standard (δ = 0 ppm). Polymerase chain reaction (PCR), restriction enzyme digestion, and DNA ligation were performed using TaKaRa PCR Thermal Cycler Dice® mini (Takara Bio, Shiga, Japan).

3.4.2 Synthesis of cyclic nitrogen-containing compounds

N-Boc-2-pyrrolidone

A solution of 2-pyrrolidone (5.43 g, 63.82 mmol) and *N*,*N*-(dimethylamino)pyridine (17.3 mg) in CPME (10 mL) was added to di-*tert*-butyl dicarbonate (13.91 g, 63.75 mmol) at room temperature, and the mixture was stirred at 25–30°C overnight. The reaction mixture was diluted with 200 mL ethyl acetate, washed with 5% (w/v) NaH_2PO_4, dried over anhydrous Na_2SO_4, and concentrated under reduced pressure. The crude product was purified by column chromatography (silica gel, *n*-hexane:ethyl acetate = 3:2 and 1:1) to yield *N*-Boc-2-pyrrolidone (11.07 g, 94% yield) as a colorless oil. ^{1}H NMR (600 MHz, $CDCl_3$): δ (ppm) 1.53 (s, 9H), 2.00 (quin, J = 7.7 Hz, 2H), 2.52 (t, J = 8.1 Hz,

2H), 3.75 (t, J = 14.4 Hz, 2H); ^{13}C NMR (150 MHz, $CDCl_3$): δ (ppm) 17.35, 28.0, 32.91, 46.43, 82.72, 150.18, 174.30.

2-Phenyl-1-pyrroline

Phenyl magnesium bromide (1 M solution in THF, 43.6 mL) was added dropwise to a solution of *N*-Boc-2-pyrrolidone (6.05 g, 32.69 mmol) in CPME at −78°C under nitrogen atmosphere, and the mixture was stirred overnight. The reaction was quenched by adding 2 M HCl (22 mL) and 10% (w/v) NaH_2PO_4 (20 mL). The mixture was extracted with ethyl acetate (3 x 100 mL). The combined organic phases were dried over anhydrous Na_2SO_4, and concentrated under reduced pressure to give white solid (8.47 g). This crude product was dissolved in THF (5 mL) and CPME (30 mL). 4 M HCl in CPME (40 mL) was added to the solution and stirred at room temperature overnight. The resulting precipitate was filtered and washed with ethyl acetate. The white solid was dissolved in H_2O (20 mL) and MTBE (20 mL), and 20% (w/v) NaOH (40 mL) was then added dropwise. The mixture was extracted with MTBE (3 x 70 mL). The combined organic phases were dried over anhydrous Na_2SO_4, and concentrated under reduced pressure to give 2-phenyl-1-pyrroline (4.55 g, 97% yield) as a red-brown oil. ^{1}H NMR (600 MHz, $CDCl_3$): δ (ppm) 2.02 (quin, J = 7.8 Hz, 2H), 2.91 (tt, J = 1.8, 8.4 Hz, 2H), 3.84 (s, 3H), 4.03 (tt, J = 1.8, 7.2 Hz, 2H), 6.92 (dt, J = 3.0, 8.4 Hz, 2H), 7.79 (dt, J = 2.4, 9.0 Hz, 2H). ^{13}C NMR (150 MHz, $CDCl_3$): δ (ppm) 22.69, 34.80, 55.27, 61.29, 113.66, 127.45, 129.12, 161.23, 172.55.

2-(4-Methoxyphenyl)-1-pyrroline

To a stirred suspension of Mg (0.51 g, 20.95 mmol) and small piece of iodine in dry THF (10 mL) under nitrogen atmosphere, 4-bromoanisole (3.74 g, 20.00 mmol) in dry THF (7 mL) was added dropwise at room temperature and stirred for 1 h. After the mixture was cooled to −78°C, *N*-Boc-2-pyrrolidone (3.50 g, 18.90 mmol) in CPME (15 mL) was added dropwise and stirred overnight. The reaction was quenched by adding 2 M HCl (10 mL) and 10% (w/v) NaH_2PO_4 (20 mL). The mixture was extracted with ethyl acetate (3 x 70 mL). The combined organic phases were dried over anhydrous Na_2SO_4, and concentrated under reduced pressure to give off-white solid (5.11 g). This crude product was dissolved in THF (5 mL) and CPME (5 mL). 4 M HCl in CPME (20 mL) was added to the solution and stirred at room temperature overnight. The resulting precipitate was filtered and washed with ethyl acetate. The white solid was dissolved in H_2O (20 mL) and MTBE (20 mL), and 20% (w/v) NaOH (40 mL) was then added dropwise. The mixture was extracted with MTBE (3 x 70 mL). The combined organic phases were dried over anhydrous Na_2SO_4, and concentrated under reduced pressure to give 2-(4-methoxyphenyl)-1-pyrroline (1.51 g, 46% yield) as a pale-orange solid. ^{1}H NMR (600 MHz, $CDCl_3$): δ (ppm) 2.02 (quin, J = 7.8 Hz, 2H), 2.91 (tt, J = 1.8, 8.4 Hz, 2H), 3.84 (s, 3H), 4.03 (tt, J = 1.8, 7.2 Hz, 2H), 6.92 (dt, J = 3.0, 8.4 Hz, 2H), 7.79 (dt, J = 2.4, 9.0 Hz, 2H). ^{13}C NMR (150 MHz,

$CDCl_3$): δ (ppm) 22.69, 34.80, 55.27, 61.29, 113.66, 127.45, 129.12, 161.23, 172.55.

rac-2-(4-Methoxyphenyl)pyrrolidine

2-(4-methoxyphenyl)-1-pyrroline (179 mg, 1.02 mmol) and $NaBH_4$ (38.8 mg, 1.03 mmol) were dissolved in *i*PrOH (5 mL). Methanol (2 mL) was added and the mixture was stirred at room temperature overnight. The reaction was quenched by adding 2 M HCl (2 mL) and the mixture was stirred for 30 min. 2 M NaOH (5 mL) was then added and the mixture was extracted with MTBE (3 x 20 mL). The combined organic phases were dried over anhydrous Na_2SO_4, and concentrated under reduced pressure. The crude product was purified by column chromatography (methanol-washed silica gel, methanol) to yield *rac*-2-(4-methoxyphenyl)pyrrolidine (135 mg, 74% yield) as a pale-yellow oil. ^{1}H NMR (600 MHz, $CDCl_3$): δ (ppm) 1.66 (dq, *J* = 8.6, 12.6 Hz, 1H), 1.80–1.95 (m, 2H), 2.14 (dddd, *J* = 4.2, 7.2, 7.8, 12.6 Hz, 1H), 2.73 (bs, 1H), 2.98 (ddd, *J* = 7.2, 8.4, 10.2 Hz, 1H), 3.18 (ddd, *J* = 5.4, 7.8, 10.2 Hz, 1H), 3.79 (s, 3H), 4.05 (t, *J* = 7.8, 1H), 6.85 (dt, *J* = 3.0, 8.4 Hz, 2H), 7.28 (d, *J* = 8.4 Hz, 2H). ^{13}C NMR (150 MHz, $CDCl_3$): δ (ppm) 25.40, 34.03, 46.68, 55.22, 62.04, 113.70, 127.65, 136.13, 158.51.

1-Methyl-3,4-dihydroisoquinoline

Acetyl chloride (7.8 mL, 109 mmol) was added to a solution of 2-phenylethylamine (12.16 g, 99.55 mmol) and triethylamine (10.24 g, 101.2 mmol) in acetonitrile (100 mL) at 0°C with stirring. The reaction mixture was stirred at room temperature overnight. CPME (20 mL) was added and the mixture was filtered. The supernatant was concentrated under reduced pressure. The residue was diluted with 200 mL ethyl acetate, washed with 0.2 M HCl and 5% (w/v) $NaHCO_3$, dried over anhydrous Na_2SO_4, and concentrated under reduced pressure. The resulting yellow solid (15.71 g, 97% yield) was used without further purification. The afforded *N*-acetyl-2-phenylethylamine (1.42 g, 8.716 mmol) was added to polyphosphoric acid (21.4 g) and P_2O_5 (2.2 g). The mixture was heated to 110°C for 15 min then 180°C for 4 h. 11% (w/v) NaOH (200 mL) was added to the reaction mixture cooled with ice water. The mixture was extracted with ethyl acetate (3 x 100 mL), dried over anhydrous Na_2SO_4, and concentrated under reduced pressure. The crude product was purified by column chromatography (silica gel, ethyl acetate) to yield 1-methyl-3,4-dihydroisoquinoline (0.837 g, 66% yield) as a yellow oil. ^{1}H NMR (600 MHz, $CDCl_3$): δ (ppm) 2.39 (t, *J* = 1.5 Hz, 3H), 2.71 (t, *J* = 7.5 Hz, 2H), 3.66 (tq, *J* = 1.6, 7.4 Hz, 2H), 7.18 (dd, *J* = 0.9, 7.5 Hz, 1H), 7.30 (tt, *J* = 0.7, 7.6 Hz, 1H), 7.35 (td, *J* = 1.2, 14.4 Hz, 1H), 7.48 (dd, *J* = 0.9, 7.5 Hz, 1H); ^{13}C NMR (150 MHz, $CDCl_3$): δ (ppm) 23.23, 25.99, 46.86, 125.26, 126.83, 127.37, 129.52, 130.52, 137.36, 164.28.

3.4.3 Cloning and overexpression

Plasmid construction

pET-21a(+)/SIR46

The *SIR46* gene on pT7Blue vector was amplified by PCR with *TaKaRa Ex Taq*® (Takara Bio) using two primers containing *Nde* I or *EcoR* I restriction site. The amplified DNA fragment and pET-21a(+) vector (Merck KGaA) were digested with *Nde* I and *EcoR* I, and ligated using DNA Ligation Kit (Takara Bio). The resulting plasmid was transformed into *E. coli* JM109 and isolated from the recombinant cells.

pACYDuet-1/BsGDH and pACYCDUet-1/BsGDH-SIR46

The genome DNA of *Bacillus subtilis* NBRC3026 was prepared using ISOPLANT II (NIPPON GENE, Tokyo, Japan). The *BsGDH* gene on the genome DNA was amplified by PCR with *TaKaRa Ex Taq*® (Takara Bio) using two primers containing *Nde* I or *Xho* I restriction site. The amplified DNA fragment and pT7Blue T-vector (Merck KGaA) were ligated using DNA Ligation Kit (Takara Bio). The resulting plasmid was transformed into *E. coli* JM109. The obtained plasmid was digested with *Nde* I and *Xho* I, and subcloned into MCS2 of pACYCDuet-1 vector (Merck KGaA) using DNA Ligation Kit (Takara Bio). The resulting plasmid was transformed into *E. coli* JM109 and isolated from the recombinant cells. The *SIR46* gene was further subcloned into MCS1 of the obtained pACYCDuet-1/BsGDH(MCS2). pACYCDuet-1/BsGDH(MCS1) and pACYCDuet-1/BsGDH(MCS1)-SIR46(MCS2) were also prepared in the same way as shown above, using *Nco* I and *EcoR* I restriction site for subcloning into MCS1 of pACYCDuet-1 vector.

pTipRT2/SIR46 and pTipQC1/BsGDH

The *SIR46* or *BsGDH* gene on pT7Blue vector were amplified by PCR with PrimeSTAR® Max DNA Polymerase (Takara Bio) using two primers containing *Nde* I or *Xho* I restriction site. Additionally, a *BsGDH* gene was commercially synthesized with codon optimization for efficient expression in *Rhodococcus* (Eurofins Genomics, Tokyo, Japan) and used in the same way as shown here. The amplified DNA fragment and pTip vectors (Hokkaido System Science, Hokkaido, Japan) were digested with *Nde* I and *Xho* I, and ligated using DNA Ligation Kit (Takara Bio). The resulting plasmid was transformed into *E. coli* JM109 and isolated from the recombinant cells.

Expression

Co-expression of SIR46 and BsGDH genes in *E. coli* BL21 (DE3)

E. coli BL21 (DE3) was transformed with pET-21a(+)/SIR46 according to SEM transformation.[22] The resulting transformant was further used for transformation with pACYDuet-1/BsGDH. The obtained recombinant cells were cultivated at 120 rpm and 28°C in LB medium supplemented with 50 μg mL^{-1}

ampicillin and 20 μg mL^{-1} chloramphenicol. When the optical density at 610 nm (OD_{610}) reached to 0.6–1.0, 0.5 mM isopropyl-β-D-thiogalactopyranoside (IPTG) was added for induction of protein expression and the culture was incubated at 28°C and 120 rpm for 5 h. The cells were harvested by centrifugation, washed with 0.85 (w/v) NaCl, and resuspended in 50 mM potassium phosphate buffer (pH 7.0). To prepare cell-free extract, 0.1 mM dithiothreitol was added and disrupted by ultrasonication at 100 W for 5 min at 0°C using a cell disrupter (19 kHz, Insonator 201 M; Kubota, Japan). The cell debris was removed by centrifugation at 4°C and 12,000 rpm for 30 min and the supernatant solution was used as cell-free extract. The amount of the protein extracted from the cells was approximately 0.5 g per liter of culture medium.

Expression of SIR46 gene in *R. erythropolis* L88

R. erythropolis L88 (Hokkaido System Science) was transformed with pTipRT2/SIR46 by electroporation using Eporator® (Eppendorf, Hamburg, Germany). The transformant was cultivated with 10 μg mL^{-1} tetracycline at 120 rpm and 28°C in 5 mL of nutrient medium A containing 10 g L^{-1} tryptone, 5 g L^{-1} yeast extract, 4 g L^{-1} Na_2HPO_4, 1 g L^{-1} KH_2PO_4, 1 g L^{-1} NaCl, 0.2 g L^{-1} $MgSO_4 \cdot 7H_2O$, and 10 mg L^{-1} $CaCl_2 \cdot 2H_2O$ in tap water. The preculture was inoculated in 90 mL of the nutrient medium with 0.2 μg mL^{-1} thiostrepton and incubated at 20°C and 120 rpm for 24 h. The cells were harvested by centrifugation and washed twice with 50 mM potassium phosphate buffer (pH 7.0). To prepare cell-free extract, the cells were resuspended in 50 mM potassium phosphate buffer (pH 7.0) with 1.0 mg mL^{-1} lysozyme and 0.1 mM dithiothreitol, and incubated at 4°C overnight. The treated cells were disrupted by ultrasonication at 100 W for 20 min at 0°C using a cell disrupter (19 kHz, Insonator 201 M; Kubota, Japan). The cell debris was removed by centrifugation at 4°C and 12,000 rpm for 30 min and the supernatant solution was used as cell-free extract. The amount of the protein extracted from the cells was 0.5–0.6 g per liter of culture medium.

Co-expression of SIR46 and BsGDH genes in *R. erythropolis* L88

The recombinant *R. erythropolis* L88_pTipRT2/SIR46 was cultivated at 120 rpm and 28°C in 5 mL of nutrient medium A supplemented with 10 μg mL^{-1} tetracycline until OD_{610} reached to 1.0. The cells were harvested by centrifugation, washed with water, and resuspended in 10% (v/v) glycerol supplemented with 1% (v/v) trehalose. The cell suspension was used for transformation of *R. erythropolis* L88_pTipRT2/SIR46 with pTipQC1/BsGDH. The resulting transformant was cultivated with 10 μg mL^{-1} tetracycline at 120 rpm and 28°C in 5 mL of nutrient medium A supplemented with 10 μg mL^{-1} tetracycline and 30 μg mL^{-1} chloramphenicol. Induction of protein expression in the recombinant cells was performed in the same way as single expression of *SIR46* in *R. erythropolis* L88. The amount of the protein extracted from the cells was approximately 0.5 g per liter of culture medium.

3.4.4 Variant construction

SIR46 variants were generated by amplifying full-length plasmid pTipRT2-SIR46 by PCR according to the instructions of PrimeSTAR® Mutagenesis Basal Kit (Takara-Bio). The PCR products were digested with *Dpn* I and purified by gel electrophoresis. The resulting DNAs were used to transform *E coli* JM109 for plasmid preparation. Introduced mutations were verified by dye-terminator sequencing.

3.4.5 Biotransformation

Biotransformations were performed at 30°C with shaking (120 rpm) in potassium phosphate buffer (pH 7.0) containing imine substrate, glucose and whole cells or cell-free extract. Samples were collected multiple times and analyzed by HPLC after amine derivatization with GITC.

3.4.6 Enzyme assay

Imine reductase activity was determined by monitoring the decrease of NADPH with UV1600PC (Shimadzu, Tokyo, Japan) at 340 nm (ε = 6.22 mM^{-1} cm^{-1}) at 30°C. The reaction mixture (1 mL) generally contained 100 mM potassium phosphate buffer (pH 7.0), 10 mM 2-methyl-1-pyrroline, 0.15 mM NADPH and 20–100 µL cell-free extract. The reaction was started by adding cell-free extract to the mixture. One unit (U) of imine reductase activity was defined as the amount of protein that oxidized 1 µmol of NADPH at 30°C per minute. Glucose dehydrogenase activity was determined by monitoring the increase of NADPH. The reaction mixture (1 mL) generally contained 100 mM potassium phosphate buffer (pH 7.0), 10 mM glucose, 0.15 mM $NADP^+$ and 0.4 µL cell-free extract. One unit (U) of glucose dehydrogenase activity was defined as the amount of protein that reduced 1 µmol of $NADP^+$ at 30°C per minute. To examine the activity of NADPH regeneration in the cell-free extract of *Rhodococcus* expressing wild-type SIR46 gene, 0.5 mM ATP and 1 mM $MgCl_2$ were further added if necessary. The NADPH-regenerating activity with glucose 6-phosphate instead of glucose was also examined.

3.4.7 Effect of temperature, pH and organic solvent on SIR46 activity

To determine the thermal stability of SIR46, the cell-free extract containing SIR46 variant was pre-incubated at temperatures from 40 to 60°C for 30 min and cooled on ice before imine reductase activity was determined. Effect of temperature was examined in a 100 mM potassium phosphate buffer (pH 7.0) containing 10 mM 2-methyl-1-pyrroline, 0.15 mM NADPH and 20 or 50 µL cell-free extract at temperatures from 35 to 60°C. Effect of pH was examined at 30°C using various 100 mM buffers with different pH values including potassium phosphate buffer (KPB) (pH 6.0–8.0), Tris-HCl (pH 7.5–9.5) and HEPES (pH 7.0–8.0), containing 10 mM 2-methyl-1-pyrroline, 0.15 mM NADPH and 50 µL cell-free extract. Effect of organic solvent was examined at 30°C in 100 mM potassium phosphate buffer

containing 10 mM 2-methyl-1-pyrroline, 0–20% (v/v) organic solvent, 0.15 mM NADPH and 50 µL cell-free extract.

3.4.8 Protein analysis

Protein concentration was determined by the Bradford method, using a protein assay kit (Bio-Rad Laboratories, Inc., California, USA) and bovine serum albumin as a standard.[23] In column chromatography, absorbance at 280 nm was measured to detect eluted protein. SDS-PAGE was performed on 12% (w/v) polyacrylamide gel with Tris-glycine buffer system according to Laemmli.[24] Proteins were stained with Coomassie Brilliant Blue R250 and gels destained in ethanol/acetate/H_2O (3:1:6, v/v/v).

3.4.9 DNA and amino acid sequences

(*S*)-Selective imine reductase from *Streptomyces* sp. GF3546 (SIR46)

Wild-type SIR46 DNA sequence

ATGAGCAAGCAGTCGGTAACGGTCATCGGTCTGGGCCCGATGGGCCAGGCGATGGTGAA
CACCTTCCTGGACAACGGCCACGAGGTGACCGTGTGGAACCGGACCGCCAGCAAGGCC
GAGGCGCTCGTGGCCCGGGGTGCCGTACTGGCTCCCACCGTCGAGGACGCGCTCAGCGC
CAATGAGCTGATCGTGCTCAGCCTGACGGACTACGACGCGGTGTACGCCATTCTTGAGCC
GGTGACGGGTTCCCTGTCCGGCAAGGTCATCGCCAACCTCAGCTCCGACACCCCGGACA
AGGCCCGCGAGGCGGCCAAGTGGGCGGCCAAGCACGGTGCGAAGCACCTCACCGGTGG
TGTGCAGGTGCCGCCGCCGCTGATCGGCAAGCCCGAGTCCTCCACCTACTACAGCGGTC
CCAAGGATGTCTTCGACGCCCATGAGGACACCCTGAAGGTCCTCACCAACGCGGACTAC
CGCGGCGAGGACGCCGGCCTCGCGGCCATGTACTACCAGGCCCAGATGACCATCTTCTG
GACCACGATGCTGAGCTACTACCAGACCCTCGCGCTGGGCCAGGCCAACGGTGTCTCGG
CGAAGGAACTGCTGCCCTACGCCACGATGATGACGTCGATGATGCCGCACTTCCTGGAG
CTGTACGCCCAGCACGTGGACTCCGCGGACTACCCGGGCGACGTGGACCGGCTCGCGAT
GGGGGCGGCCAGTGTCGACCACGTCCTGCACACGCACCAGGACGCGGGCGTCAGCACC
GTGCTGCCGGCCGCCGTCGCCGAGATCTTCAAGGCGGGCATGGAGAAGGGCTTCGCCGA
GAACAGCTTCTCCAGCCTCATCGAGGTGCTCAAGAAGCCGGCGGTCTGA

Wild-type SIR46 amino acid sequence

MSKQSVTVIGLGPMGQAMVNTFLDNGHEVTVWNRTASKAEALVARGAVLAPTVEDALSAN
ELIVLSLTDYDAVYAILEPVTGSLSGKVIANLSSDTPDKAREAAKWAAKHGAKHLTGGVQVP
PPLIGKPESSTYYSGPKDVFDAHEDTLKVLTNADYRGEDAGLAAMYYQAQMTIFWTTMLS

YYQTLALGQANGVSAKELLPYATMMTSMMPHFLELYAQHVDSADYPGDVDRLAMGAASV
DHVLHTHQDAGVSTVLPAAVAEIFKAGMEKGFAENSFSSLIEVLKKPAV*

SIR46 M9 variant DNA sequence

ATGAGCAAGCAGTCGGTAACGGTCATCGGTCTGGGCCCGATGGGCCAGGCGATGGTGAA
CACCTTCCTGGACAACGGCCACGAGGTGACCGTGTGGAACCGGACCGCCAGCAAGGCC
GAGCCGCTCGTGGCCCGGGGTGCCACGCTGGCTCCCACCGTCGAGGACGCGCTCAGCG
CCAATGAGCTGATCGTGCTCAGCCTGACGGACTACGACGCGGTGTACGCCATTCTTGAGC
CGGTGACGGGTTCCCTGTCCGGCAAGACCATCGTCAACCTCAGCTCCGACACCCCGGAC
AAGGCCCGCGAGATGGCCAAGTGGGCGGCCAAGCACGGTGCGAAGCACCTCACCGGTG
GTGTGCAGGTGCCGCCGCCGCTGATCGGCAAGCCCGAGTCCTCCACCTACTACAGCGGT
CCCAAGGATGTCTTCGACGCCCATGAGGACACCCTGAAGGTCCTCACCAACGCGGACTA
CCTCGGCGAGGACCCCGGCCTCGCGGCCATGTACTACCAGGCCCAGATGACCATCTTCTG
GACCACGATGCTGAGCTACTACCAGACCCTCGCGCTGGGCCAGGCCAACGGTGTCTCGG
CGAAGGAACTGCTGCCCTACGCCACGATGACCACGCGCATGATGCCGCACTTCCTGGAG
CTGTACGCCCAGCACGTGGACTCCGCGGACTACCCGGGCGACGTGGACCGGCTCGCGAT
GGGGGCGGCCAGTGTCGACCACGTCCTGCACACGCACCAGGACGCGGGCGTCAGCACC
GTGCTGCCGGCCGCCGTCGCCGAGATCTTCAAGGCGGGCATGGAGAAGGGCTTCGCCGA
GAACAGCTTCTCCAGCCTCATCGAGGTGCTCAAGAAGCCGGCGGTCTGA

SIR46 M9 variant amino acid sequence

MSKQSVTVIGLGPMGQAMVNTFLDNGHEVTVWNRTASKAEPLVARGATLAPTVEDALSAN
ELIVLSLTDYDAVYAILEPVTGSLSGKTIVNLSSDTPDKAREMAKWAAKHGAKHLTGGVQVP
PPLIGKPESSTYYSGPKDVFDAHEDTLKVLTNADYLGEDPGLAAMYYQAQMTIFWTTMLSY
YQTLALGQANGVSAKELLPYATMTTRMMPHFLELYAQHVDSADYPGDVDRLAMGAASVD
HVLHTHQDAGVSTVLPAAVAEIFKAGMEKGFAENSFSSLIEVLKKPAV*

Glucose dehydrogenase from *Bacillus subtilis* NBRC3026 (BsGDH)

BsGDH DNA sequence

ATGGGCCACCATCACCATCACCATATGTATCCGGATTTAAAAGGAAAAGTCGTCGCTATTA
CAGGAGCTGCTTCAGGGCTCGGAAAGGCGATGGCCATTCGCTTCGGCAAGGAGCAGGC
AAAAGTGGTTATCAACTATTATAGTAATAAACAAGATCCGAACGAGGTAAAAGAAGAGGT
CATCAAGGCGGGCGGTGAAGCTGTTGTCGTCCAAGGAGATGTCACGAAAGAGGAAGAT
GTAAAAAATATCGTGCAAACGGCAATTAAAGAGTTCGGCACACTCGATATTATGATTAATA
ATGCCGGTCTTGAAAATCCTGTACCATCTCACGAAATGCCGCTCAAGGATTGGGATAAAG

TCATCGGCACGAACTTAACGGGTGCCTTTTTAGGAAGCCGTGAAGCGATTAAATATTTCG
TAGAAAACGATATCAAGGGAAATGTCATTAACATGTCCAGTGTGCACGAAGTGATTCCTT
GGCCGTTATTTGTCCACTATGCGGCAAGTAAAGGCGGGATAAAGCTGATGACAGAAACAT
TAGCGTTGGAATACGCGCCGAAGGGCATTCGCGTCAATAATATTGGGCCAGGTGCGATCA
ACACGCCAATCAATGCTGAAAAATTCGCTGACCCTAAACAGAAAGCTGATGTAGAAAGC
ATGATTCCAATGGGATATATCGGCGAACCGGAGGAGATCGCCGCAGTAGCAGCCTGGCTT
GCTTCGAAGGAAGCCAGCTACGTCACAGGCATCACGTTATTCGCGGACGGCGGTATGAC
ACAATATCCTTCATTCCAGGCAGGCCGCGGTTGA

Codon-optimized BsGDH DNA sequence
ATGGGCCACCATCACCATCACCATATGTACCCCGACCTCAAGGGGAAGGTGGTCGCCATC
ACCGGCGCGGCCTCCGGCCTGGGTAAGGCCATGGCGATCCGCTTCGGCAAGGAGCAGGC
GAAGGTCGTCATCAACTACTACAGCAACAAGCAGGACCCGAACGAGGTCAAGGAGGAA
GTCATCAAGGCCGGCGGCGAAGCCGTCGTCGTGCAGGGCGACGTCACGAAGGAGGAGG
ACGTCAAGAACATCGTCCAGACCGCCATCAAGGAGTTCGGCACGCTCGACATCATGATC
AACAACGCCGGCCTGGAGAACCCCGTCCCGTCGCACGAGATGCCGCTGAAGGACTGGG
ACAAGGTGATCGGCACCAACCTGACCGGCGCCTTCCTCGGCAGCCGGGAGGCCATCAAG
TACTTCGTGGAGAACGACATCAAGGGCAACGTGATCAACATGTCCTCCGTGCACGAGGT
CATCCCGTGGCCGCTGTTCGTCCACTACGCCGCCTCCAAGGGCGGGATCAAGCTGATGAC
CGAAACCCTGGCGCTGGAGTACGCCCCGAAGGGCATCCGCGTGAACAACATCGGTCCCG
GCGCCATCAACACGCCCATCAACGCCGAGAAGTTCGCGGACCCGAAGCAGAAGGCCGA
CGTCGAGTCGATGATCCCCATGGGCTACATCGGGGAACCGGAGGAGATCGCCGCGGTGG
CGGCGTGGCTGGCCTCGAAGGAGGCGTCGTACGTCACCGGCATCACGCTCTTCGCCGAC
GGCGGCATGACCCAGTACCCGTCCTTCCAGGCGGGTCGCGGGTGA

BsGDH amino acid sequence
MGHHHHHHMYPDLKGKVVAITGAASGLGKAMAIRFGKEQAKVVINYYSNKQDPNEVKEE
VIKAGGEAVVVQGDVTKEEDVKNIVQTAIKEFGTLDIMINNAGLENPVPSHEMPLKDWDKV
IGTNLTGAFLGSREAIKYFVENDIKGNVINMSSVHEVIPWPLFVHYAASKGGIKLMTETLALE
YAPKGIRVNNIGPGAINTPINAEKFADPKQKADVESMIPMGYIGEPEEIAAVAAWLASKEASY
VTGITLFADGGMTQYPSFQAGRG*

3.4.10 Preparative-scale biotransformation of 2-MPN

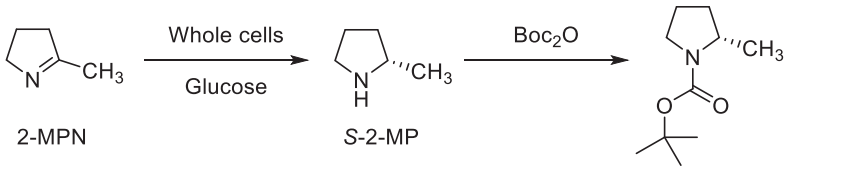

Cell suspension of *R. erythropolis* L88 expressing SIR46 M9 and BsGDH genes in 50 mM potassium phosphate buffer (5.0 mL, OD_{610} = 50, pH 7.0) was added to a solution of 2-MPN (0.25 g, 3.00 mmol) and glucose (0.54 g, 3.60 mmol) in potassium phosphate buffer (5.0 mL, 200 mM, pH 7.75). The mixture (10 mL) was incubated at 30°C and 70 rpm for 7 days in 50 mL falcon tube. The reaction mixture was centrifugated to remove the cells. NaOH (0.51 g, 12.6 mmol) in 10 mL H_2O and di-*tert*-butyl dicarbonate (1.07 g, 4.92 mmol) in 10 mL MTBE was added to the supernatant, and the mixture was stirred at room temperature overnight. After MTBE (40 mL) was added to the reaction mixture, organic phase was washed with H_2O (20 mL) and 5% (w/v) NaH_2PO_4 (2 x 25mL), dried over anhydrous Na_2SO_4, and concentrated under reduced pressure. The crude product was purified by column chromatography (silica gel, *n*-hexane:ethyl acetate = 20:1) to yield (*S*)-*N*-Boc-2-methylpyrrolidine (0.33 g, 1.79 mmol, 60% yield, 92.4% *ee*) as a colorless oil. ^{1}H NMR (600 MHz, $CDCl_3$): δ (ppm) 1.15 (bs, 3H), 1.46 (s, 9H), 1.51–1.56 (m, 1H), 1.75–1.81 (m, 1H), 1.85–1.90 (m, 1H), 1.98 (bs, 1H), 3.36 (bs, 2H), 3.87 (bd, J = 50.4 Hz, 1H); ^{13}C NMR (150 MHz, $CDCl_3$): δ (ppm) 20.11, 20.75, 22.93, 23.60, 28.54, 32.52, 33.28, 46.09, 46.41, 52.74, 78.76, 154.58.

3.5 Supplementary information

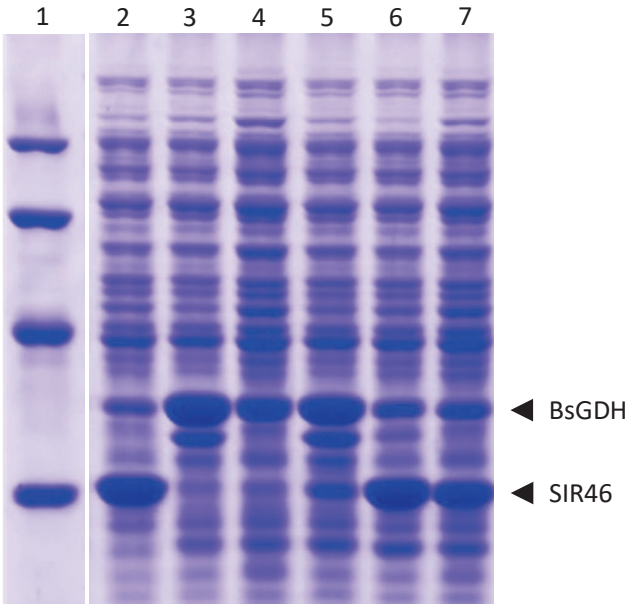

Figure S1. SDS-PAGE analysis of wild-type SIR46 and BsGDH expressed in *E. coli* BL21. Lane 1: molecular weight markers 97 kDa, 66 kDa, 45 kDa, 30 kDa. Lane 2: cell-free extract of *E. coli* BL21 (pET-21a(+)/SIR46) expressing wild-type SIR46 (CFE pET/SIR46). Lane 3: CFE pACYCDuet/BsGDH(MCS2). Lane 4: CFE pACYCDuet/BsGDH (MCS1). Lane 5: CFE pACYCDuet/SIR46(MCS1)-BsGDH(MCS2). Lane 6: CFE pET-21a(+)/SIR46 and pACYCDuet/BsGDH(MCS2). Lane 7: CFE pACYCDuet/BsGDH(MCS1)-SIR46(MCS2).

Table S1. Bioconversion of 2-MPN by whole cells of *E. coli* BL21 (DE3) expressing wild-type SIR46 and BsGDH genes.[1]

Plasmid vector	Whole cells[2]	2-MPN (mM)	Glucose (mM)	Product (mM)
pACYCDuet/SIR46(MCS1)-BsGDH(MCS2)	10-fold	10	50	2.8 (with NADPH) 1.9 (no coenzyme)
pACYCDuet/BsGDH(MCS1)-SIR46(MCS2)	10-fold	10	50	4.8 (with NADPH) 1.7 (no coenzyme)
pET-21a(+)/SIR46 and pACYCDuet/BsGDH(MCS2)	5-fold	10	50	9.4 (with NADPH) 9.9 (with $NADP^+$) 3.3 (no coenzyme)
	10-fold	30	100	27.1 (with $NADP^+$)

[1] Reactions were performed at 30°C for 24 h in 100 mM potassium phosphate buffer (pH 7.0) containing 2-MPN, glucose, 0 or 0.2 mM NADP(H), and whole cells expressing wild-type SIR46 and BsGDH genes.
[2] One-fold whole cell is the turbidity of culture broth when harvested.

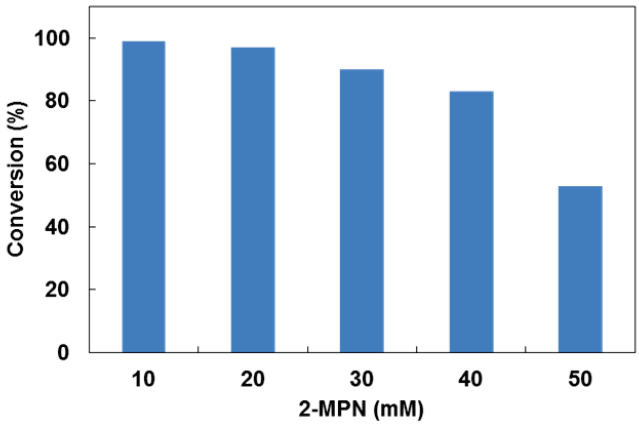

Figure S2. Effect of 2-MPN concentration on conversion of 2-MPN by wild-type SIR46. Reactions were performed at 30°C for 24 h in 100 mM potassium phosphate buffer (pH 7.0) containing 10–50 mM 2-MPN, 100 mM glucose, 0.2 mM $NADP^+$, and 10-fold whole cells of *E. coli* BL21 (pET-21a(+)/SIR46WT and pACYCDuet/BsGDH (MCS2)).

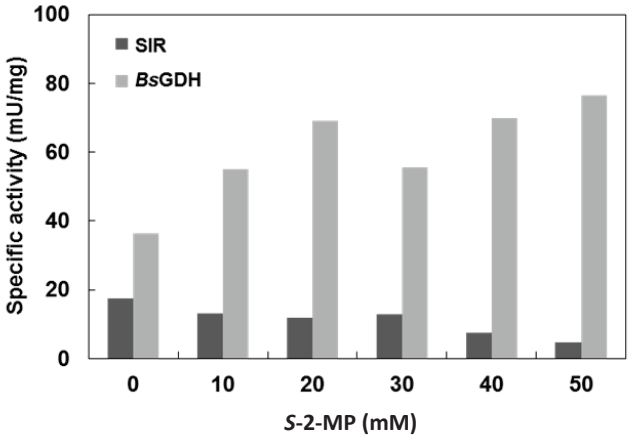

Figure S3. Effect of *S*-2-MP concentration on wild-type SIR46 and BsGDH activities.

Table S2. NADPH-generating activity in the cell-free extract of *Rhodococcus* expressing wild-type SIR46 gene

Coenzyme	Substrate	Specific activity (mU mg^{-1})
NAD^+	Glucose	3.3
NAD^+	Glucose 6-phosphate	1.3
$NADP^+$	Glucose	5.6
$NADP^+$	Glucose 6-phosphate	31.9
$NADP^+$, ATP	Glucose	5.6

```
SIR46            ------------------MSKQSVTVIGLGPMGQAMVNTFLDNGHEVTVWNRTASKAEAL    42
WP_093601729.1   ------------------MGKQSVTVIGLGPMGQAMVNTFLDNGHGVTVWNRTAAKAEAL    42
WP_206300583.1   ------------------MSKQSVTVIGLGPMGQAMVNTFLENGHEVTVWNRTASKAEAL    42
WP_189220594.1   ------------------MSKKSLTLIGLGPMGQAMVNTYLDNGYDVTVWNRTASKAEPL    42
WP_037679270.1   ------------------MSKQSVTVIGLGPMGQAMVGAFIDNGHEVTVWNRTASKAEAL    42
WP_086884371.1   ------------------MSKQPVTVIGLGPMGQAMVSTFLEQGHAVTVWNRTPAKAEAL    42
WP_229819828.1   ------------------MSKQAVTVIGLGPMGQAMVTAFLENGHPVTVWNRTASKADEL    42
WP_229356653.1   -------------MRGEPVSKQAVTVIGLGPMGQAMVAAFLENGHPVTVWNRTASKAAEL    47
WP_127489187.1   MNSSNLKEDSSVGNASAATNRKSVTVMGLGPMGQAMAGVFLECGYAVTVWNRTASKADEL    60
WP_144878318.1   -MNQNDQRSKHEATSAGERNRPSVTIIGLGPMGQAMAAVFLDRGYEVTVWNRTAGKSDAL    59
WP_043615602.1   -----------------MSGKQSVTVIGLGPMGQAMVQAFLDKGHPVTVWNRTPSRADAL    43
WP_030554141.1   ----------------MSSTKQSVTVIGLGPMGQAMAGAFLDRGYDVTVWNRTASRADAL    44
WP_129772310.1   ------MPGTSATPVTPTASATPVTVIGLGPMGRAMVGAFLDGGHQVTVWNRTASRADEL    54
WP_073792319.1   ------------------MDKQAVTLIGLGPMGQAMGAAFLDRGHALTVWNRSPGKADGL    42
WP_063484289.1   ------------------MSKHEVTVIGLGPMGRAMASTFLGKGYRVTVWNRTAGKADEL    42
RIR87            ----------------MGDNRTPVTVIGLGLMGQALAAAFLEAGHTTTVWNRSAGKAEQL    44
WP_164356008.1   ----------------MGDNRTPVTVIGLGLMGQALAAAFLEAGHTTTVWNRSAGKAEQL    44
WP_192770552.1   -------------MRNHDAGHTPVTVIGLGLMGQALAGAFLRAGHPTTVWNRTAAKAEDL    47
WP_189106074.1   -----------------MNATTPVTVLGLGLMGRALAEKFLREGHATTVWNRTAARAEPL    43
WP_132386371.1   ----------------MGDGRVPVTVIGLGMMGRALARAFLSGEHPTTVWNRTAGRAEEL    44
                                       :*::*** **:*:   ::   :  *****:..::  *

SIR46            VARGAVLAPTVEDALSANELIVLSLTDYDAVYAILEPVTGSLSGKVIANLSSDTPDKARE    102
WP_093601729.1   VARGAVLAPTVEAALGANELIVLSLTDYDAVYAVLEPVTDALSGKVIANLSSDTPDKARQ    102
WP_206300583.1   VAKGATLAPTVEDALGANELIVLSLTDYDAVNAILEPVAASLSGKVIANLSSDTPDKTRE    102
WP_189220594.1   VARGAVLAPTVEEALAANELIVLSLTDYDAVYAILEPVADHLSGKVIANLTSDTPEKARE    102
WP_037679270.1   VAKGAVLAPTLRDALAANELVVLSLTDYDAVYAVLKPVADSLSGKVIANLSSDTPERARE    102
WP_086884371.1   VAKGAVLASTVSEALAANELIVLSLTDYDAVYAVLEQAPDALSGKVIANLSSDTPERARE    102
WP_229819828.1   VAKGAVLAPSIEDALKANELVVLSLTDYDAMYAILEPATAALDGRVLINLSSDTPEKARA    102
WP_229356653.1   VAKGAVLAPSVEDALRANELVVLSLTDYDAMYAILEPATAALDGRVLINLSSDTPEKARA    107
WP_127489187.1   VAKGATRASTVNEALAANELVILSLTDYDVMYAILEPASMNLSGKVLVNLSSDTPEKVRK    120
WP_144878318.1   AAKGAIKASSVDEAIAANDLIILSLTDYDAMYAILEKAARDLSGKVFVNLSSDTPEKARE    119
WP_043615602.1   VARGAVLAGSVEEALAANELVILSLTDYDAMYTVLEPAAHALSGRVLVNLSSDTPEKTRA    103
WP_030554141.1   VTRGAVLAPNVKEALAAHELVILSLTDYDAMYAVLEPAEAALTGRTLVNLSSDTPEKARD    104
WP_129772310.1   VARGAVRAATVDEALAANELVILSLTDYDAMYALLGPATGALAGRVLVNLSSDTPKRAHE    114
WP_073792319.1   VARGAVLADSVEAALRANDLVVLSLTDYDATYGVLGPAQDALAGRVVVNLSSDTPDRARE    102
WP_063484289.1   VVAGAHRAATVRDALTASELVILSLTDHHAMYAVLESATDALSGRTLVNLGSDTPESARR    102
RIR87            VSQGAVQAATPADAVAASELVVVCLSTYDNMHDVIGSLGESLRGKVIVNLTSGSSDQGRE    104
WP_164356008.1   VSQGAVQAATPADAVAASELVVVCLSTYDNMHDVIGSLGESLRGKVIVNLTSGSSDQGRE    104
WP_192770552.1   VAQGATLAGSVGDAVAASPLVVVCVSNYEAMHELLDPLGGVLDGRVLVNLTSGTSRVARE    107
WP_189106074.1   VAEGAELAGSVADAVAASPLVVVCVLDYDAVHALLDPVGDALDGRVLVNLTSGTSEGARE    103
WP_132386371.1   VAAGATSTDNVAAAVSASPLVVVCVRDYQAAYEILGPVSDTLAGRVLVNLTSGTSAQARA    104
                 .  **  : .   *: *  *:::.:  :.    ::      * *:.. ** *.:.   :

SIR46            AAKWAAKHGAKHLTGGVQVPPPLIGKPESSTYYSGPKDVFDAHEDTLKVLTN-ADYRGED    161
WP_093601729.1   AATWAAEHGAKHLTGGVQVPPPLIGKPGSATYYSGPKDVFDAHEDTLKVLTD-ADYRGED    161
WP_206300583.1   AAKWATKHGAKHLTGGVQVPPPLIGKPGSSTYYSGPRDVFEAHEETLKVLTD-ADYRGED    161
WP_189220594.1   AFKWAAKHGAQHITGGVQVPPPLIGKPESSTYYSGPKDAFDTHEEALKVLTN-ADYRGED    161
WP_037679270.1   AAKWAAEHGAQHLTGGVQVPPPMIGTSDASAYYSGPEDVFNAHRSTLAVLTN-TDFRGED    161
WP_086884371.1   AAKWAERHGAVHITGGVQVPPPMIGKPESSTYYSGPKDAFDKYESTLKVLTG-ADFRGED    161
WP_229819828.1   AFEWAAGHGAKHVTGGVQVPPPLIGKEGSSTYYSGPRDVFDTYKETLEVLTA-ADYRGED    161
WP_229356653.1   AFAWAAGHGARHLTGGVQVPPPMIGKEGSSTYYSGPRDVFDTYRETLAVLTG-TDYRGED    166
WP_127489187.1   AAKWLAGRGARHVTGGVQVPPSGIGKSESSTYYSGPREVFEAHRETLEVLTG-TDYRGED    179
WP_144878318.1   AAKWLEARGARHLTGGVQVPPSGIGKAESSTYYSGTREVFDAHKKTLEVLTG-ADYRGED    178
WP_043615602.1   GAKWVAGHGGVQLSGGVTVPPSGIGKPESSTFYSGPRGPFETHRPTLEALTG-TDYRGED    162
WP_030554141.1   AARWAAEQGAVQLTGGVTVPPSGIGQAESSTFYSGPRDVFDRHRPALEVITGRTDHRGED    164
WP_129772310.1   AAAWAAGHGARHLSGGVQVPPSGIGKPESATFYSGPKDVFEEHAATLGVLTG-TDYLGED    173
WP_073792319.1   AAAWIAERGATHLTGGVRVPPSGIGQPGTSTFYSGPREVFERHKETLETLTG-ADYLGED    161
WP_063484289.1   AARWASEHGARYLTGGVQASPPGIGQPGFSTFYSGPQEVFDAHQEALEALTG-ADYRGED    161
RIR87            TAAWAEKQGVEYLDGAIMITPPGIGTETAVLFYAGTQSVFEKYEPALKLLGGGTTYLGTD    164
WP_164356008.1   TAAWAEKQGVEYLDGAIMITPPGIGTETAVLFYAGTQSVFEKYEPALKLLGGGTTYLGTD    164
WP_192770552.1   TAQRAAPLGGTYLDGAIMAIPQAIGTADAVILYSGPQAAFDSYESTLRSLG-AGTYLGAD    166
WP_189106074.1   MAEWAAGHGATYLDGAILSDPDGVGTADAVILYSGPRAAFDAHEPVLKLLGGATTHLGED    163
WP_132386371.1   MAGWAAERGAGYLDGAIMMTPPGIGTAEALILYSGPSETFAAHRPALTALGGGTTHLGAD    164
                        *   : *.:   *  :*       *:*.   *  :  .*  :     . * *
```

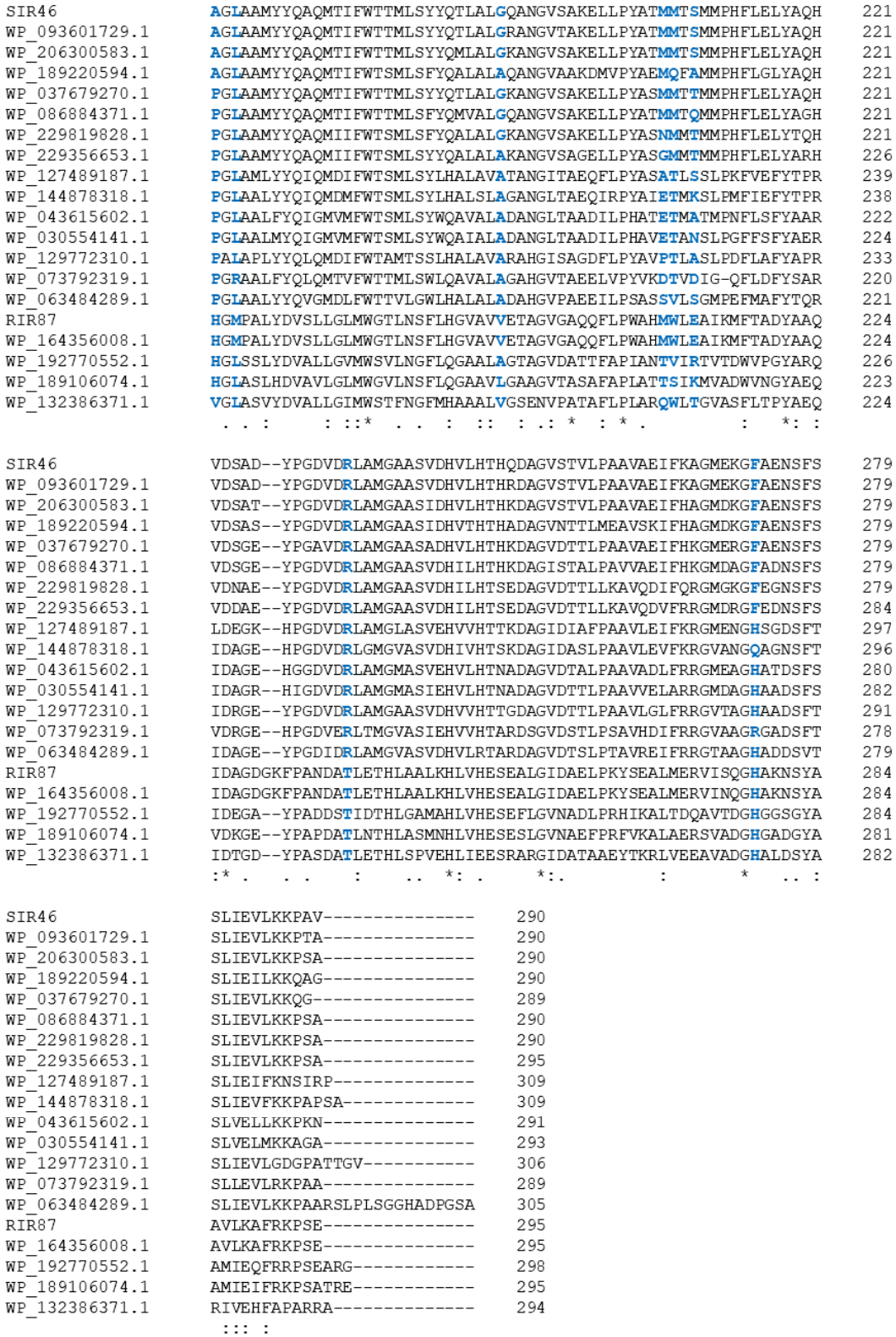

Figure S4. Multiple sequence alignments with SIR46. Alignments performed with clustal W using protein sequences obtained by BLAST searches with protein sequences of SIR46 and RIR87. The mutation candidates for improvement of SIR46 were shown in blue.

Table S3. Target residues in SIR46 (pdb 4oqy) (browsed by RCSB PDB web site)

Residue	Structual position	Residue	Structual position
S5	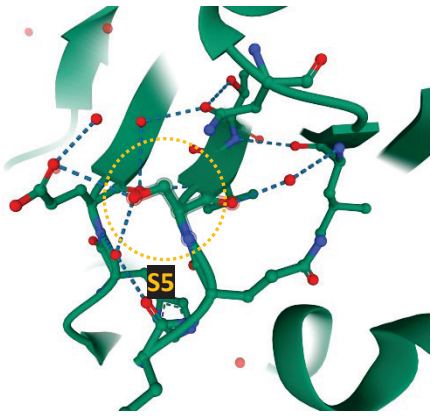	A41	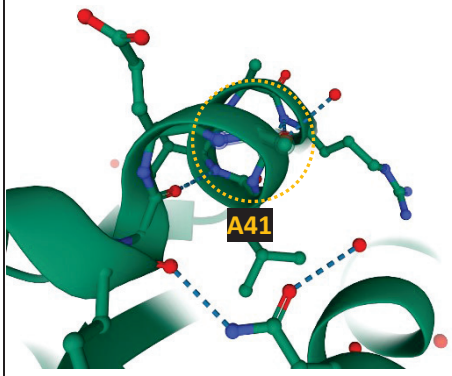
V48	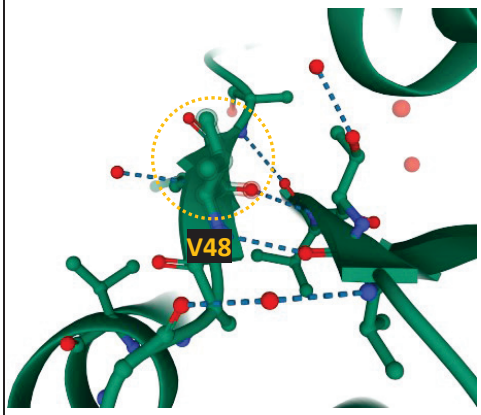	S58	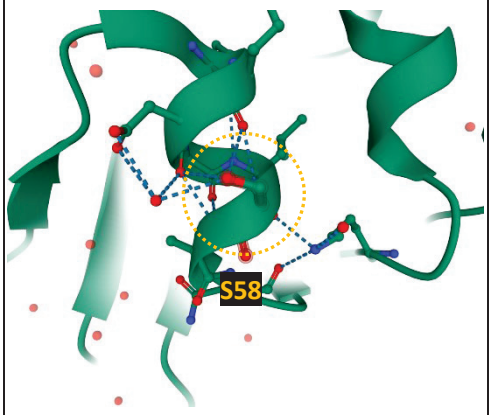
V88	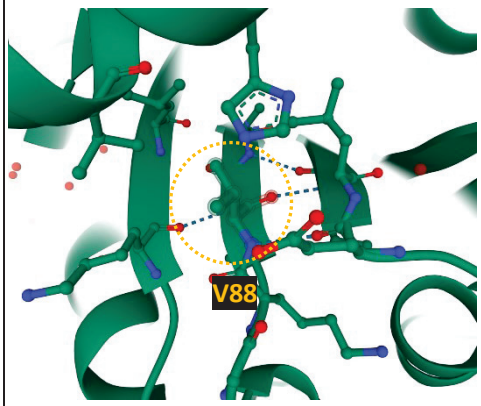	A90	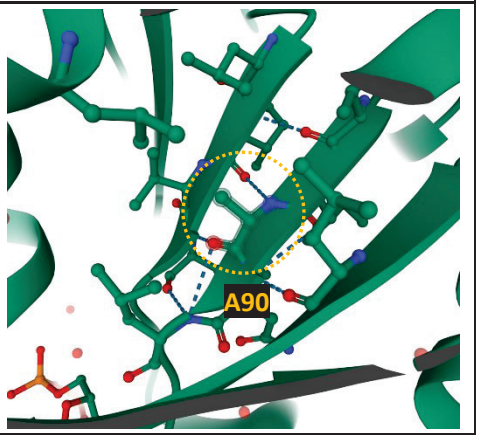

A103	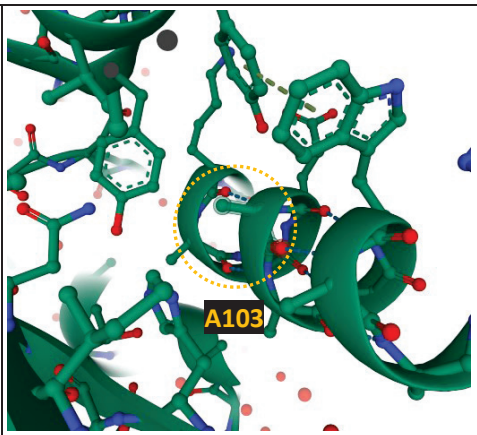	L115	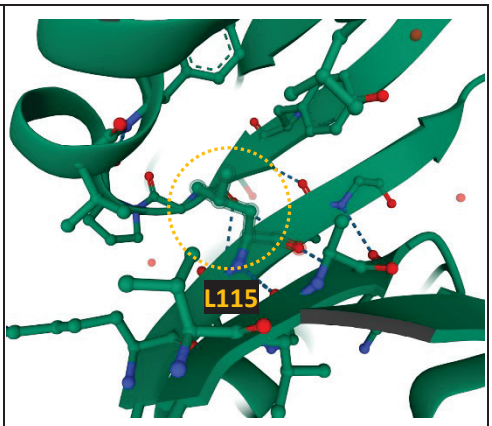
A144	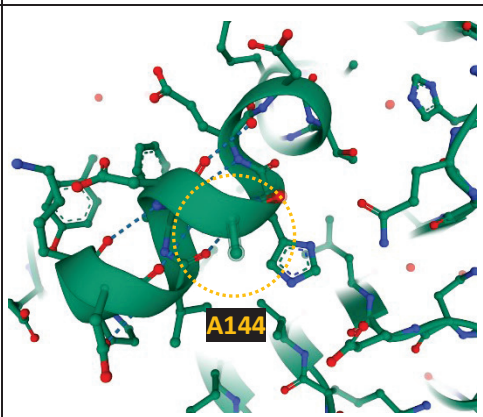	R158	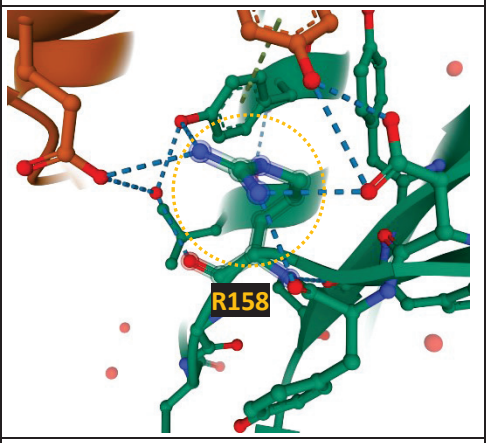
A162	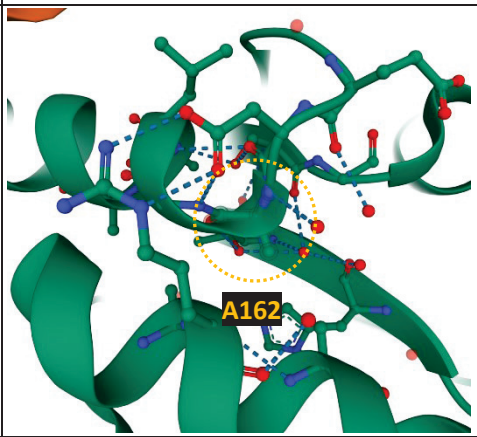	L164	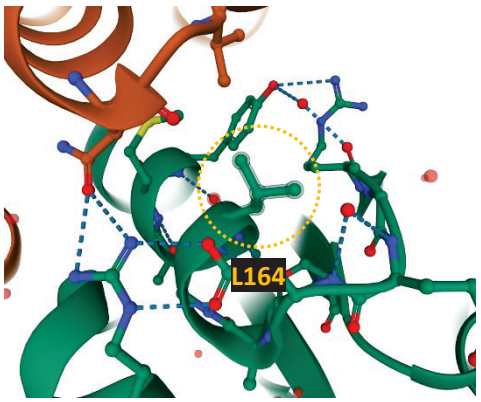
G190	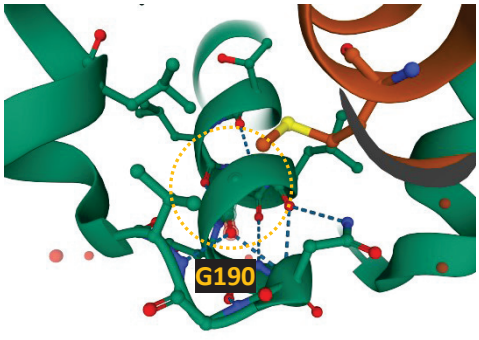	M206	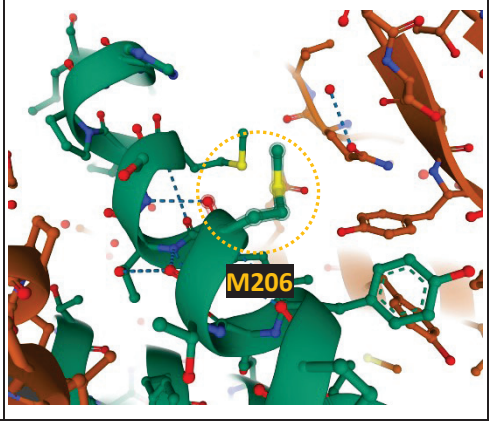

M207	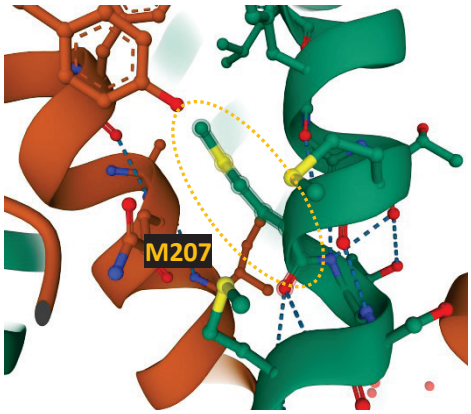	S209	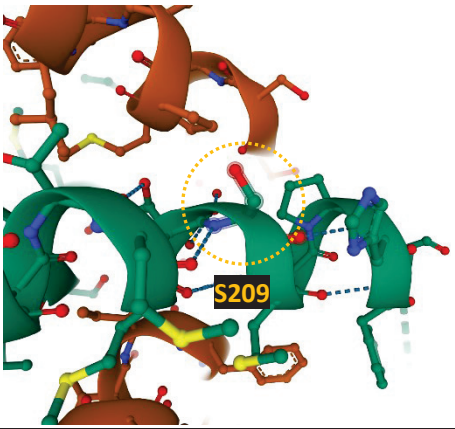
R233	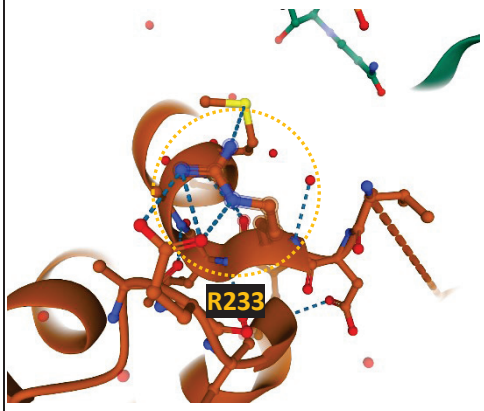	F273	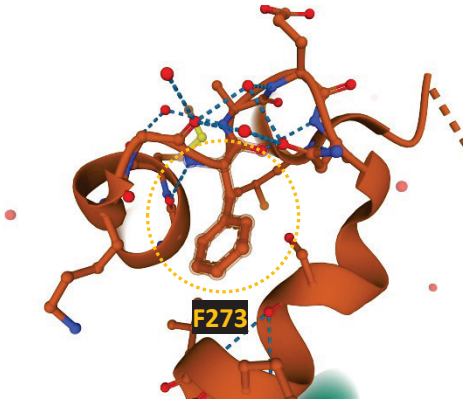
V73 and A103	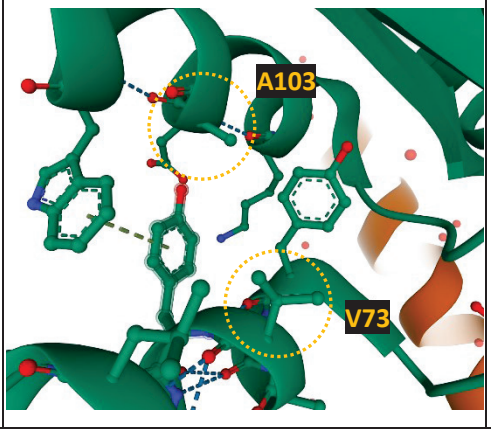		

Table S4. Specific activity and thermostability of SIR46 variants

Variant	Specific activity	Residual activity[1] (%)			
	(mU mg^{-1})	40°C	45°C	50°C	55°C
Wild type (WT)	12.6	66	0	n.d.	n.d.
WT + His6	8.8	58	0	n.d.	n.d.
R158L	23.4	91	6	n.d.	n.d.
V48T	16.2	57	0	n.d.	n.d.
A90V	4.6	78	0	n.d.	n.d.
A103M	21.2	85	15	n.d.	n.d.
S209R	20.4	88	27	n.d.	n.d.
S5P	13.8	60	0	n.d.	n.d.
A41P	13.4	67	0	n.d.	n.d.
L164R	13.1	0	n.d.	n.d.	n.d.
M206E	2.4	0	n.d.	n.d.	n.d.
R233T	9.0	93	34	n.d.	n.d.
S58R/R158L	19.7	96	16	n.d.	n.d.
R158L/G190A	7.4	69	0	n.d.	n.d.
R158L/F273H	9.5	10	0	n.d.	n.d.
M7	35.7	n.d.	n.d.	100	48
M7 + His6	33.4	n.d.	n.d.	97	33
M7 + V88T	31.6	n.d.	n.d.	104	58
M7 + L115V	35.1	n.d.	n.d.	87	0
M7 + A144R	31.8	n.d.	n.d.	105	55
M7 + M207T (M8)	36.6	n.d.	n.d.	94	63
M8 + V88T (M9)	32.9	n.d.	n.d.	102	70
M9 + A144R (M10)	32.6	n.d.	n.d.	98	71
M10 + L115V	30.6	n.d.	n.d.	97	54

[1] Residual activity after incubation at 40°C–55°C for 30 min.

Table S5. Effect of various organic solvents on SIR46 M9 or M10 activity for selection of the best variant.

Organic solvent	SIR46 M9	SIR46 M10
None	100% (35.0 mU mg^{-1})	100% (35.0 mU mg^{-1})
5% MeOH	89	85
10% MeOH	76	70
15% MeOH	65	59
20% MeOH	50	45
5% DMSO	77	75
10% DMSO	59	54
15% DMSO	43	41
20% DMSO	30	26
5% EtOH	60	51
10% EtOH	35	32
5% MeCN	41	40
5% AcOEt	4	6

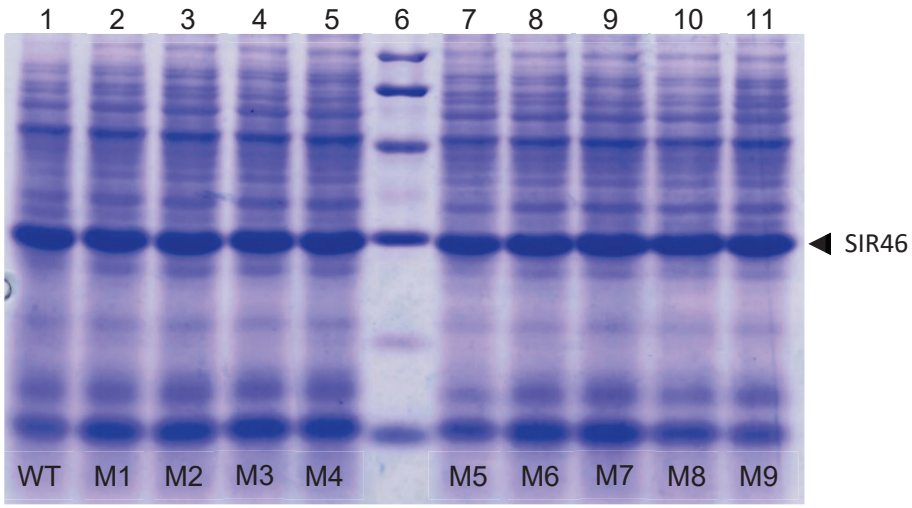

Figure S5. SDS-PAGE analysis of SIR46 variants expressed in *R. erythropolis* L88. Lanes 1–5, 7–11: cell-free extract of *R. erythropolis* L88 expressing SIR46 variants gene. Lane 6: molecular weight markers 97 kDa, 66 kDa, 45 kDa, 30 kDa, 20.1 kDa, 14.4 kDa.

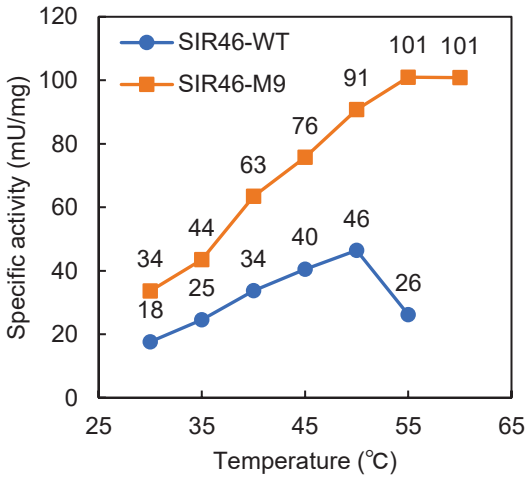

Figure S6. Effect of temperature on SIR46 activity.

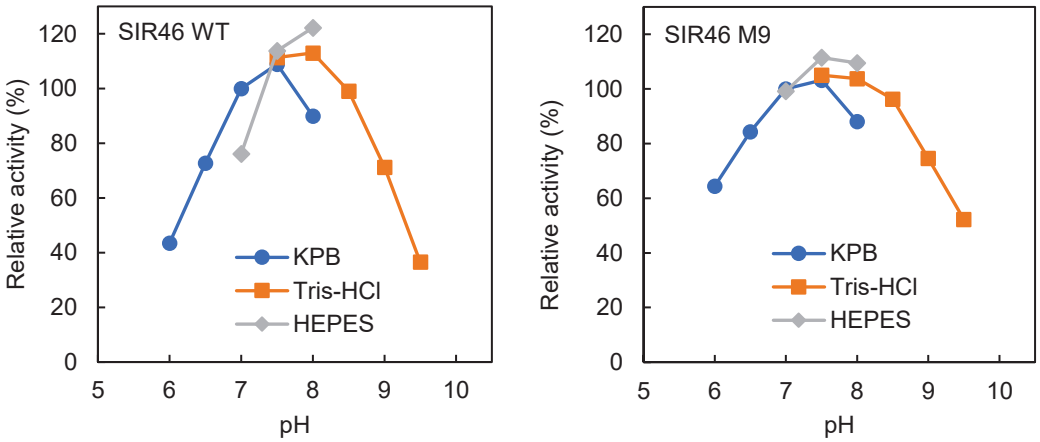

Figure S7. Effect of pH on SIR46 activity. 100% = 18.0 mU mg^{-1} (WT), 33.7 mU mg^{-1} (M9) in 100 mM KPB (pH 7.0).

Table S6. Residual activity of wild-type SIR46 and the variant M9 in cell-free extract on several conditions.

Condition	Residual activity (%)	
	Wild type	M9
None	100 (17.6 mU mg^{-1})	100 (32.7 mU mg^{-1})
Storage at 4°C for 15 days	65	107
Storage at 4°C for 35 days	34	110
Storage at 4°C for 53 days	15	106
Incubation at 35°C for 24 h	4	102

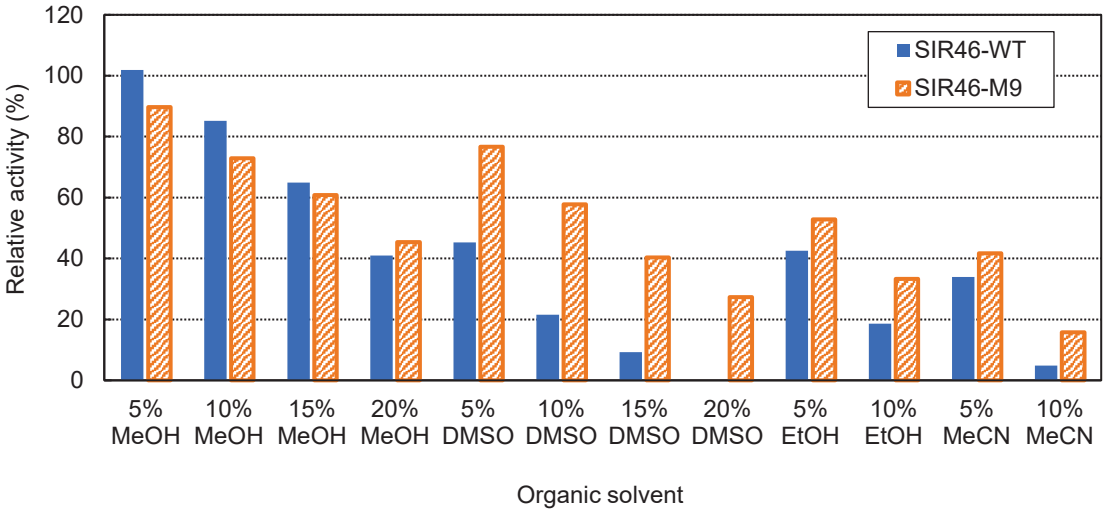

Figure S8. Effect of various organic solvents on SIR46 activity. None = 100% = 17.6 mU mg^{-1} (WT), 33.6 mU mg^{-1} (M9)

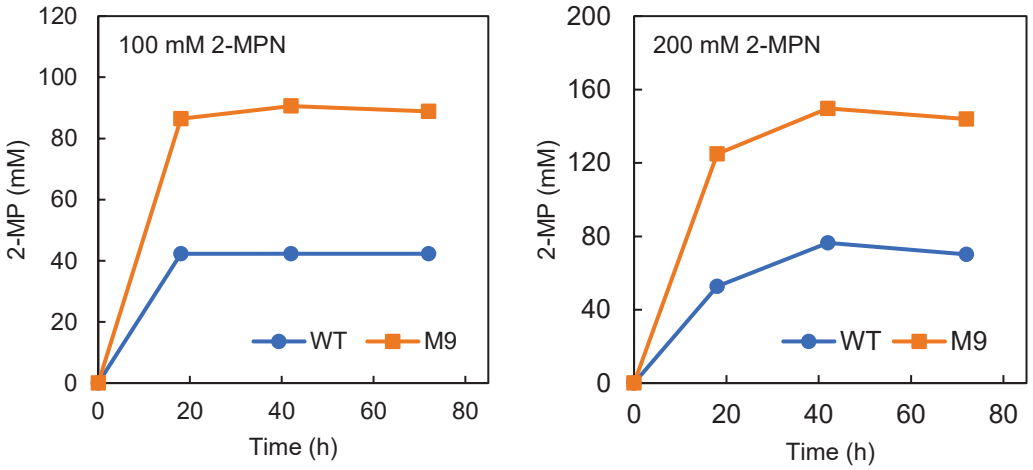

Figure S9. Evaluation of imine reductase activity of SIR46 WT or M9 in the presence of high concentration of 2-MPN. Reactions were performed at 30°C in potassium phosphate buffer (pH 7.5) containing 100 or 200 mM 2-MPN, glucose (1.25 eq.), 0.2 mM $NADP^+$, and 3.0 mg mL^{-1} cell-free extract of the recombinant cells overexpressing SIR46 and BsGDH genes.

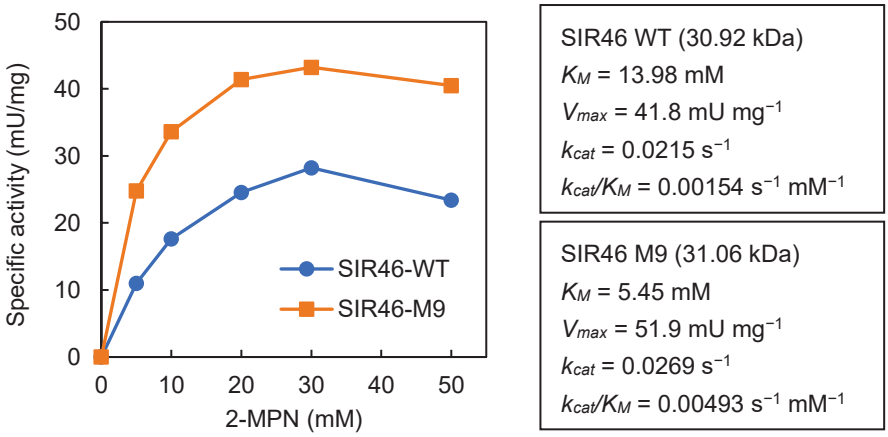

Figure S10. Determination of kinetic constants for 2-MPN reduction by SIR46. Kinetic constants were calculated using the values of specific activity at 5–30 mM 2-MPN.

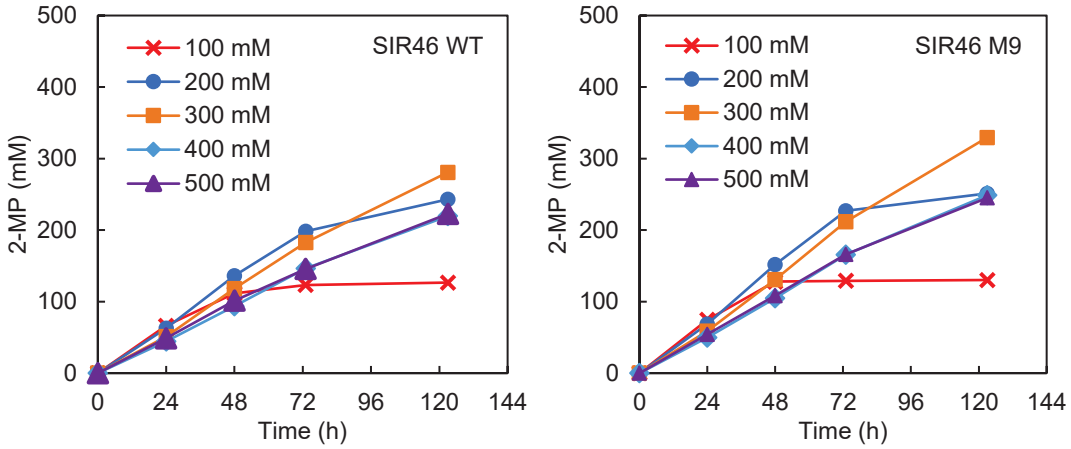

Figure S11. Bioconversion of high concentration of 2-MPN by SIR46 WT or M9. The reactions were performed at 30°C in potassium phosphate buffer (pH 7.5) containing 100–500 mM 2-MPN, glucose (1.2 eq.), and whole cells expressing SIR46 WT or M9 gene (OD_{610} = 25).

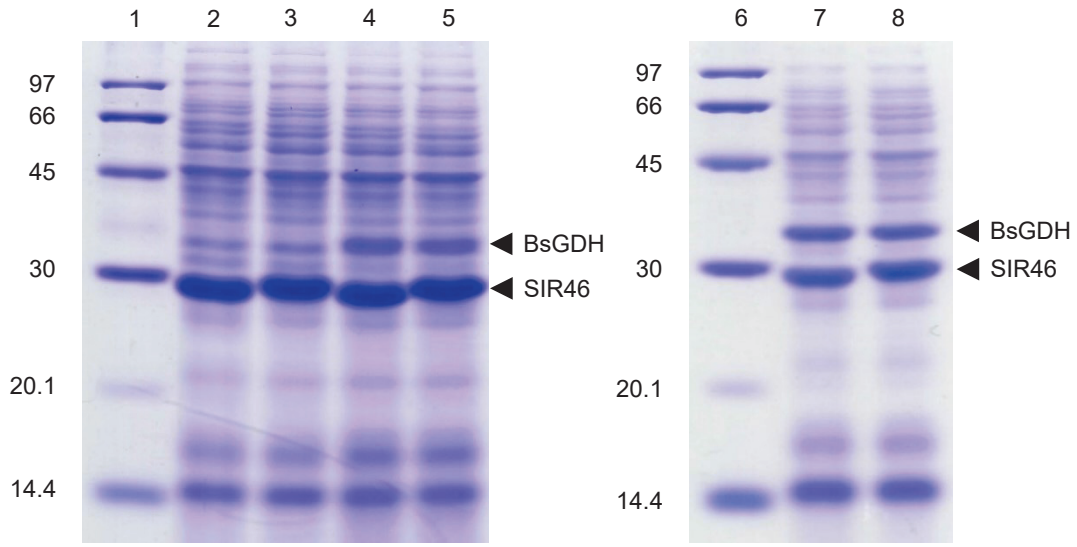

Figure S12. SDS-PAGE analysis of SIR46 M9 and BsGDH expressed in *R. erythropolis* L88. Lane 1, 6: molecular weight markers 97 kDa, 66 kDa, 45 kDa, 30 kDa, 20.1 kDa, 14.4 kDa. Lanes 2: cell-free extract of *R. erythropolis* L88 / wild-type SIR46 (CFE SIR46WT). Lanes 3: CFE SIR46WT. Lanes 4: CFE SIR46 WT and BsGDH. Lanes 5: CFE SIR46 M9 and BsGDH. Lane 7: CFE SIR46 WT and BsGDH (codon-optimized gene). Lane 8: CFE SIR46 M9 and BsGDH (codon-optimized gene).

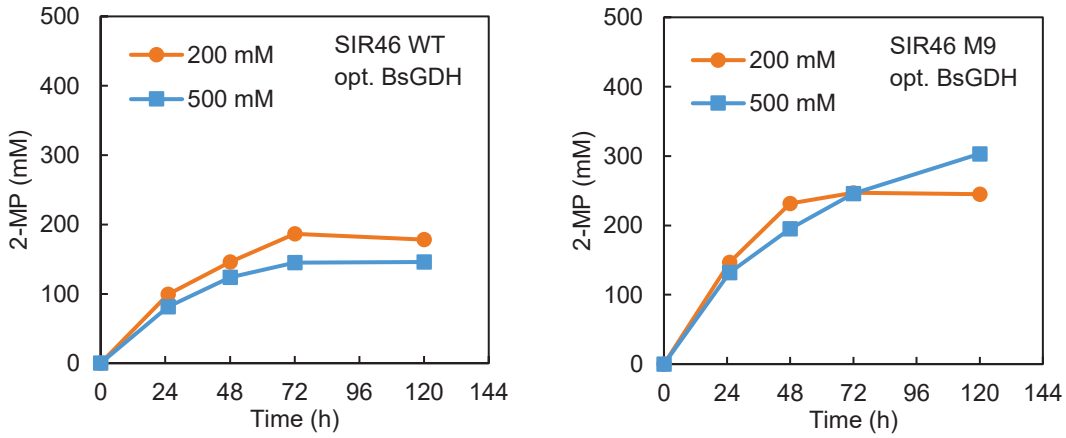

Figure S13. Bioconversion of high concentration of 2-MPN by SIR46 WT at 35°C. Reactions were performed at 35°C in potassium phosphate buffer (pH 7.5) containing 200 or 500 mM 2-MPN, glucose (1.2 eq.), and whole cells expressing SIR46 WT and codon-optimized BsGDH gene (OD_{610} = 25).

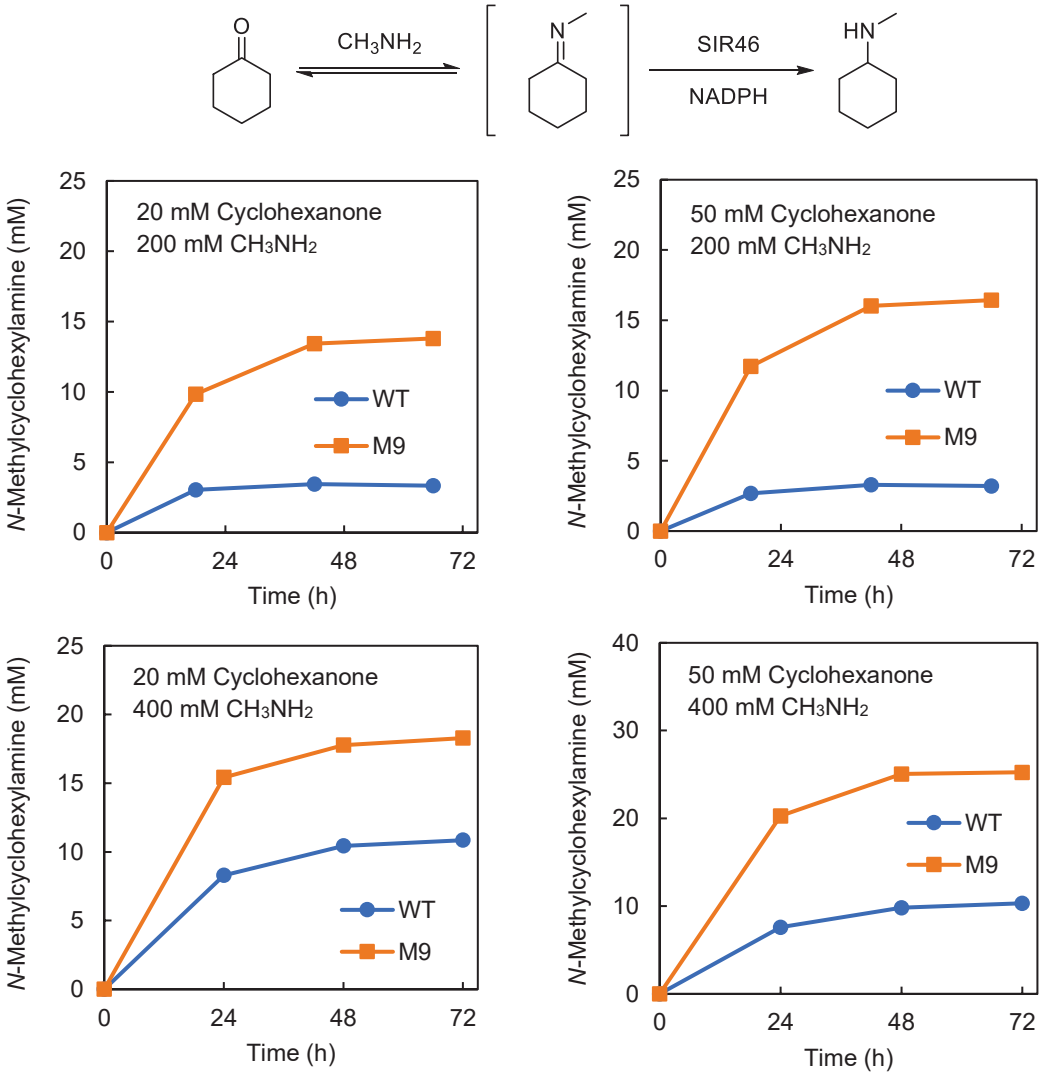

Figure S14. Reductive amination activity of SIR46 WT or M9. Reactions were performed at 30°C in potassium phosphate buffer (pH 8.0) containing 200 or 400 mM methylamine hydrochloride, 100 mM glucose, 0.2 mM $NADP^+$, 20 or 50 mM cyclohexanone, and 1.5 mg mL^{-1} cell-free extract of the recombinant cells overexpressing SIR46 and BsGDH genes.

Table S7. Specific activities of SIR46 and BsGDH in the cell-free extract of the recombinant cell.

Coexpression system	Substrate	Coenzyme	Specific activity (mU mg^{-1})
E. coli BL21 (DE3) pACYCDuet/SIR46(MCS1)-BsGDH(MCS2)	2-MPN	NADPH	2.3
	Glucose	$NADP^+$	628.3
E. coli BL21 (DE3) pACYCDuet/BsGDH(MCS1)-SIR46(MCS2)	2-MPN	NADPH	10.0
	Glucose	$NADP^+$	1.4
E. coli BL21 (DE3) pET-21a(+)/SIR46 and pACYCDuet/BsGDH(MCS2)	2-MPN	NADPH	22.7
	Glucose	$NADP^+$	133.1
R. erythropolis L88 pTipRT2/SIR46 WT and pTipQC1/BsGDH	2-MPN	NADPH	14.4
	Glucose	$NADP^+$	5.2
R. erythropolis L88 pTipRT2/SIR46 M9 and pTipQC1/BsGDH	2-MPN	NADPH	33.2
	Glucose	$NADP^+$	4.5
R. erythropolis L88 pTipRT2/SIR46 WT and pTipQC1/opt. BsGDH [1]	2-MPN	NADPH	11.1
	Glucose	$NADP^+$	6841
	Glucose	NAD^+	7314
R. erythropolis L88 pTipRT2/SIR46 M9 and pTipQC1/opt. BsGDH [1]	2-MPN	NADPH	25.1
	Glucose	$NADP^+$	6110
	Glucose	NAD^+	6083

[1] Codon-optimized BsGDH gene was expressed in the recombinant cell.

Table S8. HPLC analysis conditions for detection of cyclic amines.

Cyclic amine[1]	Column	Solvent	Retention time[2] (min)
2-Methylpyrrolidine (2-MP)[3]	Atlantis dC18 5μm 4.6×150 mm and YMC-Triart C18 5μm 4.6×150 mm	Sodium phosphate buffer (10 mM, pH 3.0) : MeOH = 11 : 10	32.8 (*S*) 34.6 (*R*)
2-Phenylpyrrolidine (2-PP)	Atlantis dC18 5μm 4.6×150 mm	Sodium phosphate buffer (10 mM, pH 3.0) : MeOH = 4 : 5	14.9 (S) 15.7 (*R*)
2-(4-Methoxyphenyl) pyrrolidine (2-MeOPP)	Atlantis dC18 5μm 4.6×150 mm	Sodium phosphate buffer (10 mM, pH 3.0) : MeOH = 4 : 5	16.4 (*S*) 16.9 (*R*)
1-Methyl-1,2,3,4-tetrahydroisoquinoline (1-MTIQ)	CHIRALPAK AD-RH 5μm 4.6×150 mm	sodium phosphate buffer (10 mM, pH 3.0) : MeCN = 3 : 2	12.8 (*R*) 13.7 (*S*)
N-Methyl-cyclohexylamine	Atlantis dC18 5μm 4.6×150 mm	sodium phosphate buffer (10 mM, pH 3.0) : MeOH = 4 : 5	18.0

[1] Cyclic amines except for 1-MTIQ were derivatized with GITC to determine the yield and optical purity. 1-MTIQ was derivatized with MITC.

[2] Absolute configurations of chiral cyclic amines were determined by using commercially available chiral reagents or the reference.

[3] HPLC analysis of 2-MP was performed with two columns connected in series (Atlantis column in front, YMC column in back).

References

(1) K. Mitsukura, M. Suzuki, S. Shinoda, T. Kuramoto, T. Yoshida, T. Nagasawa, Purification and Characterization of a Novel (*R*)-Imine Reductase from *Streptomyces* sp. GF3587, *Biosci. Biotechnol. Biochem.*, **2011**, 75, 1778–1782.

(2) K. Mitsukura, T. Kuramoto, T. Yoshida, N. Kimoto, H. Yamamoto, T. Nagasawa, A NADPH-dependent (*S*)-imine reductase (SIR) from *Streptomyces* sp. GF3546 for asymmetric synthesis of optically active amines: purification, characterization, gene cloning, and expression, *Appl Microbiol Biotechnol*, **2013**, 97, 8079–8086.

(3) M. Rodríguez-Mata, A. Frank, E. Wells, F. Leipold, N. J. Turner, S. Hart, J. P. Turkenburg, G. Grogan, Structure and Activity of NADPH-Dependent Reductase Q1EQE0 from *Streptomyces kanamyceticus*, which Catalyses the *R*-Selective Reduction of an Imine Substrate, *ChemBioChem*, **2013**, 14, 1372–1379.

(4) P. N. Scheller, S. Fademrecht, S. Hofelzer, J. Pleiss, F. Leipold, N. J. Turner, B. M. Nestl, B. Hauer, Enzyme Toolbox: Novel Enantiocomplementary Imine Reductases, *ChemBioChem*, **2014**, 15, 2201–2204.

(5) T. Huber, L. Schneider, A. Präg, S. Gerhardt, O. Einsle, M. Müller, Direct Reductive Amination of Ketones: Structure and Activity of *S*-Selective Imine Reductases from *Streptomyces*, *ChemCatChem*, **2014**, 6, 2248–2252.

(6) D. Wetzl, M. Gand, A. Ross, H. Müller, P. Matzel, S. P. Hanlon, M. Müller, B. Wirz, M. Höhne, H. Iding, Asymmetric Reductive Amination of Ketones Catalyzed by Imine Reductases, *ChemCatChem*, **2016**, 8, 2023–2026.

(7) G. A. Aleku, S. P. France1, H. Man, J. Mangas-Sanchez, S. L. Montgomery, M. Sharma, F. Leipold, S. Hussain, G. Grogan, N. J. Turner, A reductive aminase from *Aspergillus oryzae*, *Nat. Chem.*, **2017**, 9, 961–969.

(8) S. Velikogne, V. Resch, C. Dertnig, J. H. Schrittwieser, W. Kroutil, Sequence-Based *In-silico* Discovery, Characterisation, and Biocatalytic Application of a Set of Imine Reductases, *ChemCatChem*, **2018**, 10, 3236–3246.

(9) E. Vázquez-Figueroa, J. Chaparro-Riggers,A. S. Bommarius, Development of a Thermostable Glucose Dehydrogenase by a Structure-Guided Consensus Concept, *ChemBioChem*, **2007**, 8, 2295–2301.

(10) C. K. Savile, J. M. Janey, E. C. Mundorff, J. C. Moore, S. Tam, W. R. Jarvis, J. C. Colbeck, A. Krebber, F. J. Fleitz, J. Brands, P. N. Devine, G. W. Huisman, G. J. Hughes, Biocatalytic Asymmetric Synthesis of Chiral Amines from Ketones Applied to Sitagliptin Manufacture, *Science*, **2010**, 329, 305–309.

(11) M. A. Huffman, A. Fryszkowska, O. Alvizo, M. Borra-Garske, K. R. Campos, K. A. Canada, P.

N. Devine, D. Duan, J. H. Forstater, S. T. Grosser, H. M. Halsey, G. J. Hughes, J. Jo, L. A. Joyce, J. N. Kolev, J. Liang, K. M. Maloney, B. F. Mann, N. M. Marshall, M. McLaughlin, J. C. Moore, G. S. Murphy, C. C. Nawrat, J. Nazor, S. Novick, N. R. Patel, A. Rodriguez-Granillo, S. A. Robaire, E. C. Sherer, M. D. Truppo, A. M. Whittaker, D. Verma, L. Xiao, Y. Xu, H. Yang, Design of an in vitro biocatalytic cascade for the manufacture of islatravir, *Science*, **2019**, 366, 1255–1259.

(12) W. Qian, L. Ou, C. Li, J. Pan, J. Xu, Q. Chen, G. Zheng, Evolution of Glucose Dehydrogenase for Cofactor Regeneration in Bioredox Processes with Denaturing Agents, *ChemBioChem*, **2020**, 21, 2680–2688.

(13) H. Lu, D. J. Diaz, N. J. Czarnecki, C. Zhu, W. Kim, R. Shroff, D. J. Acosta, B. R. Alexander, H. O. Cole, Y. Zhang, N. A. Lynd, A. D. Ellington, H. S. Alper, Machine learning-aided engineering of hydrolases for PET depolymerization, *Nature*, **2022**, 604, 662–667.

(14) M. Schober, C. MacDermaid, A. A. Ollis, S. Chang, D. Khan, J. Hosford, J. Latham, L. A. F. Ihnken, M. J. B. Brown, D. Fuerst, M. J. Sanganee, G.-D. Roiban, Chiral synthesis of LSD1 inhibitor GSK2879552 enabled by directed evolution of an imine reductase, *Nat. Catal.*, **2019**, 2, 909–915.

(15) R. Kumar, M. J. Karmilowicz, D. Burke, M. P. Burns, L. A. Clark, C. G. Connor, E. Cordi, N. M. Do, K. M. Doyle, S. Hoagland, C. A. Lewis, D. Mangan, C. A. Martinez, E. L. McInturff, K. Meldrum, R. Pearson, J. Steflik, A. Rane, J. Weaver, Biocatalytic reductive amination from discovery to commercial manufacturing applied to abrocitinib JAK1 inhibitor, *Nat. Catal.*, **2021**, 4, 775–782.

(16) J. R. Marshall, P. Yao, S. L. Montgomery, J. D. Finnigan, T. W. Thorpe, R. B. Palmer, J. Mangas-Sanchez, R. A. M. Duncan, R. S. Heath, K. M. Graham, D. J. Cook, S. J. Charnock, N. J. Turner, Screening and characterization of a diverse panel of metagenomic imine reductases for biocatalytic reductive amination, *Nat. Chem.*, **2021**, 13, 140–148.

(17) G. A. Aleku, H. Man, S. P. France, F. Leipold, S. Hussain, L. Toca-Gonzalez, R. Marchington, S. Hart, J. P. Turkenburg, G. Grogan, N J. Turner, Stereoselectivity and Structural Characterization of an Imine Reductase (IRED) from *Amycolatopsis orientalis*, *ACS Catal.*, **2016**, 6, 3880–3889.

(18) H. Li, P. Tian, J. Xu, G. Zheng, Identification of an Imine Reductase for Asymmetric Reduction of Bulky Dihydroisoquinolines, *Org. Lett.*, **2017**, 19, 3151–3154.

(19) Y. Fukawa, Y. Mizuno, K. Kawade, K. Mitsukura, T. Yoshida, Novel (*S*)-Selective Hydrolase from *Arthrobacter* sp. K5 for Kinetic Resolution of Cyclic Amines, *Catalysts*, **2021**, 11, 809.

(20) H. Man, E. Wells, S. Hussain, F. Leipold, S. Hart, J. P. Turkenburg, N. J. Turner, G. Grogan, Structure, Activity and Stereoselectivity of NADPH-Dependent Oxidoreductases Catalysing the *S*-Selective Reduction of the Imine Substrate 2-Methylpyrroline, *ChemBioChem*, **2015**, 16, 1052–1059.

(21) M. Moustakim, T. Christott, O. P. Monteiro, J. Bennett, C. Giroud, J. Ward, C. M. Rogers, P. Smith, I. Panagakou, L. Díaz-Sáez, S. L. Felce, V. Gamble, C. Gileadi, N. Halidi, D. Heidenreich, A. Chaikuad, S. Knapp, K. V. M. Huber, G. Farnie, J. Heer, N. Manevski, G. Poda, R. Al-awar, D. J. Dixon, P. E. Brennan, O. Fedorov, Discovery of an MLLT1/3 YEATS Domain Chemical Probe, *Angew.*

Chem. Int. Ed., **2018**, 57, 16302–16307.
(22) Inoue, H., Nojima, H., and Okayama, H. High efficiency transformation of *Escherichia coli* with plasmids. *Gene* **1990**, 96, 23–28.
(23) Bradford, M.M. A rapid and sensitive method for the quantitation of microgram quantities of protein utilizing the principle of protein-dye binding. *Anal. Biochem.* **1976**, 72, 248–254.
(24) Laemmli, U.K. Cleavage of structural proteins during the assembly of the head of bacteriophage T4. *Nature* **1970**, 227, 680–685.

Acknowledgement

I deeply appreciate Professor Toyokazu Yoshida for his kind and appropriate guidance in this study. I also wish to express my thanks to Associate Professor Koichi Mitsukura for his kind support and warmest encouragement in the accomplishment of this work. They have always given me freedom to have my own ideas and experiment anything I want to do, which developed my ability to think. I will never forget the precious opportunity.

I would like to thank the support of the Life Science Research Center, Gifu University, for NMR analysis and whole-genome sequencing.

I greatly appreciate the kind support by the members who belonged to our laboratories at Department of the Chemistry and Biomolecular Science, Faculty of Engineering, Gifu University.

Finally, I would like to express my gratitude to my family and friends for their clear guidance and unconditional support.

March 2023

Yuta Fukawa

List of publications

Chapter 2

1. Y. Fukawa, Y. Mizuno, K. Kawade, K. Mitsukura, T. Yoshida
   Novel (*S*)-selective hydrolase from *Arthrobacter* sp. K5 for kinetic resolution of cyclic amines
   Catalysts, **2021**, 11, 809.

Chapter 3

2. Y. Fukawa, K. Yoshida, S. Degura, K. Mitsukura, T. Yoshida
   Improvement of (*S*)-selective imine reductase GF3546 for the synthesis of chiral cyclic amines
   ChemComm, **2022**, 58, 13222–13225.